MARINE GEOLOGY OF UPPER JERVIS INLET

by

ROBERT DRUMMOND MACDONALD
B.A.Sc. University of British Columbia 1965

A THESIS SUBMITTED IN PARTIAL FULFILMENT OF
THE REQUIREMENTS FOR THE DEGREE OF

MASTER OF APPLIED SCIENCE

in the Department
of
Geology

We accept this thesis as conforming to the
required standard

THE UNIVERSITY OF BRITISH COLUMBIA

April 1970

In presenting this thesis in partial fulfilment of the requirements for an advanced degree at the University of British Columbia, I agree that the Library shall make it freely available for reference and study. I further agree tha permission for extensive copying of this thesis for scholarly purposes may be granted by the Head of my Department or by his representatives. It is understood that copying or publication of this thesis for financial gain shall not be allowed without my written permission.

Department of Geology

The University of British Columbia
Vancouver 8, Canada

Date April 30 1970.

ABSTRACT

Manganese-iron oxide concretions are presently forming on Patrick Sill in upper Jervis Inlet. The marine geology of Patrick Sill and the adjoining basins (Queen's Reach and Princess Royal Reach) was studied to define the environment in which the concretions form.

The river at the inlet head is the principal source of sediment to the upper basin. The average grain size of surficial bottom sediments within this basin decreases uniformly with distance from the source. Patrick Sill separates the upper from the lower basin. The sediment distribution pattern within the lower basin differs markedly from the upper basin as there is no dominant source of material but rather many localized sources.

Abundant shallow marine faunal remains recovered in deep water sediment samples indicate that sediments deposited as deltas off river and stream mouths periodically slump to the basin floors. Geologic and optical turbidity information for the upper basin can best be explained by slumping from the delta at the inlet head with the initiation of turbidity or density currents. Patrick Sill appears to create a downstream barrier to this flow.

The mineralogy of the bottom sediments indicates derivation from a granitic terrain. If this is so, the sediments presently being deposited in both basins are reworked glacial materials initially derived by glacial action outside the present watershed. Upper Jervis Inlet is mapped as lying within a roof pendant of pre-batholithic rocks, principally slates.

Patrick Sill is thought to be a bedrock feature mantled with Pleistocene glacial material. The accumulation rate of recent sediments on the sill is low especially in the V-notch or medial depression. The manganese-iron oxide concretions are forming within the depression and apparently nowhere else in the study area. Also forming within the depression are crusts of iron oxide and what are tentatively identified as glauconite-montmorillonoid pellets. The concretions are thought to form by precipitation of manganese-iron oxides on pebbles and cobbles lying at the sediment water interface. The oxide materials are mobile in the reducing environment of the underlying clayey-sand sediment but precipitate on contact with the

oxygenating environment of the surficial sediments. The iron crusts are thought to be forming on extensive rocky surfaces above the sediment water interface. The overall appearance and evidence of rapid formation of the crusts suggests they formed from a gel in sea water.

Reserves of manganese-iron concretions on Patrick Sill were estimated to be 117 metric tons. Other deposits of concretions have recently been found in other inlets and in the Strait of Georgia but, to date, the extent of these has not been determined.

Table of Contents

List of Tables

List of Figures

CHAPTER 1

INTRODUCTION

I. History and Purpose of the Study

Little work has been done on the marine geology of British Columbia inlets. Sediment studies have been made in Bute Inlet (Toombs 1956), Saanich Inlet (Gucleur and Gross 1964), and Howe Sound (Murray and Ricker--unpublished report).

A sedimentologic survey of Jervis Inlet was undertaken in May, 1966 (I.O.U.B.C. Cruise 66/12) to obtain information for comparison with sediment data from Howe Sound. Systematic sampling of upper Jervis Inlet revealed a localized deposit of manganese-iron concretions, or nodules, on a submarine sill (Patrick Sill). Thereupon, a more intensive study of Patrick Sill and adjacent basins of upper Jervis Inlet was conducted.

Chemical studies of the concretions, the interstitial water of the sediments, and the water column are being made by Dr. E. V. Grill of the Institute of Oceanography at the University of British Columbia.

A study of all the oceanographic aspects of the upper Jervis Inlet system may lead to a better understanding of the formation of manganese concretions in shallow coastal waters.

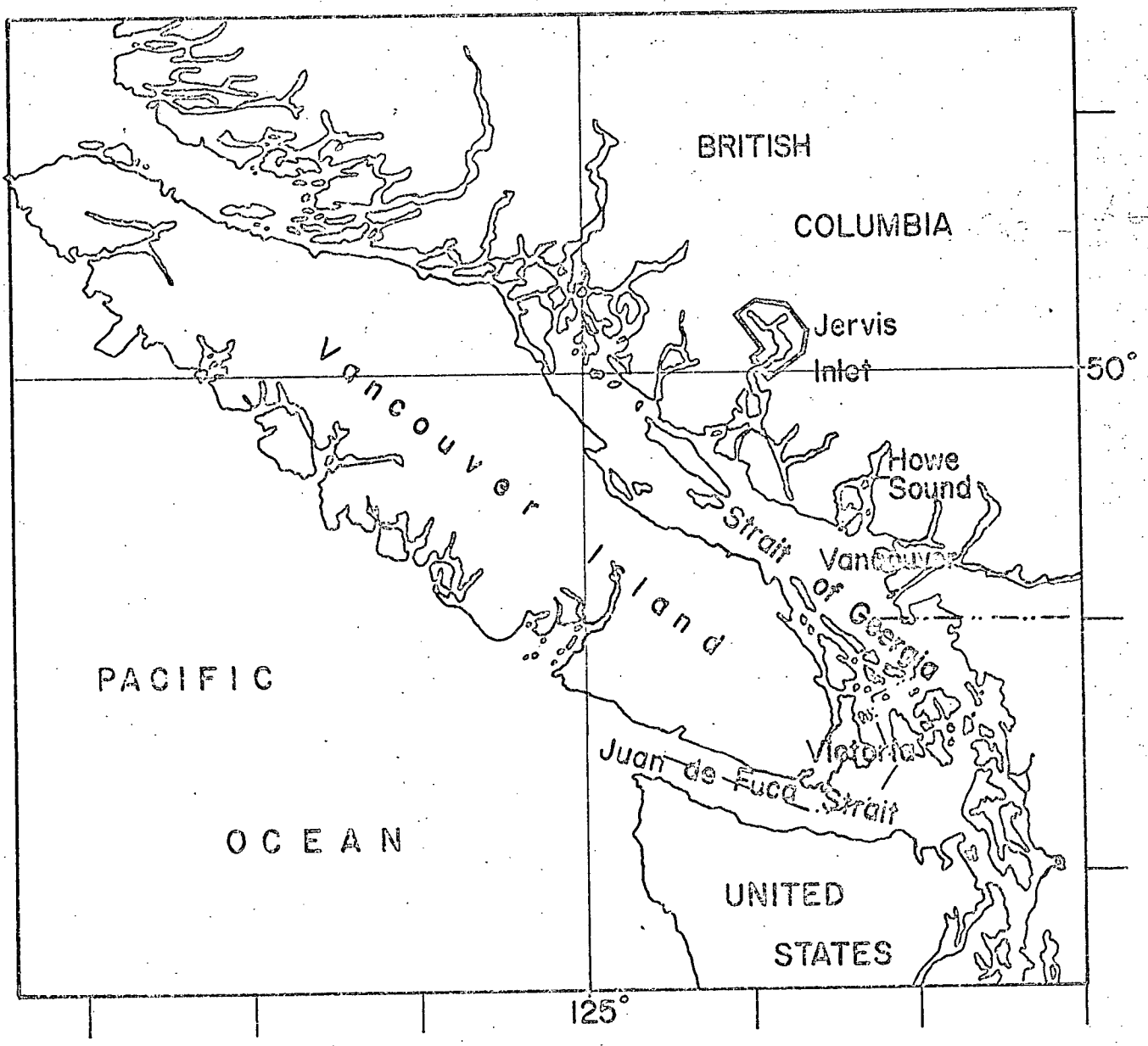

FIG. 1 LOCATION MAP — Showing upper Jervis Inlet study area

II. Location and Physical Setting

Jervis Inlet is located in the northwesterly trending Pacific Range of the Coast Mountains. The mouth of the inlet lies approximately 46 nautical miles (85 kilometers) west-northwest of Vancouver, British Columbia, on the eastern margin of the Strait of Georgia. The inlet is 48 nautical miles (89 kilometers) long and the width averages 1.7 (3.2 kilometers) and seldom exceeds 2.5 nautical miles (4.6 kilometers).

The study area (Figure 1) encompasses the northern or upper part of the inlet which is divided into two legs or reaches by a right-angle change in strike of the axis. Queen's Reach is uppermost and has a north-westerly trend while Princess Royal Reach trends to the north-east. Princess Louisa Inlet, which opens into Queen 's Reach, was not included in the study.

Patrick Sill lies perpendicular to the axis of Queen's Reach at the point where Queen's Reach turns into Princess Royal Reach. The manganese concretions occur on the southern flank of Patrick Sill at $50^{o}06.2'$ north latitude and $123^{o}47.8'$ west longitude.

Access to the area is by boat or aircraft only.

Jervis Inlet is a glacially modified Pliocene river valley which was invaded by the sea with the waning of the Pleistocene ice sheet. The mountains surrounding the inlet tower to 6,000 to 8,000 feet (1800 to 2200 meters) above sea level. Steep mountain sides dip at angles averaging 30° to 35° to the water's edge and disappear with no change of slope. Deep striations on rock surfaces, mountain sides too steep and polished to trap soil to support vegetation, and hanging valleys all indicate extensive glaciation.

The watershed area of upper Jervis Inlet is small, and many of the streams are intermittent. Queen's Reach and Princess Royal Reach have watershed areas of 273 and 167 square miles (855 and 523 square kilometers) respectively. Unlike the majority of long inlets, the run-off into Jervis follows the coastal rainfall pattern closely, i.e. above average in the spring and winter months and below average during July through September. This is due to the absence of large, permanent snowfields within the watershed to store precipitation.

The mean annual fresh water discharge into Jervis Inlet is 236 cubic yards (180 cubic meters) per second. Howe Sound, which has a length of 23 nautical miles (42 kilometers), receives a mean annual discharge of 630 cubic yards (480 cubic meters) per second. (Trites 1955). The average rainfall for southern inlets is estimated to be 60 to 100 inches (150 to 250 centimeters) annually at lower elevations (B.C. Atlas of Resources,1956). However, with altitude, the amount of precipitation can increase to 100 to 150 inches (250 to 380 centimeters) annually, especially towards the heads of the inlets. The inlets funnel moist Pacific air inland until, at the head, this air is forced to rise abruptly. About 10 to 15 per cent of precipitation falls as snow.

The mean monthly temperature at the heads of fjords along the west coast ranges from 20° to 25°F (-7°to -4°C) in January, to 38° to 62°F (3°to 17°C) in July. On a daily basis, the mean maximum temperature is 70° to 75°F (21° to 24°C). The average minimum temperature and the number of frost-free days increase from the heads to the mouths of the inlets (B.C.Atlas of Resources, 1956).

With some exceptions, the mountain slopes are covered with vegetation to an elevation of approximately 4600 feet (1400 meters). This elevation does not represent the true tree line, but reflects a general lack of soil at higher elevations. The lower, vegetated areas are classified as Coast Forest biotic region. Characteristic are extensive stands of sitka spruce, red and yellow cedar, fir, western and mountain hemlock, and western white pine. These stands of timber support many small logging operations along the length of the inlet. Typical of the Coast Forest region is a dense underbrush of maple, alder, ferns, salal, devil's club, huckleberry, salmonberry and thimbleberry. With increase in elevation, the Coast Forest gives way to the Subalpine Forest biotic region. Alpine varieties of spruce, fir, and pine in open stands and a matting of blueberry and heather typify this region.

III. Previous Work

Prior sedimentologic work in Jervis Inlet has been done only on a reconnaissance basis as part of an overall study of the B. C. coastline (Pickard, 1956), and the continental shelf (Cockbain 1963). More detailed geologic studies have been made in

Bute Inlet (Toombs 1956), Saanich Inlet (Gucleur and Gross 1964) and Howe Sound (Murray and Ricker - unpublished).

The surficial geology of the upper Jervis Inlet area was mapped on a reconnaissance basis by LeRoy (1908). Since then no further work has been published for this area. Bacon (1957) described the geology of the lower Jervis Inlet area. The coast mapping project of the Geological Survey of Canada, which is presently underway, will give the first unified map of the geology of Jervis Inlet.

The physical oceanography of Jervis Inlet has been studied by many workers. Pickard (1961) described and classified the inlets of the B.C. coast and presented observations of optical turbidity (Pickard and Giovando 1960). Lazier (1963) studied Jervis Inlet as an example of a deep silled inlet and described a circulation of unknown period.

IV. Field Work and Acknowledgments

Field work was carried out from the vessels C.S.S.Ehkoli and C.S.S.Vector of the Department of Energy, Mines and Resources of the Federal Government. The assistance of the officers and crew of

these vessels was invaluable.

Detailed bathymetric charts (field sheets) of the study area were generously supplied by the Canadian Hydrographic Service.

Financial support was gratefully received from the Dean's Research Fund of the University of British Columbia, National Research Council of Canada, Geological Survey of Canada (Contract EMR-68-IU), Special Projects Division of Bear Creek Mining Company and the International Nickel Company of Canada.

Dr. J. W. Murray of the Department of Geology at the University of British Columbia was the supervisor of this work.

CHAPTER 2

GEOLOGIC HISTORY AND REGIONAL GEOLOGY

I. Geologic History of Southwestern B.C.

Early Jurassic marked the beginning of tectonic events which were to ultimately form the Insular and Coast Mountain region. This orogenic episode, which was to continue in stages to mid-Tertiary time, involved a late Paleozoic eugeosynclinal-like succession of sedimentary and submarine volcanic rocks. Intense folding, metamorphism and uplift were accompanied by volcanism and the development of large plutonic masses. Successive stages of tectonism followed by erosion removed much of the rock cover from the batholithic cores. The derived sediments were deposited in flanking basins under marine and brackish conditions. The resulting land surface was a peneplain of low relief and average elevation of 900 to 1200 feet (270 to 370 meters) below the present average. (Holland, 1964). Differential uplift of this erosion surface occurred during early Tertiary with greatest movement along two main axes of intrusion. Separating these axes, now the Insular and Coast Mountains, was a trough now corresponding to the Strait of Georgia. Sediments dervied from further erosion of rejuvenated areas were deposited in this Coastal Trough along with lavas and fragmental products of regional volcanism. Erosion continued through the middle Pliocene and further unroofed the granitic

cores of the uplifted areas. The land surface was reduced to one of low to moderate relief, co-extensive with a similar surface with a relief of 1500 to 2000 feet (460 to 610 meters) in Central British Columbia. (Holland, 1964). Late Pliocene time marked the advent of renewed differential uplift along the previously active axes resulting in rejuvenation of the erosive power of all the streams. A transverse upwarping divided the coastal trough into the Hecate Depression to the north, and the Georgia Depression to the south. The late Tertiary erosion surface was deeply dissected and partially to almost completely destroyed. The present topography is essentially that of the late Pliocene, considerably modified by Pleistocene glaciations.

During Pleistocene time, southwestern B.C. was extensively glaciated by cirque, valley, and continental glaciers. Like the tectonic history of the area, the glacial history is very complex. Studies indicate at least two major Cordilleran ice sheet glaciations separated by an interglacial stage. Some peripheral areas may have been subject to three or more major ice advances. The sequence of major Pleistocene events in southwestern B.C. is given below.

Table I. Time Stratigraphic Units for Pleistocene of Southwestern B.C.
(after Armstrong et al, 1965)

1) Salmon Springs Glaciation > 37,000 years B.P.

2) Olympia Interglaciation $<24,500>15,000$ - 37,000 years B.P.

During this period, ice was absent from the lowlands of southwestern B.C.

3) Fraser Glaciation approx.$9,500 - >15,000 <25,000$ years B.P.

This glaciation is probably the regional equivalent of the Wisconsin Glaciation of the mid-western United States.

a) Evans Creek Stade 17,000 - 25,000 years B.P.

By definition, during this period, large alpine glaciers formed and reached their maximum extent. In British Columbia, expansion of the glaciers apparently resulted in ice-sheet formation.

b) Vashon Stade $13,000 - <21,000 >15,000$ years B.P.

By definition, the Vashon is the last major climatic episode during which drift was deposited by continental ice originating in British Columbia, and occupying the lowlands of southwestern B.C. and northwestern Washington.

c) Everson Interstade 11,000 - 13,500 years B.P.

This period began with the invasion of the lowlands by the sea, and ended with either the advance of the Sumas ice sheet or, the withdrawal of the sea and the disappearance of the floating ice.

d) Sumas Stade 9,500 - 11,000 years B.P.

A climatic episode during final stages of emergence of the Fraser Lowland when a valley glacier occupied the eastern part of the lowland. This glacier may have been only a local advance of the Cordilleran ice sheet.

The valley glaciers widened and deepened trunk valleys to a U-shaped cross-section leaving truncated spurs, hanging valleys and scoured rock surfaces. A result, perhaps not immediately evident, was the over-deepening of many of the valleys. For example, the maximum depth in Jervis Inlet is 385 fathoms (705 meters) and occurs about 10 nautical miles (18 kilometers) from the mouth, just north of Nelson Island. This depth exceeds by 178 fathoms (326 meters), the maximum depth in the Strait of Georgia. The valley glaciers which flowed into the Strait of Georgia coalesced and flowed south and southeast down the Strait then southwest to west across the end of Vancouver Island.

The ice sheet which accumulated during the Vashon attained an estimated thickness of from 5,000 to 8,000 feet (1500 to 2400 meters). The weight of the ice sheet depressed the land surface with respect to sea level. The net effect on the crust of unloading, due to the waning of the ice sheet, was the emergence of the land surface. The height of emergence, as measured from raised beach deposits, in the vicinity of the mouth of Jervis Inlet was 424 feet (129 meters) at Texada Island

and 500 feet (152 meters) at Campbell River. (Holland,1964). With the retreat of the Cordilleran ice sheet, the heavily scoured and probably nearly sediment-free inlets became depositional basins for glacial and glaciomarine sediments.

II. Original of Fjords

The structural pattern of the B. C. coastline has two components--one dominant and forming a crudely rectangular network in the north-west and north-east directions, and the other subordinate in the north and east directions (Peacock 1935). The former is concordant with the north-westward trending grain of the coastline and is thought to have originated from Jurassic tectonism. The subordinate trend is thought to have resulted from early Tertiary tectonism (Peacock 1935).

A majority of the inlets have abrupt high angle changes in strike of their axes-a feature explainable by structurally controlled fluvial erosion. Rejuvenation of the earlier Pliocene erosion surface during the late Pliocene created a deeply dissected and immature topography before Pleistocene glaciations. Thus fjords are the drowned lower parts of immature valleys developed by fluvial erosion and modified by intense glacial

action (Peacock, 1935).

Characteristic of fjords is extensive over-deepening and general presence of one or more thresholds or sills along their length. Over-deepening is apparently related to glacial erosion but the origin of the sills is debatable. Some sills are resistant granitic rock which for part of their length rise above sea level as islands or extend the shoreline to create a narrows. Sills formed intermediate along the length of many inlets are thought to represent terminal moraines deposited at points of furthest advance of valley glaciers.

III. Regional Geology

The reconnaissance map of upper Jervis Inlet by LeRoy (1908) shows Queen's Reach and Princess Royal Reach to be incised in a roof pendant of pre-Coast intrusive rocks. LeRoy stated these rocks were Paleozoic but James (1929) considers them early Mesozoic. LeRoy recognized two pre-Coast intrusive rock units consisting of a sequence of igneous rocks which he correlated with similar rocks on Texada Island (the Texada Group) and a series of sedimentary rocks correlated with rocks at Britannia Beach (the Britannia Group). LeRoy

found the Britannia Group rocks to be by far the most abundant in the upper Jervis Inlet area. The Texada Group outcrops near sea level in a narrow band along the north-east shore of Queen's Reach between Malibu Rapids and the head of Jervis Inlet. James' (1929) work on the Britannia Beach area shows a sequence of volcanics and sediments which he correlated with LeRoy's Britannia Group. Bacon (1957) combined the Texada and Britannia Groups of LeRoy with two other rock units and used the term Jervis Group to include all rocks of pre-batholithic age.

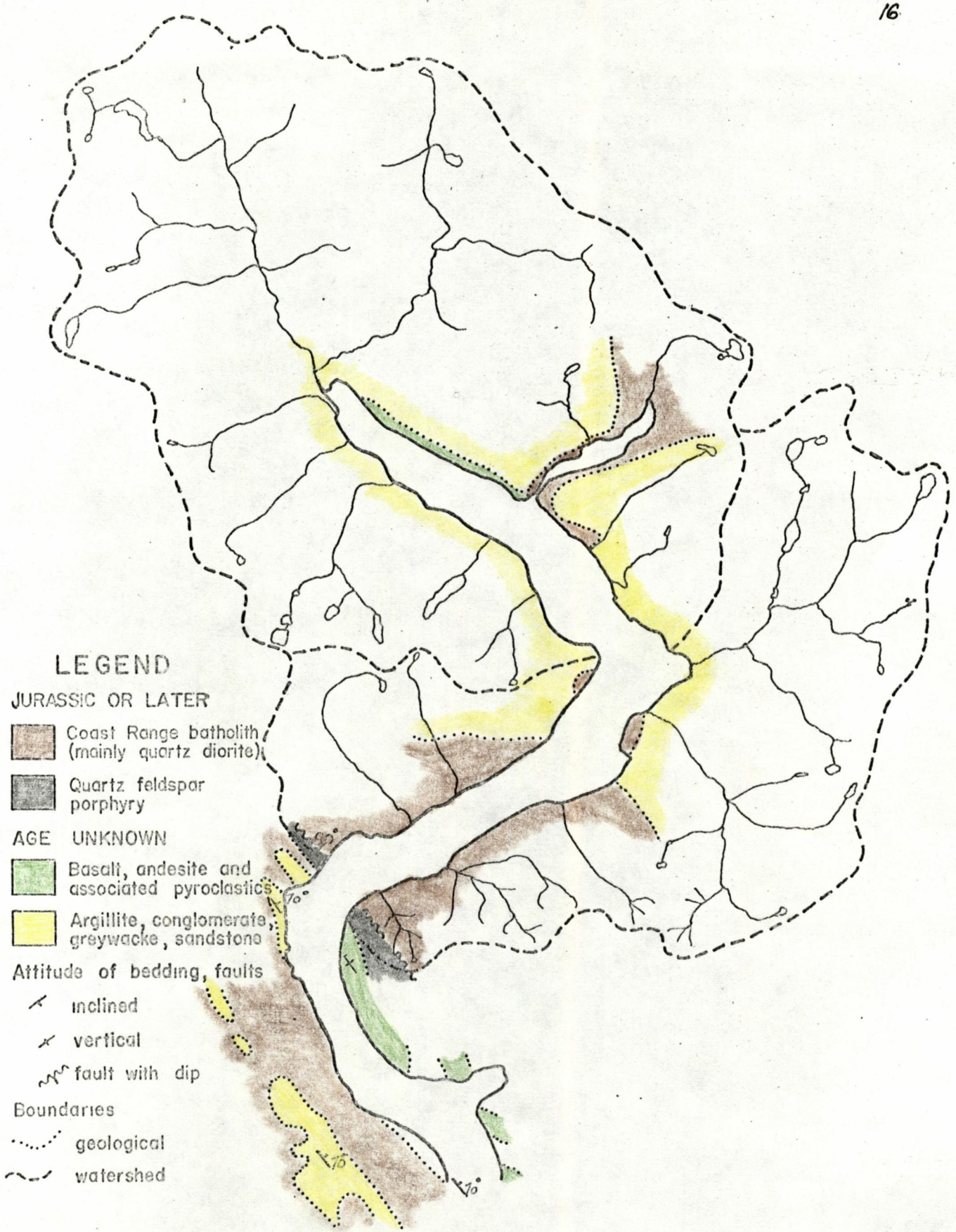

FIG. 2 MIDDLE AND UPPER JERVIS INLET

SHOWING GEOLOGY AND DRAINAGE PATTERN

GEOLOGY AFTER BACON (1957) AND LEROY (1908)

Table 2 Table of Map Units
(after Bacon, 1957)

Age	Map Unit		Description
Jurassic or later	Coast Intrusions	8	mainly coarse grained hornblende granodiorite
		7	medium grained biotite granodiorite
		6	main batholithic mass; quartz diorite, granodiorite
		5	quartz feldspar porphyry
Intrusive Contact			
Age Unknown	Jervis Group	4	basalt, andesite and associated pyroclastics, minor limestone, dolomitic limestone, chert, argillite
		3	mainly conglomerate, greywacke, sandstone, argillite, greenstone
		2	metavolcanic rocks, metasedimentary rocks, metadiabase
		1	Gneiss

Discrepancies exist where the pertinent areas of geologic maps by Bacon (lower Jervis Inlet) and LeRoy (upper Jervis Inlet) overlap. However, a tentative map of the geology of middle and upper Jervis Inlet was compiled (Figure 2) using Bacon's

nomenclature. Judging from rock specimen descriptions given by both authors, LeRoy's Texada and Britannia Groups are approximately equivalent to Bacon's map units 4 and 3 respectively.

Figure 4 a 1/6 square meter Petterssen grab sampler ready to be lowered

b Edgerton, Germeshausen and Grier underwater camera assembly. Not visible in picture is the compass and vane which is suspended beneath the camera.

c Rigging a Phleger corer just prior to lowering. The triangular-shaped part with arm is a bottom contact trip.

CHAPTER 3

METHODS OF STUDY

I. Field Methods

1) Positioning

The sample localities were chosen beforehand and plotted on a large-scale chart of the area. Positioning was done by combined use of echo sounder and Decca radar. Since the inlet is narrow and very steep-sided in most instances, radar was used to good advantage. However, when more accurate positions were desired so that a station could be reoccupied, the position was taken by sextant. Sampling station locations are show in Figure 3 (in pocket).

2) Sample Collection

Samples of surficial sediments were collected by use of a Petterssen grab sampler (Figure 4a) which sampled an area of 5.9 square feet (1/6 square meter). The awkwardness of this sampler, due to its weight, was more than compensated for by its reliability, especially when sampling the deep basins or precipitous sides of the inlet. The usually gelatinous block of sediment recovered was broken open and the laboratory sample was taken from the relatively undisturbed interior. This sample was placed in a one-quart plastic container and sealed with plastic

a

b

c

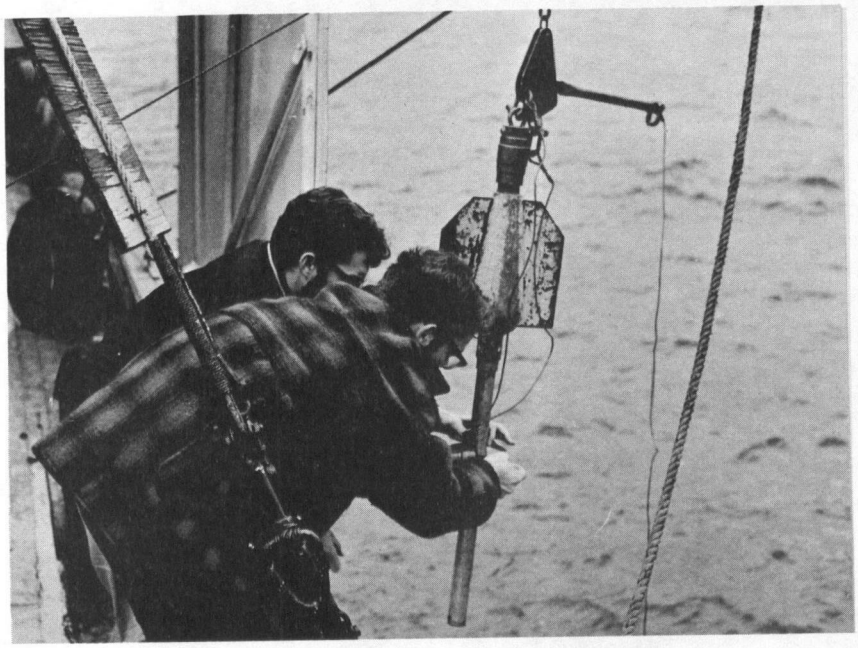

FIGURE 4

electrical tape. The remainder of the sampler contents was discarded. However, if the sample contained coarse sand or greater-sized material, the remainder of the sample was seived with a 10 mesh (2 mm) seive and the +10 mesh material was also collected.

Gravity cores were taken along the axes of the basins using a 1¼" (3.2 cm) diameter Phleger corer (Figure 4c) and a 2 3/8" (6 cm) diameter gravity corer. In both instances the sample was retained within a clear plastic barrel liner which was removed from the corer, capped and used for sample storage. Experience showed it was advantageous to use both corers in the free-fall mode rather than with a bottom contact tripping device. The corer was lowered until the meter block indicated the cutting edge was about 12 feet (4 m.) above the bottom. The winch was then stopped, taken out of gear and allowed to"free-wheel". Adequate penetration was achieved using a minimum number of weights.

3) Photography

Underwater photographs were taken at selected stations using an Edgerton, Germeshausen and Grier photographic assembly (Figure 4b). This consists of an automatically timed 35 mm. camera and a 110 joule strobe flash housed in identical but separate stainless

steel pressure resistant cylinders. Both cylinders are mounted on a frame - the camera in the vertical plane and the strobe flash angled so the intersection of the axes to the two units occurs at the focal point of the camera. Once started, the unit takes one picture every 12 seconds until the battery is drained, the film is consumed, or the unit is raised to the surface and stopped by disconnection of the synchronizing or power lead. Generally, 100 foot rolls of Kodak Plus-X film with an ASA rating of 125 were used. With the camera focused at 6 feet (1.8 meters), the optimum diaphragm opening was found to be f8 - f11. A compass was hung from the frame in the camera field. The compass needle is usually visible in the photograph (sometimes special processing is required). The compass assembly includes a 10 inch (25 cm) vane, which, by proportioning, can be used to determine scale as well as to indicate current direction.

At the time the photographic stations in Jervis Inlet were occupied, the assembly was positioned at the correct distance off the bottom by trial and error. The assembly was followed by echo-sounder until near the bottom.

When 3 to 6 fathoms off bottom, the rate of lowering was decreased until the bottom was touched by the legs of the frame. This touchdown could be detected at the winch. The assembly was then raised to the desired height off the bottom. This procedure was repeated every 5 to 10 minutes while on station. Useable pictures were obtained but the success ratio was only about one frame in twelve and sometimes one in twenty depending on the depth of operation.

Subsequently, a bottom-finding pinger has been included in the assembly. An omnidirectional transducer pings at a set rate thus allowing the distance from the assembly to the bottom to be measured from the difference in arrival times between the direct pulse and the reflection of the pulse from the bottom. The use of this pinger on other projects resulted in an increase of the success ratio to one frame in five or sometimes ~~less~~ better.

The films were processed commercially after the cruise returned. Lack of space, time and necessary equipment aboard ship precluded on-the-spot processing, which however, would have been advantageous.

4) Echo Sounding and Continuous Seismic Profiling

The bathymetric map of Jervis Inlet (Figure 6 - in pocket) was drawn from the Canadian Hydrographic Service Field Sheet No. 2228-L entitled "Jervis Inlet -- Northern Portion". However, a more detailed survey was made of the manganese concretion locality. Five lines were run transverse to the axes of the inlet over Patrick Sill. These were tied in by four lines run consecutively on a rectangular pattern. A 38 KHz Kelvin-Hughes sounder gave good records, even though the subsurface topography was steep. Positions were plotted every two minutes by Decca radar. This data was corrected and combined with data from the Field Sheet in order to compile a large-scale bathymetric map of Patrick Sill (Figure 37 - in pocket).

During I.O.U.B.C. Cruise 66/1, a continuous seismic profile was made from the head to the mouth of Jervis Inlet (Tiffin and Murray, 1966). The 5000 joule seismic profiling equipment consisted of Edgerton, Germeshausen, and Grier power supply, capacitor banks, and trigger, coupled to a "spark-array" transducer. Echos were picked up by hydrophone, amplified, filtered, and then recorded by an Alden wet-paper Precision Graphic Recorder.

II. Laboratory Methods

1) Grain Size Distribution in Sediments

The procedure for processing a sample is illustrated in Figure 5. Each sample was kept frozen until analyzed. To begin, the sample was first thawed and then homogenized by stirring. Three sub-samples were taken by means of a 5/8 inch (16 mm) inside diameter glass tube with a tapered cutting edge. The sub-sample was extracted by rotating the tube and applying a slight vacuum by mouth to the free end. As the tube was pushed into the sediment, the level of the sediment within the tube was kept the same as that surrounding. In this way, any biasing of grain size parameters etc. by sub-sampling techniques was hopefully minimized. The sub-samples for clay mineral analysis and total carbon content were air-dried. Carbon analyses were made using a Leco induction furnace and CO_2 absorption system.

Grain size analyses were made by dry sieving for the $> 63/u$ material and by hydrometer for the $< 63/u$ material. Before sieving, the $> 63/u$ material was given successive treatments with hydrogen peroxide in order to dissolve organic components. This step was included as the concentration of organics was sufficient to prevent disaggregation

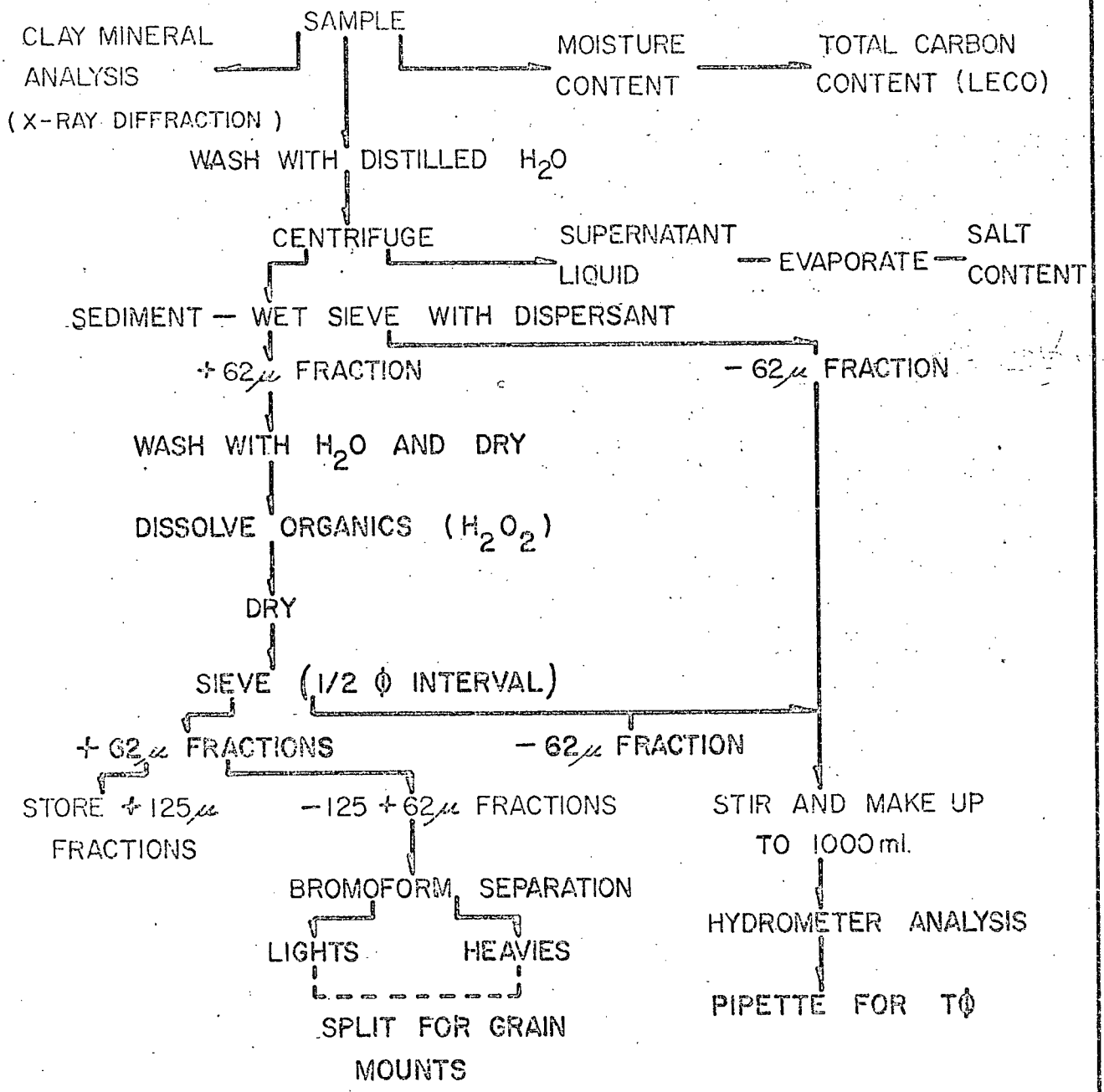

FIG. 5 PROCEDURE FOR SAMPLE ANALYSIS

especially if the sediment was dried. Grains with a diameter of $< 63/u$ derived from seiving the coarse fraction were added to the sedimentation cylinders before the hydrometer analyses were made.

Hydrometer analyses were conducted according to ASTM specification (ASTM D422-61T) using a 152H hydrometer. The initial weight of the sub-sample for grain size analysis was estimated so the $<63/u$ material would weigh from 10 to 15 grams. Preliminary analysis indicated this weight of material in suspension gave optimum results. All hydrometer analyses were done at 84°F (30°C) because room temperature was not likely to exceed this temperature. The constant temperature bath used maintained the set temperature as long as this was above ambient. However, the bath had no direct means of cooling if ambient exceeded set temperature.

Initially, the times at which hydrometer readings should be made to derive a weight distribution in even ϕ values (i.e. 4.5ϕ, 5ϕ, 6ϕ, etc. where $\phi = -\log_2$ grain diameter in mm.) were taken from a chart calculated for the settling velocities of quartz spheres. However, these times did not give the weight distribution in even ϕ values for the material being

analysed. Through a series of successive approximations, appropriate reading times were calculated.

The total weight of sediment in the -63/u fraction (tØ weight) was difficult to determine by hydrometer. Thus when a hydrometer analysis was complete, the sediment was stirred back into suspension, and the tØ weight was determined by immediately pipetting off 50 ml of suspension.

2) Mineralogy of Sediments

Mineral analyses were carried out on select samples taken from the axes of the basins. The 63/u to 88/u and the 88/u to 125/u seive samples were combined and then a heavy mineral separation was made using bromoform. Thin sections were made of both the light and heavy fractions and the mineralogy was determined petrographically by point-counting.

The clay mineral analyses were conducted on separate sub-samples of the main sample. The size fractions were separated according to the procedure described by Kittrick and Hope (1963). X-ray diffraction analyses were carried out on the 20 - 5/u, 5 - 2/u, and $< 2/u$ fractions. The $< 2/u$ fraction was given a series of treatments to aid in

identification of the clay minerals present. These were K saturation, K saturation heating to 300°C, K saturation heating to 500°C, Mg saturation and Mg and glycerol saturation, The iron extracted in preparation of the clays for X-ray analysis was determined by atomic absorption spectrophotometer.

3) Gravity Core Analyses

The large diameter gravity cores were split by using a circular saw to cut the core barrel and a piece of thin piano wire to cut the sediment. Structures in the sediments were revealed by running a stream of water down the cut face. No analyses were carried out on the sediments due to time limitations. The cores were sealed in containers for future reference.

4) Composition, Structure and Abundance of Manganese-Iron Concretions

The elemental composition of the manganese concretions was determined by Dr. E. V. Grill of the Institute of Oceanography at the University of British Columbia (Grill, Murray and Macdonald 1968). The Special Projects Division of Bear Creek Mining Company Ltd. and the B.C. Department of Mines carried out independent analyses. The mineralogy of the concretions was determined by X-ray diffraction.

Polished sections of the concretions were made for reflected light studies and photographic purposes. To make the sections, the concretions were first impregnated due to their very friable nature. Impregnation was carried out in a vacuum dessicator using Castolite resin. The proportions of resin to thinner to hardener used were in the ratio of 24 mls. to 8 mls. to 3 drops. A curing time of 24 hours in an oven at 80°C was used. The entire concretion was impregnated and then cut. A second impregnation was necessary before the cut surface could be polished satisfactorily. The final polishing was done on a diamond lap.

The estimate of the weight of dried manganese concretionary material per unit area was made from a typical 1/6 meter^2 (1.8 feet^2) Petterssen grab sample. The concretions recovered were dried and oxide materials were broken away from the nucleating rock fragments and weighed.

CHAPTER 4

OCEANOGRAPHY

I. Bathymetry

The study area encompasses two basins separated by a sill. The upper or more northerly basin coincides with Queen's Reach, while the lower coincides with the upper two-thirds of Princess Royal Reach.

The bathymetric map is presented in Figure 6 (in pocket). The sill depth of the upper basin is 160 fathoms (290 meters), while that of the lower is 220 fathoms (400 meters). The maximum depths are 190 and 290 fathoms (348 and 530 meters) respectively. The slope along the basin axis at the head of the inlet measures $1^{o}50'$, but rapidly increases to $10^{o}36'$. Beyond Station J-102, the slope slowly decreases to an average of $0^{o}14'$ for the remainder of the length of the upper basin. The slope of the bottom of the second basin is approximately $0^{o}02'$. The south-facing flank of Patrick Sill dips at $18^{o}30'$ on the axial line but the angle increases towards the inlet sides.

Transverse sections (Figure 7) illustrate the modified catenary or U-shaped cross-section which is typical of glacially-scoured valleys.

In the upper basin, the 160 fathom (293 meter) contour marks the approximate break in slope between the sides and bottom of the inlet. In the lower basin, the break in slope occurs at 280 fathoms (513 meters). The slope of the inlet sides ranges from 10^{o} to 47^{o} and probably averages about 35^{o}. Echo and wire soundings at Station J-160 indicate a very steep slope. The echo-sounder recorded a depth of 200 fathoms (366 meters), while a wire sounding gave a depth of 292 fathoms (534 meters). Pickard (1961) noted from transverse sections that a flat bottom was characteristic of the upper basin and was most pronounced just inside the sill at the deepest portion of the basin. From this and other data (i.e. optical turbidity), Pickard postulated the existence of turbidity currents within the upper basin. Also noticeable on the sections is the transverse asymmetry of the inlet at sea level and below.

The bathymetric map of Upper Jervis Inlet shows several banks within the upper basin, while none appear within the lower basin. These features are found along the margins of the inlet. Also noticeable is the biconcave or venturi shape of

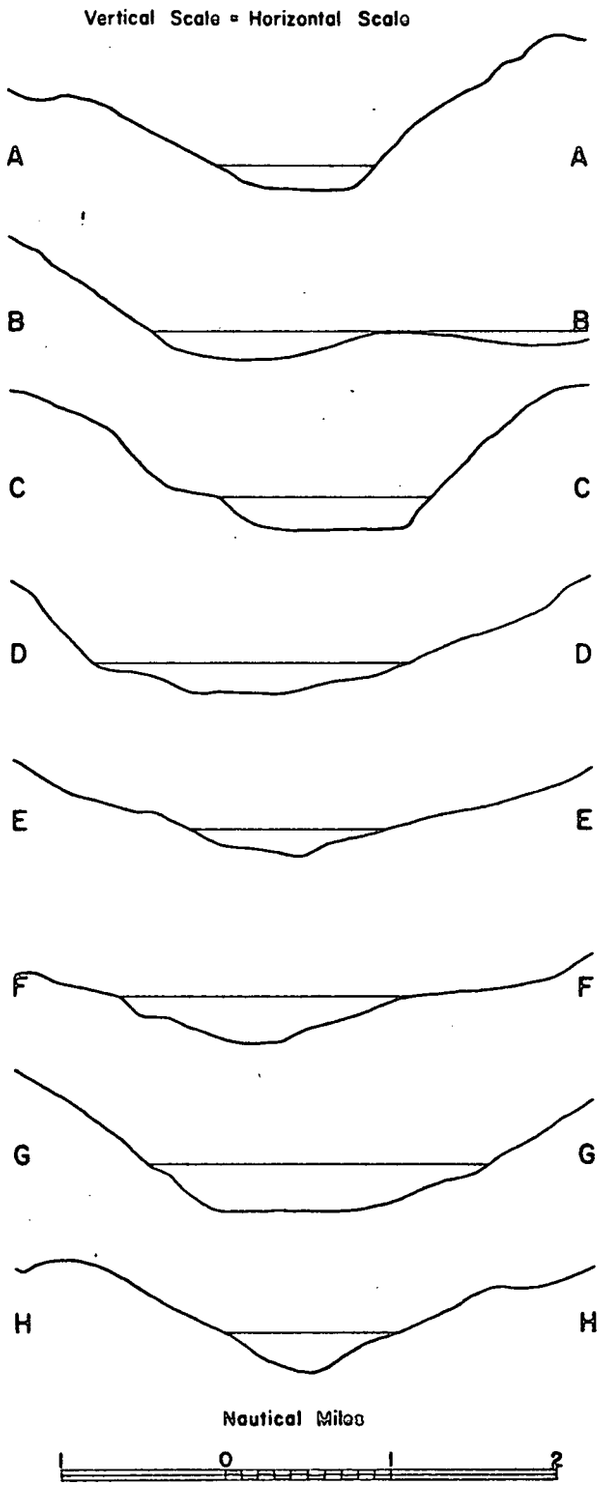

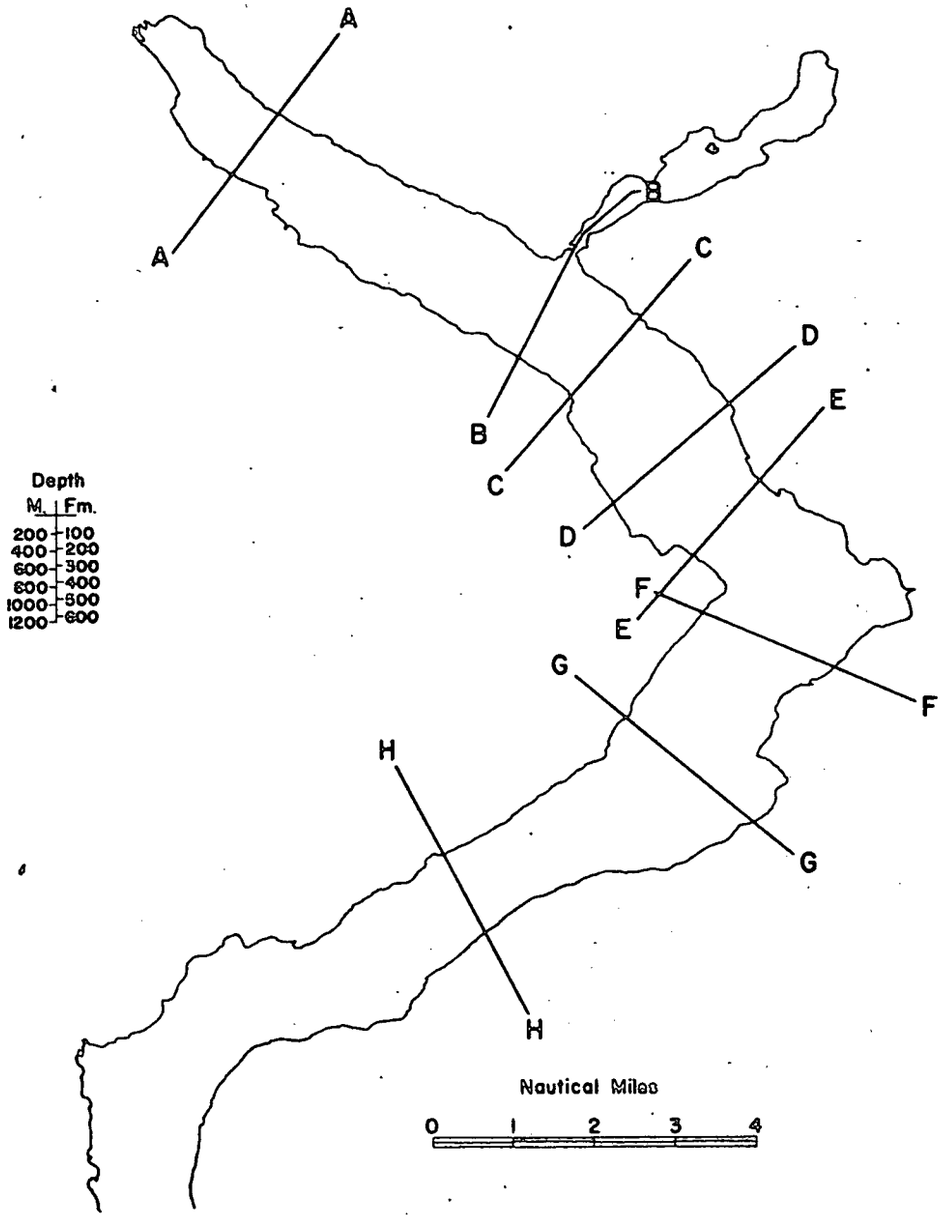

FIG. 7 TRANSVERSE SECTIONS

Patrick Sill. A section transverse to the basin axis through Patrick Sill reveals a distinct medial depression or "V" notch. The origin of these features will be discussed later.

II. Temperature and Salinity (after Lazier, 1963)

The average vertical profiles of temperature and salinity for Jervis Inlet in March 1962 are given in Figure 8. These represent more or less stable conditions during the year Lazier studied the inlet circulation (March 1962 - March 1963).

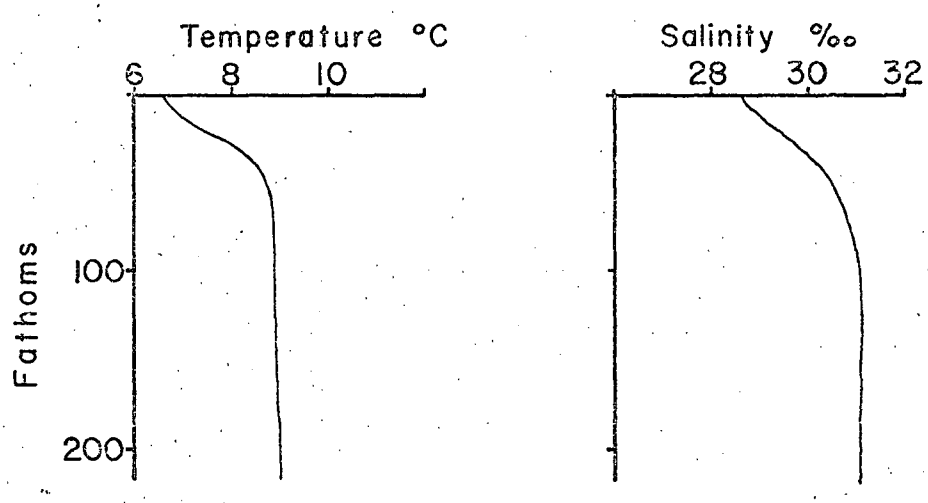

Figure 8 Average Vertical Profiles of Temperature and Salinity for Jervis Inlet during March 1962
After Lazier, 1963

The average salinity-depth profile indicates that over most of the inlet there is a lack of a homogeneous surface layer of low salinity and thus there is no distinct halocline. The salinity increases from the surface to depth with a decreasing rate. Surface water salinity reaches 50% of the deep-water salinity at a depth of about one fathom, and 90% of the deep-water salinity within a depth of between 4 to 11 fathoms.(Pickard 1961).

The average temperature-depth profile resembles the salinity-depth profile. However, as the mean daily temperature increases with the advent of summer, the surface waters warm considerably resulting in the formation of a temperature minimum at about 15 fathoms. This minimum remains in evidence until October. At this time the decreasing surface temperature results in a temperature maximum at about the 15 fathom depth.

III. Oxygen Content and Circulation (after Lazier 1963)

Jervis Inlet is classed as a deep-silled inlet in that the sill at the mouth is of sufficient depth so that tidal waters may enter and leave without unduly modifying the vertical stratification of the resident inlet waters. Flows may occur

in both directions simultaneously.

Since the surface runoff into Jervis Inlet is small, the estuarine circulation is generally weak. Changes in meteorlogical and oceanographical conditions in the area will produce flows which will dominate the estuarine circulation.

Oxygen profiles display most distinctly the circulation within the inlet.(Fig.9) Lazier described a mid-depth oscillatory flow of unknown period which occurred during the winter of 1963-63. A possible mechanism for this flow is described by Lazier as follows:

> "It was proposed that strong southwesterly winds in the autumn, particularly those associated with Typhoon Frieda, caused the water level within Jervis Inlet to rise. To compensate for the increase in water volume, a mid-depth outflow was created. This outflow produced a horizontal pressure gradient that tended to reverse the direction of the flow. When the flow reversed, the water level in the inlet again became greater, and the surface outflow increased. A negative correlation between the direction of the mid-depth flow and the depth of the surface layer was noted.
>
> The low oxygen content in the water at mid-depths near the head of Jervis Inlet was attributed to weak estuarine circulation which results in slow removal of water near the head."

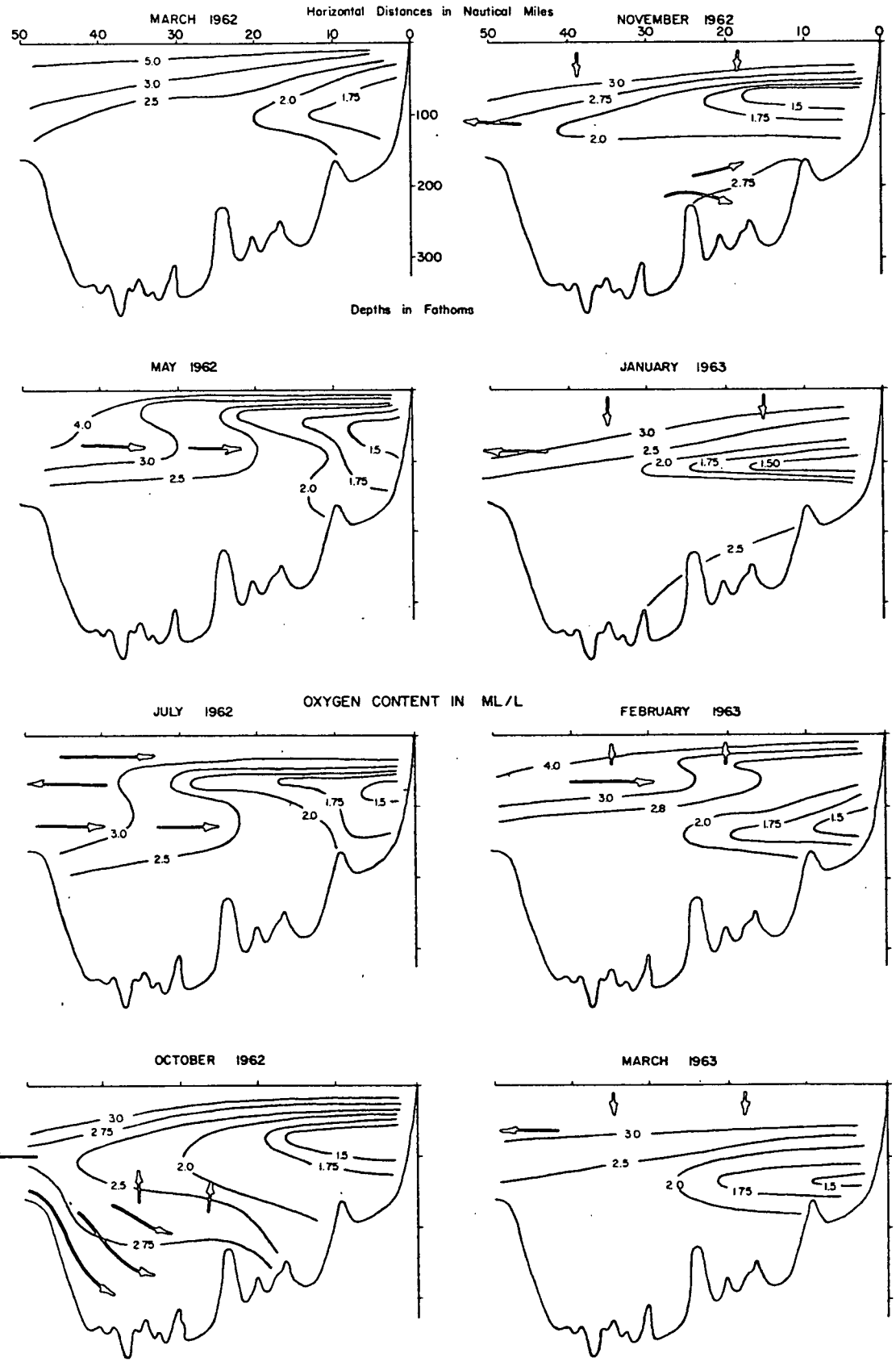

FIGURE 9 WATER CIRCULATION AS INDICATED BY LONGITUDINAL OXYGEN PROFILES AFTER LAZIER, 1963

IV. Tides

The British Columbia coast is subject to semi-diurnal tides which have marked irregularities between the heights of successive low waters. The time of either high or low water at the heads of the inlets is not more than ten minutes later than at the mouth. The range at the head is from 1 to 10 per cent greater than at the mouth (Pickard,1961).

Current directions were calculated for the manganese locality (Station J-19-67) by use of the compass which hangs in the field of view of the underwater camera. The directions indicated coincide with the direction of the surface tidal flow i.e. northwest on a flood tide and southwest on an ebb tide. Measurements were made when the compass was 1 to 2 feet from the bottom.

V. Optical Turbidity (after Pickard and Giovando, 1960)

Figure 10 illustrates measurements of optical turbidity made in Jervis Inlet on two occasions - February 1958 and June 1958.

A light-scattering method of measurement was used and values of optical turbidity represent fractional reduction in light intensity per meter length due to scattering. Data indicates that the majority of suspended material was minerogenic,

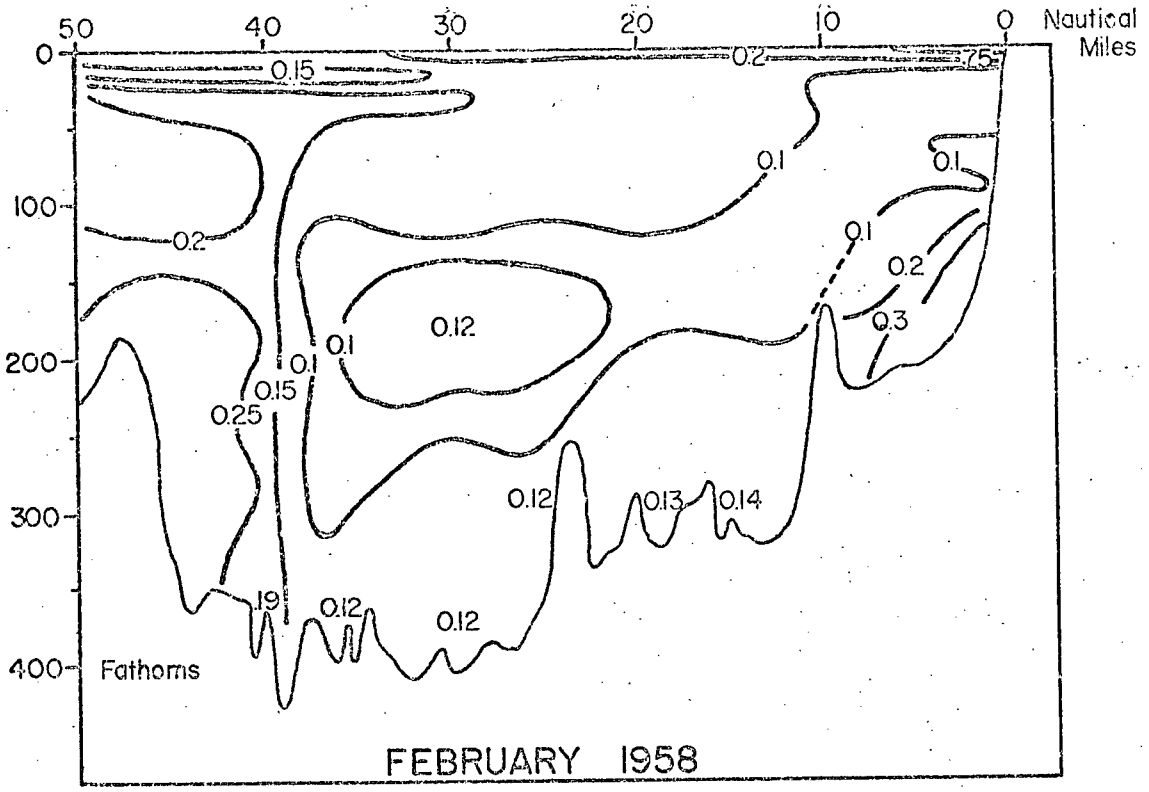

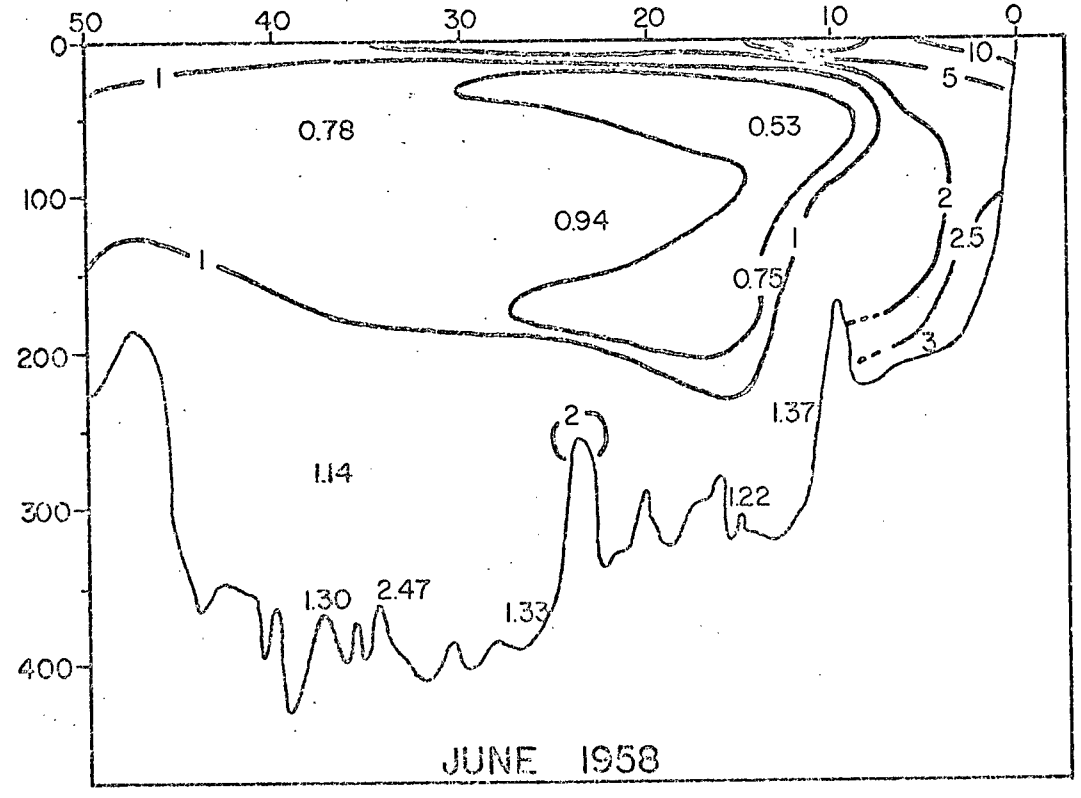

FIG. 10 OPTICAL TURBIDITY ALONG JERVIS INLET

relatively transparent, and optically anisotropic. Also indicated was the presence of white opaque particles or transparent material with multiple internal reflecting surfaces. In the surface water samples collected in June, the diameters of the suspended particles ranged from 0.75 to 49 μ with a geometric mean of 16.7 $\pm$ 1.5 μ. Inorganic materials accounted for 99 per cent of the total. Samples collected in February contained particles with diameters ranging from 0.5 to 15 μ having a geometric mean of 7.3 $\pm$ 1.5 μ. In these, inorganic materials accounted for 90 per cent of the total. Pickard suggests, as a bold estimate, a sedimentation rate of 35 cm. per 1000 years.

Current measurements made in Knight Inlet (Pickard and Rodgers, 1959) show that at a distance of 27 fathoms above the bottom in 190 fathoms of water, there exists a current of tidal period of a few centimeters per second. Thus the increase in turbidity in the bottom waters of Queen's Reach, as illustrated in Figure 10, may be due to a similar current reaching the bottom sediments. As an alternative, Pickard postulates the existence of turbidity currents.

CHAPTER 5

BASIN STRUCTURE AND SEDIMENT THICKNESS

Figure 11 is a tracing from a continuous seismic profile made by Dr. J. W. Murray and Dr. D. L. Tiffin of the Institute of Oceanography, University of British Columbia. The course along which the profile was taken appears at the lower left hand corner of the figure, and also on Figure 3 (in pocket) with positions of sample stations.

The "Spark-array" transducer produces an acoustic pulse by means of an instantaneous arc discharge underwater. The arc creates a plasma bubble, which rapidly expands and then collapses. The outgoing wave form consists of several peaks, and therefore, on the seismic record,a reflecting layer will appear as a closely spaced series of lines rather than one. Return or reflected energy is filtered and only that with a frequency in the 40 to 200 Hzrange is recorded. Use of low frequencies results in good penetration but poor definition. Tiffin (oral comm,1969) estimates that a horizontal layer must have a minimum thickness of about 5 fathoms (9 meters) before it can be detected. On a slope this minimum thickness increases.

The slow firing rate of the transducer (one or more seconds per pulse depending on depth and energy/pulse) results in a record on which the vertical scale is greatly exaggerated and apparent angles are much steeper. The vertical scale on the recorder is calibrated with respect to the speed of sound in sea water (about 4800 feet/second). However, the speed of sound in Recent and Pleistocene sediments varies from about 4800 to 7800 feet/second. (Dobrin, 1960). Therefore sediment thickness taken from a seismic record must be multiplied by the ratio of the speed of sound in the material/4800 for correction.

The record presented in Figure 11 may be confusing because many underwater peaks are evident. However, since the course followed was a zig-zag pattern, many of the apparent peaks result from approach to and turning away from the shoreline. Also, as the ship's speed was not constant, the horizontal scale is variable.

Noticeable in Figure 11 is the relatively uniform sediment thickness in the basins. With the exceptions of the very thick accumulation off Malibu Rapids, sediment thickness in the upper

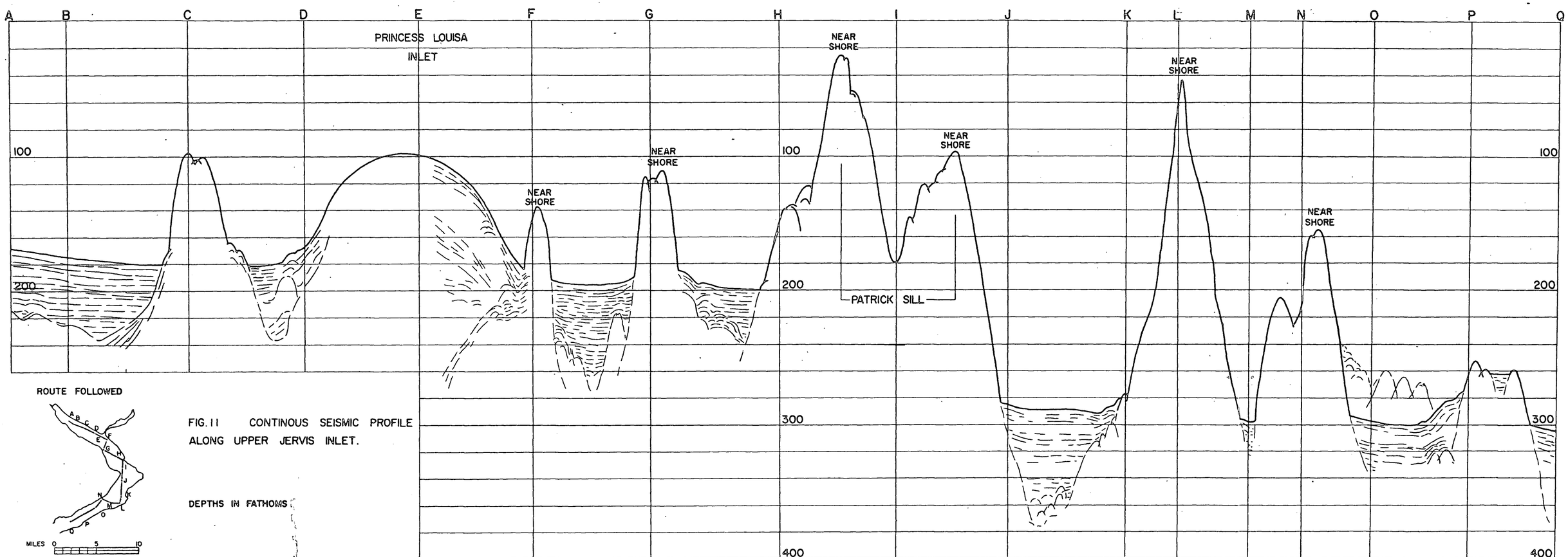

FIG. 11 CONTINOUS SEISMIC PROFILE ALONG UPPER JERVIS INLET.

DEPTHS IN FATHOMS

basin averages about 480 feet or 146 meters (assuming an average speed of sound to be 7000 feet/second). The thicknesses range from 480 feet (146 meters) for section B-C to 672 feet (205 meters) for section F-G and 336 feet (102 meters) for section G-H. The increase in thickness in section F-G is probably due to addition of material from the delta at Malibu. In the lower basin the average sediment thickness is 720 feet (220 meters).

Reflecting horizons within the sediments are thought to represent bedding planes. On the slope at the head of the inlet the more recent beds dip gently to the southeast (i.e.down the inlet). These beds appear to overlie flat-lying basal sediments, apparent in section B - C of Figure 11. Unfortunately, only the base of the slope was covered by the seismic line and therefore the extent of the unconformity is not known. If the unconformity is traceable to the inlet head, perhaps it represents the overlapping of recent sediments deposited by slumping on sediments deposited during shelf ice conditions.

Determination of sediment thickness on slopes such as the inlet walls and the sill cannot be made

because of record distortion inherent in the use of a low frequency and wide beam angle transducer. However, the action of the grab sampler as detected by hand on the winch cable and the damage done to the grab while sampling the inlet walls and V-notch of the sill, indicate that the sediment cover is often thin and sometimes lacking. Also, one of the underwater photographs (Figure 29a) taken in the concretion locality shows what is likely bedrock but possibly a large glacial erratic. Iron crusts (Figure 44) and sponges recovered from this locality appear to have been broken off rock faces. Although little or nothing can be determined about actual sediment thicknesses which have accumulated on slopes, or in the V-notch, some doubt is cast on the terminal moraine origin of sills.

Patrick Sill and other similar sills have usually been regarded as terminal moraines originating from ice advance during the Sumas Stade. The concavo-convex shape of some sills (ecg.the inner sill of Howe Sound) tend to support this explanation. However, little is known about the extent of Sumas Stade glaciation except for the advance in the Sumas area of the Fraser Valley. Evidence suggests Patrick Sill is not a terminal moraine but a bedrock feature

covered, for the most part, by a sediment veneer of varying thickness. Several exposed sills are bedrock features and their position with respect to former ice flow channels offers a possible explanation for their formation.

Major sills are generally located at points where valleys which confined the ice suddenly widen or, in the valleys of smaller glaciers where these met trunk glaciers at or near right angles. The sill creating Malibu Rapids is an example of the latter. At this point a smaller glacier would have coalesced with a much larger ice mass moving at right angles. At the point where coalescence of the ice masses occurred, the downward erosive capability of the smaller would likely be decreased resulting in a sill. The sill at Malibu is a bedrock feature and biconcave in plan view. Possibly glacial action only sculptured the sill and the basic control is structural.

Intense shearing at the point of coalescence of the ice masses would also mean that as the ice masses began to waste, these areas would melt the most rapidly due to the greater surface areas exposed by fracture surfaces. In this way, depending

on sea level, the biconcave plan and especially the V-notch of sills may be accentuated as these areas would form sinks for the initially derived glacial debris. As wasting of the ice masses progressed, more and more of the released sediments would be deposited over the basin as a whole.

The bathymetric map of the study area (Figure 6) shows the presence of bank or ridge-like features along the sides of the upper basin. These features are not present in the lower basin. Even though seismic records are poor because of the slope involved, they indicate that the banks, like the sill, are bedrock features-possibly glacially sculptured granitic plugs within the roof pendant of shale. Several such plugs are known to exist along the shore of the upper basin as the contacts have been explored for economic minerals.

CHAPTER 6

SEDIMENTS

A sample recovered with a Petterssen grab sampler represents at least the top 20 to 30 centimeters of sediment, assuming the material has the consistency of a typical marine silty clay. If Pickard's estimate of 35 cm/1000 years for the sedimentation rate in Jervis Inlet is assumed correct, a grab sample could conceivably represent a section with an age span of about 550 to 850 years. While this is only an example, it does illustrate that parameters derived from laboratory analysis of sediment collected by grab sampler represent only a crude average taken over an indeterminable number of years. Interpretation based on these parameters should be made with this in mind.

The surficial sediments were classified texturally according to a scheme proposed by Shepard (1954). Basically, the sediments consist of equal parts of silt and clay-sized particles (Figure 12) with the amount of sand and gravel varying from 0.5 to 85 per cent. This characteristic is also noticeable in data presented by Cockbain (Cockbain 1963) for Vancouver Island inlets. Cockbain's data

FIG. 12 CLASSIFICATION OF JERVIS INLET SEDIMENTS ACCORDING TO GRAIN SIZE DISTRIBUTION

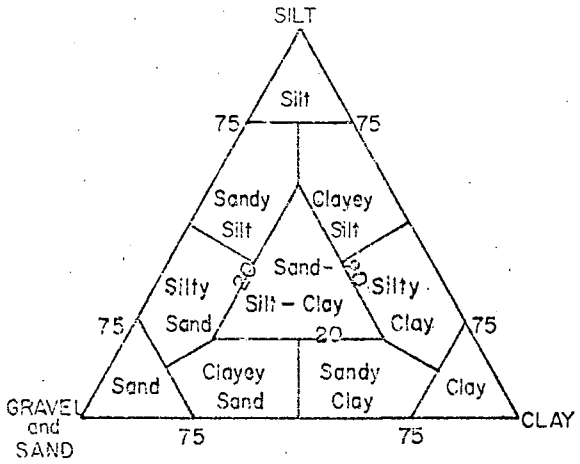

Depth less than 100 fathoms

Depth greater than 100 fathoms

GRAVEL and SAND

CLAY

for mainland inlets, plotted in the same manner, indicates a slight skewness towards clay-sized particles, with the average abundance of sand and gravel less than for Jervis Inlet. This difference may be a result of differences in sampling pattern and/or the below average sedimentation rate in Jervis Inlet.

Figure 13, showing sediment grain size distribution along the axis of upper Jervis Inlet is presented as a reference to the discussion of total carbon content, free iron content and mineralogy of the sediments. In each of the figures similar to Figure 13 the data being presented is superimposed on the bottom profile taken along the inlet axis.

I. Colour

The colour of the wet sediments is characteristic of the coastal marine province and varies from a greyish olive (10Y4/2) to an olive grey (5Y3/2). The sediments of the upper basin tend to be more lightly coloured (i.e. greyish olive) while those in the lower tend towards the darker olive grey colour. Samples collected along the axes of the lower basin from Station J-146 southward contained varve-like laminations of olive grey alternating

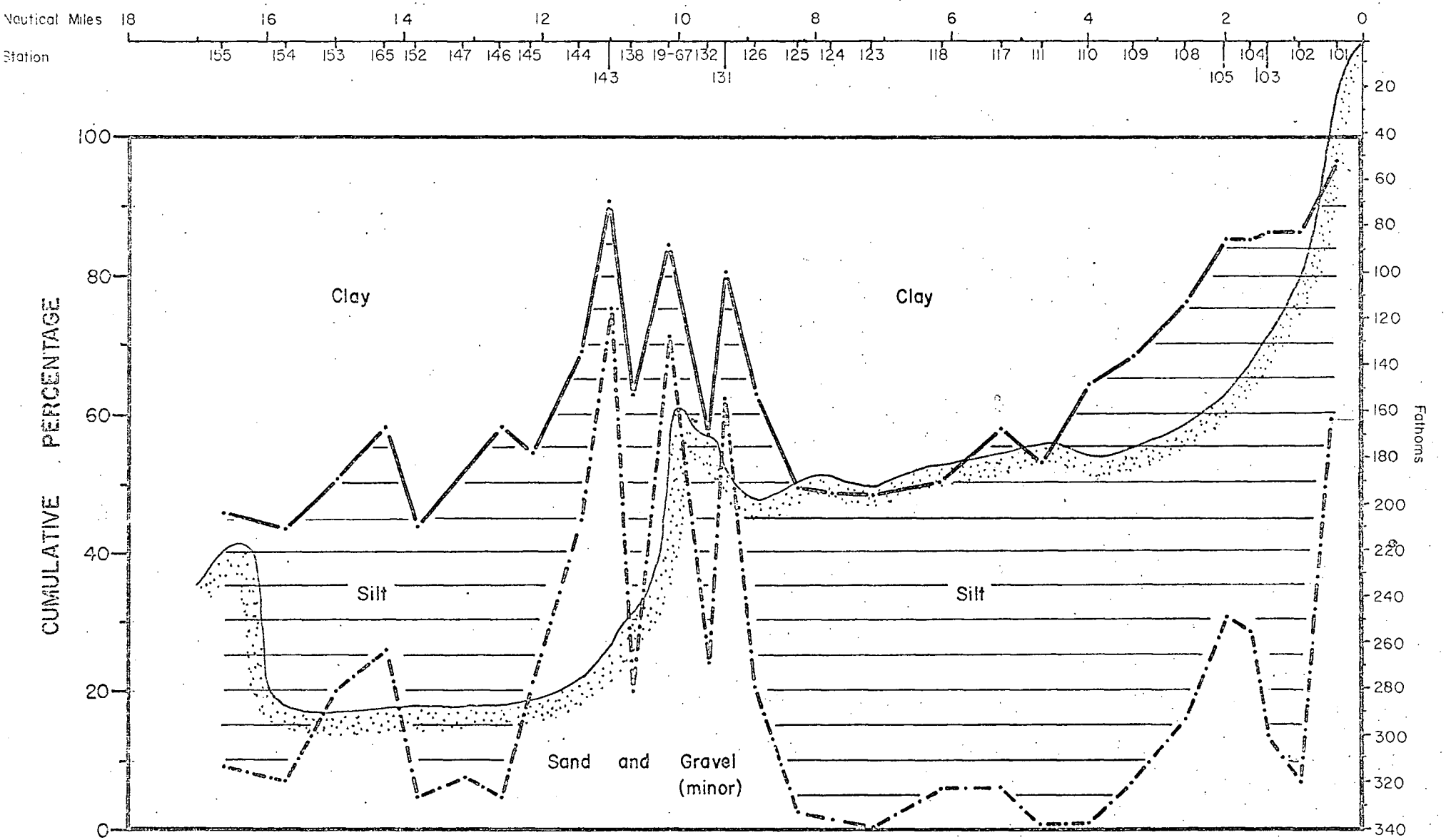

FIG.13 GRAIN SIZE DISTRIBUTION ALONG AXIS OF UPPER JERVIS INLET

with black material. These were the only samples within the lower basin to contain distinct concentrations of H_2S. Samples from the upper basin which contained noticeable concentrations of H_2S were collected nearshore in relatively shallow waters (Station J-101, J-102, and J-128).

Cores taken by Dr. E. V. Grill indicate the presence of a thin (approx. 0.5 to 1.5 cm) and very fluid, dark yellow-brown to red-brown oxidized layer which forms at the sediment-water interface over most of the study area. This oxidized layer is not noticeable in the grab samples except in those collected over the concretion locality. In this area, this layer thickens to several centimeters and includes within its depth a layer of coarse sand to cobble-sized material.

The olive-green colour of the wet sediments is thought to be due primarily to the organic content (Pantin, 1969). Reduced iron may add to the overall colour effect. Figure 16 illustrates the amount of iron extracted in preparation of samples for clay mineral analysis, and Figure 15 illustrates the total carbon content in these samples. Examination of these figures reveals a closer correlation between

total carbon content than extractable iron content with the darker colour of the sediments of the lower basin. When the samples are dried at room temperature, the colour becomes light grey to light green-grey.

II. Total Carbon Content

The total carbon content was determined for each of the surficial samples collected. Figure 14 (in pocket) shows the distribution of carbon content over the entire study area. Figure 15 shows the carbon content in comparison with the weight of clay size particles along a longitudinal profile. In order to convert a total carbon percentage into an organic matter percentage Trask recommends a multiplication factor of 1.8 (Trask, 1938).

Figure 15 shows the total carbon content to vary approximately as the weight of clay-size particles. This correlation is likely due to environmental energy factors. The organic material has a density near that of sea water with the majority of particles having an effective diameter in the silt size range. The result will be a very low settling velocity. Therefore, the maximum accumulation of organic debris will occur in the environment of

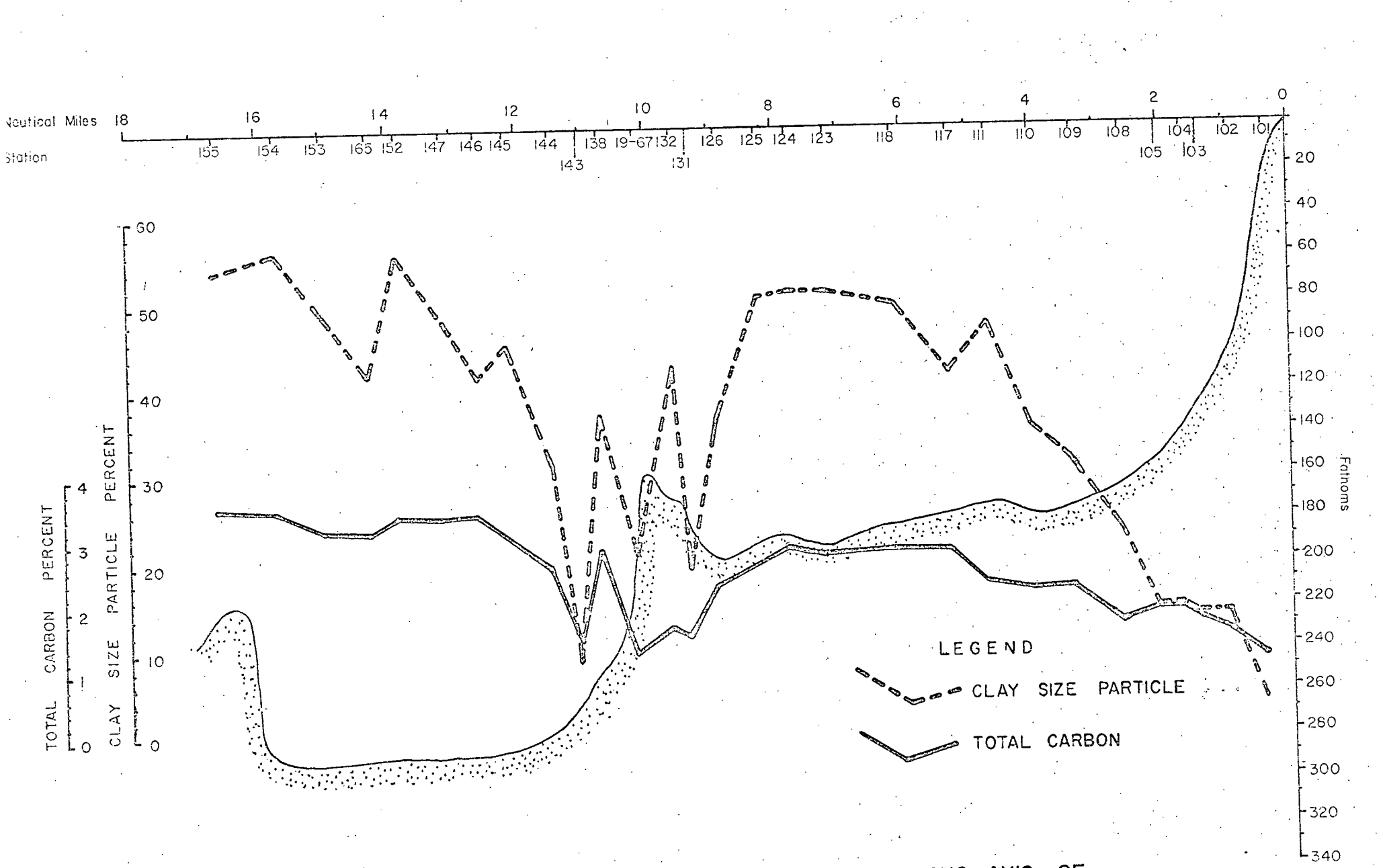

FIG. 15 CLAY SIZE PARTICLE AND TOTAL CARBON CONTENT ALONG AXIS OF UPPER JERVIS INLET.

minimal energy as will the finest of mineral particles. The trend in the total carbon content is a gradual increase with increase in distance from the head of the inlet. This trend is interrupted in the area of the V-notch of Patrick Sill as the notch represents a much higher energy environment than its surroundings. There are several possible explanations for the observed trend. Much of the organic debris is thought to originate from phytoplankton. Thus, a lower productivity of the surface waters over the upper basin would give the observed carbon distribution pattern. However, another and perhaps more plausible reason could be differing factors of dilution of the organic debris by sediment being added and deposited contemporaneously. Grain-size analyses and optical turbidity data indicate that the river at the head of the inlet is the prime source of sediment for upper Jervis Inlet. Most of the sediment is deposited in the upper basin, thus diluting the organic debris more in the upper than in the lower basin. The greater water depth through which the organic debris must settle in the lower

basin apparently has little effect on the amount oxidized before being deposited on the basin floor.

The difference in total carbon distribution between the upper and lower basins is best illustrated in Figure 14 (in pocket). Most noticeable is the relatively constant distribution in the upper basin versus the zonal distribution in the lower basin. Over a large part of the upper basin, the total carbon content is in the 2 - 3% range with exception of certain nearshore areas and the slope at the head of the inlet. Dilution and possibly lower productivity probably account for the low values at the head of the inlet. The localized, nearshore areas of higher carbon content coincide closely with log-booming grounds or streams which drain areas presently being logged. Considerable amounts of similar coarse organic debris are added from Princess Louisa Inlet to the delta on the Jervis Inlet side of Malibu Rapids.

The lower basin can be divided into three apparently distinct zones on the basis of carbon content. The nearshore zone has a low total carbon content ($< 2\%$) and is coextensive with the steep walls. The intermediate zone, with an average

carbon content of 2 - 3%, coincides with the break in slope between the walls and floor, while the deep zone, with a carbon content of 3 - 4% coincides with the basin floor. The higher values for samples collected within the bay along the southeast shore may be due to local addition of organic material by streams and/or increased productivity of the more sheltered surface waters.

III. Free Iron Content

In the preparation of a sample for X-ray diffraction analysis, it is necessary to remove free iron, the presence of which could cause fluorescence with resultant loss of sensitivity. The first stage of sample treatment was the dissolution of carbonate minerals by addition of pH5 ✱ sodium acetate (NaOAc). Organic materials were then destroyed by the addition of hydrogen peroxide (H_2O_2). Free iron was extracted by adding sodium dithionite to the heated sample to which a citrate buffer had been added, stirring every two to three minutes for a total of fifteen minutes. The supernatant liquid, as separated by centrifuge, was diluted to 1000 ml. and analyzed for iron by atomic absorption. However, the supernatant liquid derived from the organic

oxidation step was often coloured ranging from light greenish to distinct red-brown indicating the presence of iron. These solutions were saved and analyzed similarly to those from the sodium dithionite treatment. The results of the analyses are plotted in Figure 16 which shows the total free iron as a sum of that extracted by the two treatments. This procedure results in removal of only the adsorbed iron and will not destroy well crystallized iron compounds nor extract iron from interlayer positions that it may occupy in certain minerals such as chlorite.

The concentration of the iron extracted by sodium dithionite is relatively constant with distance from the head of the inlet, averaging about 0.35% (3500 ppm). The state of this iron in the sediments is probably as poorly crystalline particulate iron oxides and as iron adsorbed to clay minerals. A ratio of iron extracted by sodium dithionite to percentage of clay-size particles (all the samples had the same initial weight) indicates a pronounced decreasing trend from the head of the inlet. Work done by Dr. E. V. Grill on metal content of sea waters from upper Jervis

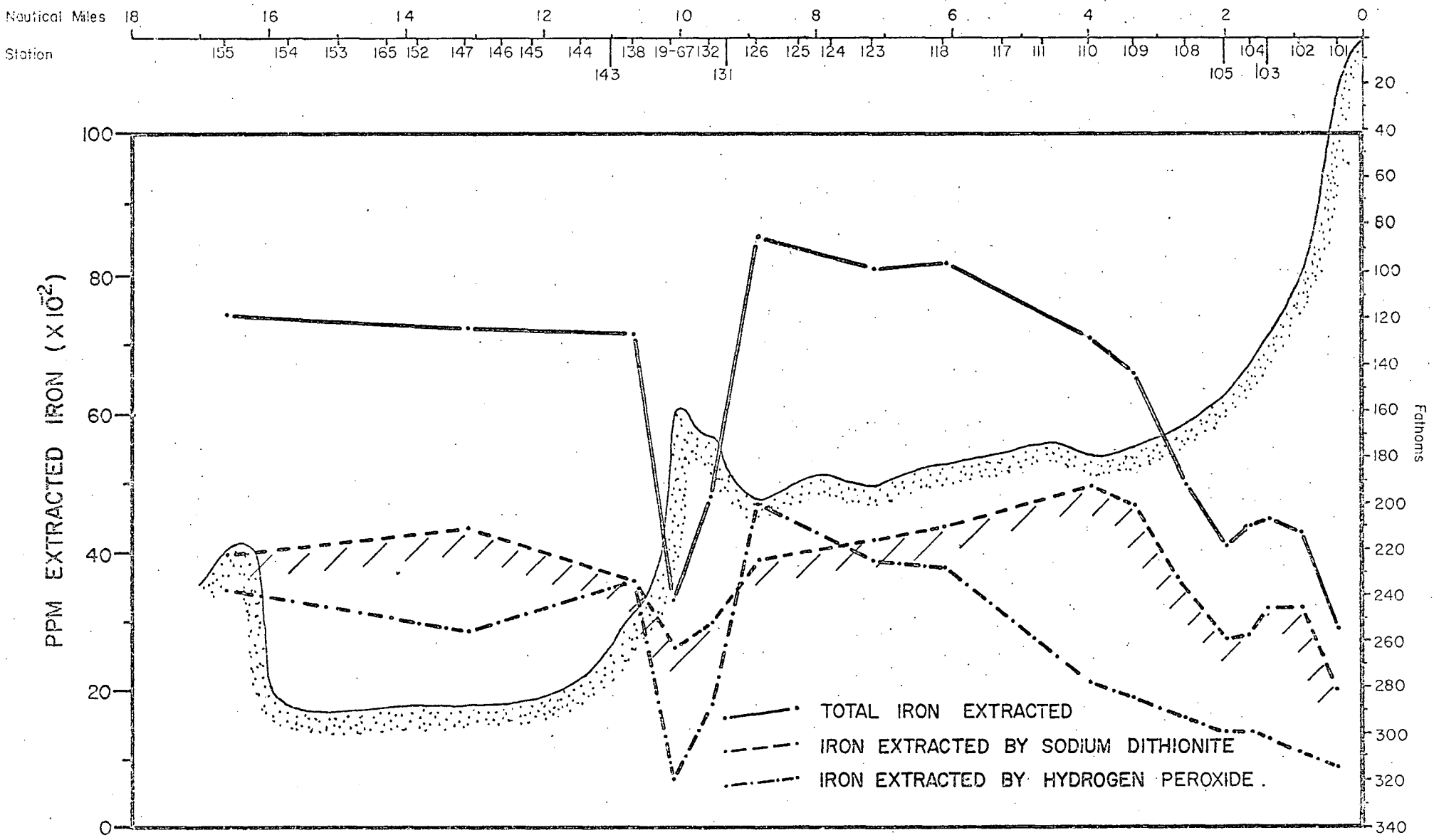

FIG. 16 IRON EXTRACTED DURING SAMPLE PREPARATION FOR X-RAY ANALYSIS

Inlet shows the source of particulate iron to be the river at the inlet head. Isopleths of suspended iron oxide content are approximately vertical with decreasing gradient from the source. Since the ratio curve tends to approach a base level, an explanation for the shape of the curve might be dilution of particulate iron with distance from the source, while iron adsorbed by clay-size particles (of which approximately 70% are clay minerals and micas) remains constant.

The chemical state of the iron within the sediment extractable by hydrogen peroxide is not known. Possibly it was associated with the organic material. Comparison of Figure 16 and Figure 15 indicates a correlation between iron extracted by peroxide and total carbon content.

The area with sediments containing minimal extractable iron corresponds to the manganese-iron concretion locality on Patrick Sill. The total carbon content and the percentage of clay-sized particles is also at a minimum because of the higher energy of the environment. Iron crusts recovered from the locality indicate iron is being precipitated on exposed rock surfaces. These crusts will be described later with the manganese concretions.

IV. Particle Morphology

Granule-sized and larger fragments, when present, showed a wide range in degree of roundness, varying from angular to sub-rounded. Evidences of a glacial origin, such as scour marks and faceting, were not confirmed on any of the samples examined. Distinct faces on some rock fragments appeared to represent jointing.

Mineral grains from the 500 - 300/u(1.0 - 1.5Ø) and 88 - 63/u (3.5 - 4Ø) fractions were examined by binocular microscope to determine the general shape and roundness and, if possible, any trends. Figures 17 and 18 are photomicrographs of the fractions examined for samples J-101, J-110, J-126 and J-19-67. Photograph J-126A shows a fragment of a sponge spicule and photograph J-19-67-B shows rounded and partially dessicated fragments which are thought to be glauconite-montmorillonoid pellets.

The shape of many grains often reflected their granitic origin. Quartz was generally equidimensional as in the assumed parent rocks. Some of the grains were elongate and very angular and probably

Figure 17 a Station J-101 (approx.110X) Photomicrograph of mineral grains from very fine sand fraction (63 to 88/u)

b Station J-101 (approx.60X) Photomicrograph of mineral grains from medium sand fraction (350 to 500/u)

c Station J-110 (approx.110X) Photomicrograph of mineral grains from very fine sand fraction (63 to 88/u)

a

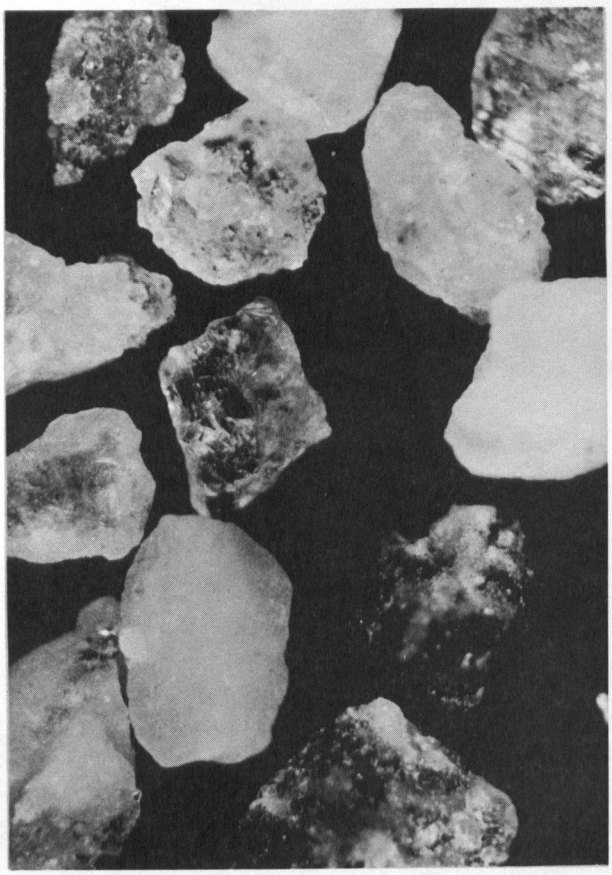

b

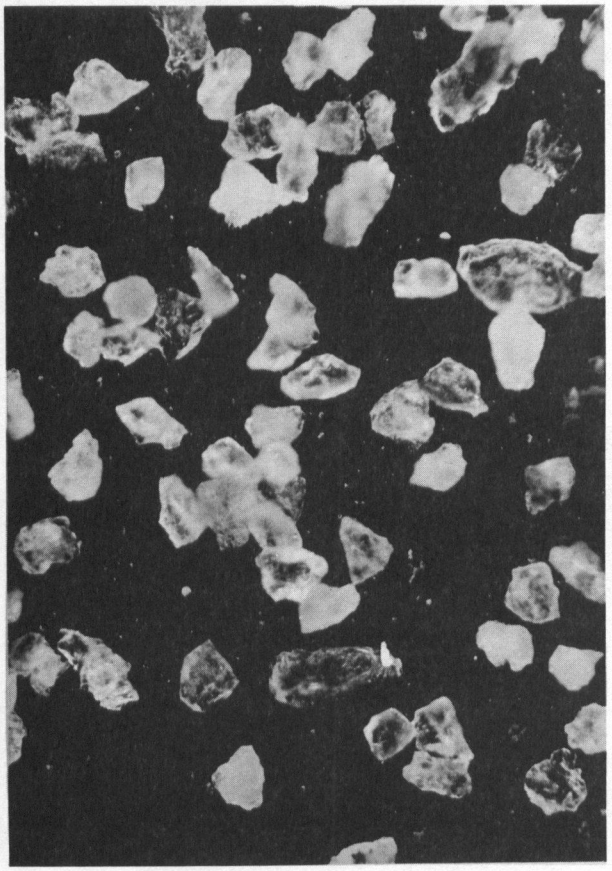

c

FIGURE 17

Figure 18 a Station J-126 (approx.110 X)Photomicrograph of mineral grains from very fine sand fraction (63 to 88/u). The long prismatic fragment is a portion of a spicule from a siliceous sponge.

b Station J-126 (approx. 60 X) Photomicrograph of mineral grains from medium sand fraction (350 to 500/u). Note angularity and apparent concoidal fracturing of quartz grains.

c Station J-19-67 (approx.110 X) Photomicrograph of mineral grains from a very fine sand fraction (63 to 88/u)

d Station J-19-67 (approx.60 X) Photomicrograph of mineral grains from medium sand fraction (350 to 500/u). Note rounded, partially dessicated pellets in lower half of photograph. These are tentatively identified as glauconite-montmorillonoid pellets.

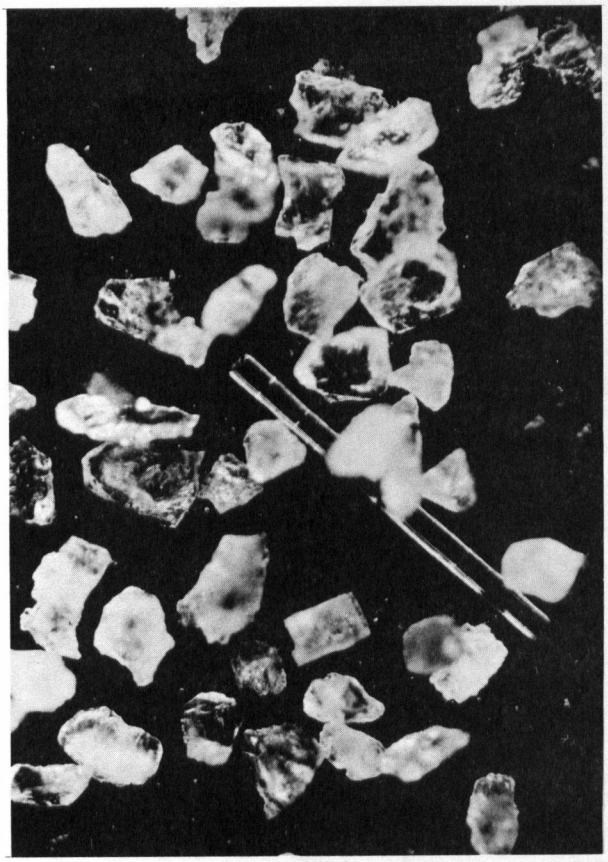

a

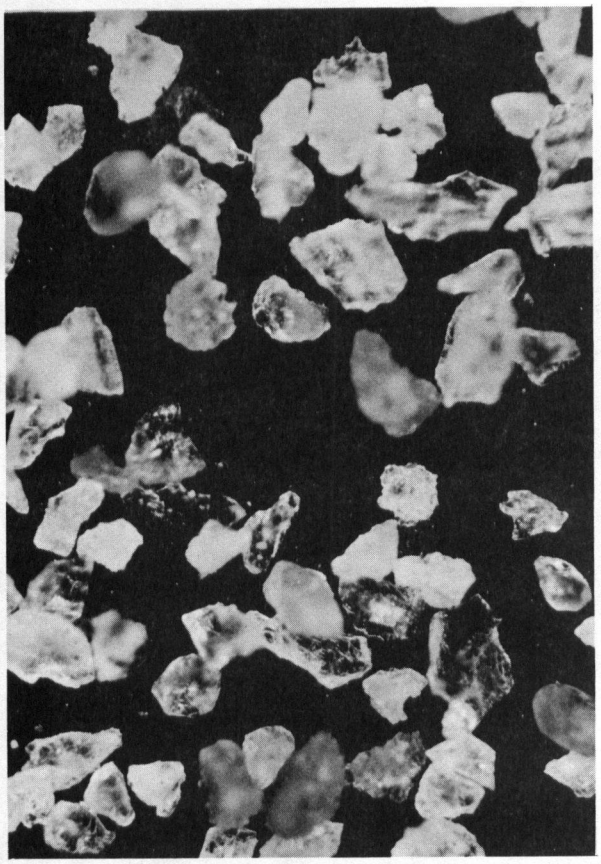

c

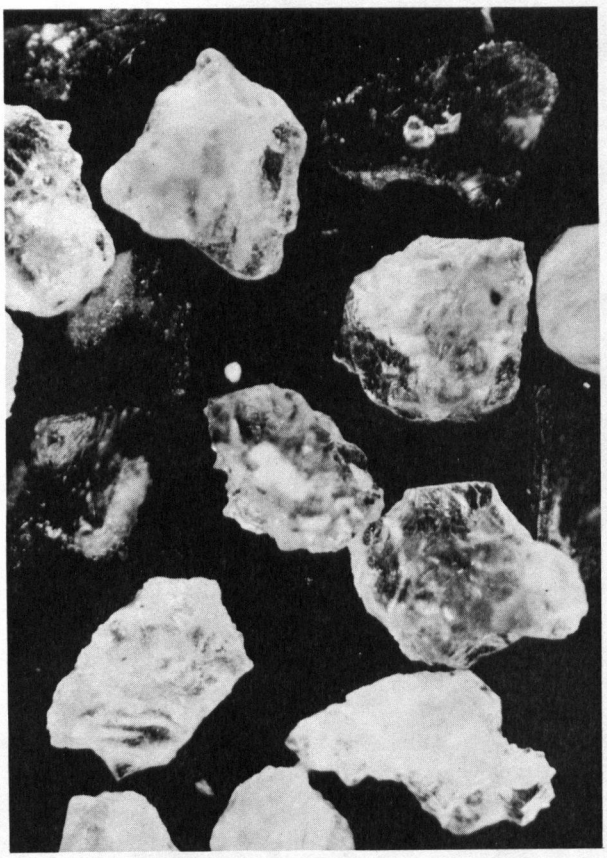

b

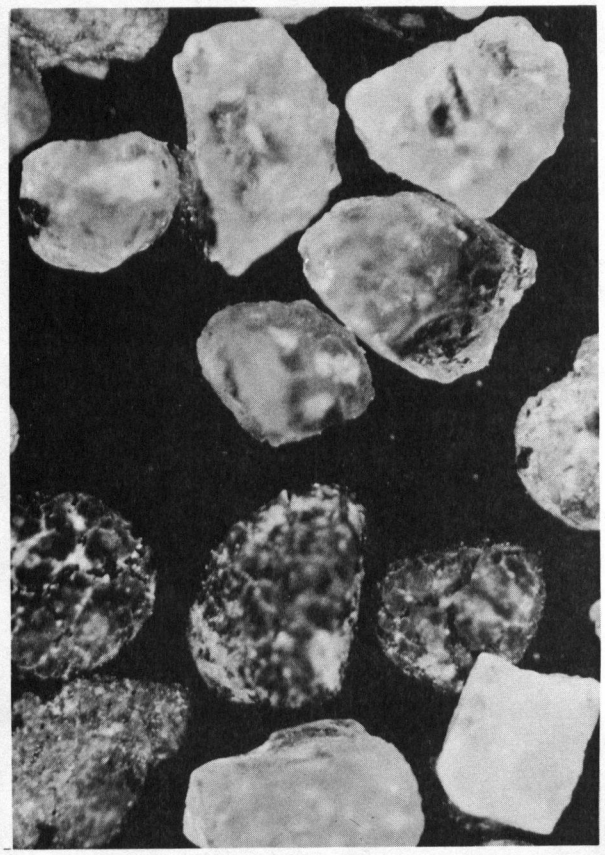

d

FIGURE 18

were formed by shattering under high stress. Plagioclase and hornblende grains ranged from approximately equidimensional to elongate or lath-like. External evidence of alteration was not common.

Generally, the mineral grains were angular indicating erosion by physical processes followed shortly by deposition with little or no re-working. Along the axis of the basins, however, subangular to subrounded grains were found at the inlet head and on the nodule locality. A transverse section, just above Princess Louisa Inlet indicated the central basin sediments to be better rounded than the slope sediments. A similar section along the crest of the sill indicated the opposite in that angularity increased with depth. A third transverse section, this one across the lower basin, indicated more rounding with depth.

If rounding of mineral grains is occurring approximately in situ, the areas with greatest current action are the head of the inlet and the nodule locality.

V. MINERALOGY

1. Granule and Larger Size Material (> 2.0 mm)

Thin sections were cut from cobble-sized fragments of each of the major rock types present in the sediments. Identification of minerals while they were still members of a rock-forming assemblage was much easier than when they were discrete grains in grain mounts.

Rocks of approximately quartz dioritic to quartz monzonitic composition accounted for 65 - 75% of the granule-sized and larger material recovered in grab samples. Granite and minor pegmatite accounted for 5 - 15%, volcanics (usually basaltic) for 5 - 20%, and slates with occasional hornfels and amphibolite fragments for 0 - 5%.

Hand specimens generally appeared fresh and revealed little evidence of alteration in the present marine environment. Where surface alteration was apparent, the mafic minerals had been most noticeably affected. Whether this alteration occurred in the marine environment is not known. A surface colouration, variable from light green to dark red-brown was particularly noticeable on leucocratic rocks. Polished sectioned revealed that this stain occurred as a rind

and extended to depths from 1 to 5 mm. The state of alteration within the stained area was no more advanced than without. The red-brown stains may have been due to absorbed iron oxides, whereas the green stains were possibly of organic origin. Thin section study indicated the state of alteration of a mineral within a fragment bore little or no relation to distance from the fragment's surface.

In a typical quartz diorite cobble, sodic plagioclase (Ab_{60-70}) accounted for about 60% of the rock. The plagioclase was generally subhedral to anhedral and often complexly twinned, although in foliated rocks, twinning was much less noticeable. A majority of grains showed little or no alteration. Quartz formed about 10% of the rock and was usually anhedral and intergranular. Extinction patterns were often wavy or undulatory. Biotite was the principal mafic mineral. The lathes were usually intertranular and sometimes bent. Pleochroism was masked by the green or sometimes yellow-green colour. Micas (in places) showed signs of alteration along contacts with other minerals. Potassium feldspar occurred in minor quantities. Unlike plagioclase, these grains

usually showed some signs of alteration. Also present were hornblende, sphene, zircon, and magnetite. In some speciments, hornblende was the principal mafic mineral. Typically the grains were subhedral. Pleochroism varied from yellow-green to blue-green.

In the more acidic quartz monzonite cobbles quartz occupied about 45% of the section, K-feldspar 25%, plagioclase 25% and mafics and opaques 5%. The constituent minerals displayed the same spatial relations. In the samples examined, alteration of feldspar species was equal and most pronounced in the cores of the crystals.

The average composition of the granites was 30 - 35% quartz, 55 - 60% K-feldspar, and 5 - 10% plagioclase. The K-feldspar was often considerably altered.

The volcanic rocks were basaltic. A specimen of porphyritic basalt contained phenocrysts of plagioclase (An_{70}) and pyroxene with minor amounts of olivine, biotite, magnetite, and hematite. The groundmass was dark brown to black. In hand specimen the rock appeared altered but thin section examination did not verify this.

Hornfels fragments were black, fine-grained, schistose and often porous. The cavities were lined with limonite and in places contained pyrite. Plagioclase feldspar and/or quartz made up 55% of the rock, hornblende 40%, and opaques 5%. Minor quantities of biotite and epidote were present. Hornblende crystals were arranged in parallel to sub-parallel alignment. There was little alteration of essential minerals.

The hand specimens of amphibolite were fine grained, slightly foliated, and dark green in colour. Hornblende comprised about 70%, plagioclase 25%, and quartz 5% of the rock. Alteration was relatively minor.

2. Sand Size Material (0.063 - 2.0 mm)

Within the sand size and coarser fractions, the mineralogy was determined for only the fine sands of diameter range 62/u to 125/u (4Ø to 3Ø). The individual grains within this fraction were essentially monomineralic. However, the majority of grains of the heavier, mafic minerals were in this size range and therefore, the calculated average composition will be skewed towards the mafic minerals.

The mineralogy of 16 samples, all collected along the basin axes, was determined. Mineral content

of the sediments along transverse profiles was not investigated. The mineral percentages (by point count) are given in Table 3. Crystallographic properties and degrees of weathering were not tabulated.

The following is a list of minerals identified petrographically in thin-sectioned grain mounts.

Essential	Accessory and Trace
Quartz	Epidote
K-feldspars	Pyroxene
Plagioclase feldspars	Magnetite
Chlorite	Apatite
Biotite	Sphene
Amphibole (principally hornblende)	Garnet
	Tourmaline
	Zircon

Sta. No.	Quartz	Feldspar			Micas		Amphib.	Pyroxene		Epidote	Magnetite	Apatite	Unident. & Misc.
		K	Plag.	Indet.	Chlor.	Biot		Clino.	Ortho				
101	20.0	4.6	35.5	7.9	2.9	0.9	15.9	0.8	0.5	6.6	1.3	-	3.0
102	23.8	4.4	31.9	13.1	8.0	3.0	12.5	1.0	0.5	3.1	0.1	0.1	3.1
103	27.0	10.4	29.0	7.5	7.1	2.2	7.4	0.5	0.3	2.9	0.4	-	5.2
104	32.6	9.8	21.4	8.5	2.5	4.1	10.5	0.5	0.1	3.0	0.3	0.6	4.4
105	27.7	7.2	21.5	8.5	13.1	4.3	12.2	0.1	-	3.7	1.0	0.1	1.9
108	19.3	2.6	15.5	6.4	2.1	4.1	28.9	0.8	2.0	12.7	1.2	0.4	4.9
109	21.1	5.1	42.1	8.9	9.1	4.8	8.2	1.8	0.3	1.7	1.1	0.2	1.0
110	24.8	8.0	34.8	9.6	-	-	-	-	-	-	-	-	-
118	18.9	8.0	50.0	3.3	8.2	1.2	6.0	0.2	1.0	0.3	0.7	-	2.1
19-67	22.6	5.7	41.5	9.3	9.9	2.2	5.0	0.1	0.2	1.0	0.7	-	1.9
126	23.8	6.7	49.5	4.3	4.4	4.9	4.1	0.2	0.4	0.3	0.3	0.1	1.0
132	29.8	3.6	46.1	1.6	2.5	10.4	3.1	-	0.3	0.5	0.2	-	1.8
138	20.8	7.2	44.2	5.7	3.3	8.2	5.7	-	0.4	1.7	0.3	-	2.6
147	18.7	5.5	41.6	2.5	13.4	13.4	2.3	-	0.1	0.6	0.1	-	2.0
155	23.5	12.6	40.3	6.3	8.9	3.5	3.2	-	0.2	0.3	0.2	-	0.9

Table 3 Mineral Abundances in Fine Sand Fraction (by percent)

From 4% to 15% of the mineral grains counted were unidentifiable. Of these, about 75% appeared to be feldspars but were altered to such an extent that identification was uncertain. Rock fragments were included as unknown minerals. However, the occurrence of these, in this fraction, was minor.

An average composition of the fine sand fraction of the recent sediments would be:

Plagioclase	37%	Biotite	5%
Quartz	24%	Epidote	3%
Amphibole	8%	Pyroxene	1%
K-feldspar	7%	Unidentifi-	9%
Chlorite	6%	able rock fragments and opaques	

There was a marked similarity of physical and optical properties of minerals between the fine sand fraction and the cobble fraction. Most of the coarse surficial sediments are thought to have been derived from Coast Range batholithic rocks, as this is the only available source of granitic rock.

Roddick (1965) discussed the Coast Range batholith of the Vancouver North, Coquitlam and Pitt Lake map areas and gave an average composition of the granitic rocks. The average was an h-quartz diorite (where h denotes hornblende is more abundant than biotite) and had the following composition:

Plagioclase	56%	K-feldspar	1%
Quartz	30%	Sericite	1%
Hornblende	7%	Opaques	0.5%
Biotite	5%	Chlorite	0.5%

Roddick's average composition does not correlate with that of the marine sediment fraction examined. However, since the mafic minerals tended to be concentrated within this fraction, discrepancies would be expected.

As the geology of the study area is unmapped, except on a reconnaissance basis, the mineralogy of rocks from possible sediment source areas is not known. Perhaps the granitic rocks of the sediment source area tend to be more acidic than in the area studied by Roddick.

The occurrence of minerals such as chlorite (6%), epidote (3%) and pyroxenes (1%) in these percentages is probably an expression of the presence of pre-batholithic rocks which are mapped as outcropping over most of the watershed of upper Jervis Inlet. The igneous rocks of the Texada Group, as described by LeRoy (1908), are extensively altered and often large percentages of the minerals are secondary with calcite, chlorite and epidote being the most common.

Since the sediment samples collected for mineralogic analysis were likely recently deposited, one would expect the influence of the surrounding outcropping rock to be more pronounced. However, if the pre-batholithic material in which the upper part of the inlet is incised is primarily slate, then the diameter of eroded particles may be smaller than the range examined. Another possibility is that the extent of the roof pendant of pre-batholithic material may not be nearly as great as presently mapped. However, assuming the gross geology, as mapped to date, to be reasonably correct, the source of sand size and larger material being deposited in the inlet must be relict Pelistocene deposits undergoing reworking in both terrestrial and marine environments. The presence of sills prevents loss of all but the very finest of material carried into the inlet.

Several trends were noted within mineral groups.(Figure 19). Biotite, which gradually increases in abundance from the head of the inlet, was usually a dark green colour. However, over the sill, a red-brown variety predominates. Whether this effect is ~~geochemical~~ diagenetic or an expression of present and/or past sedimentation patterns is not

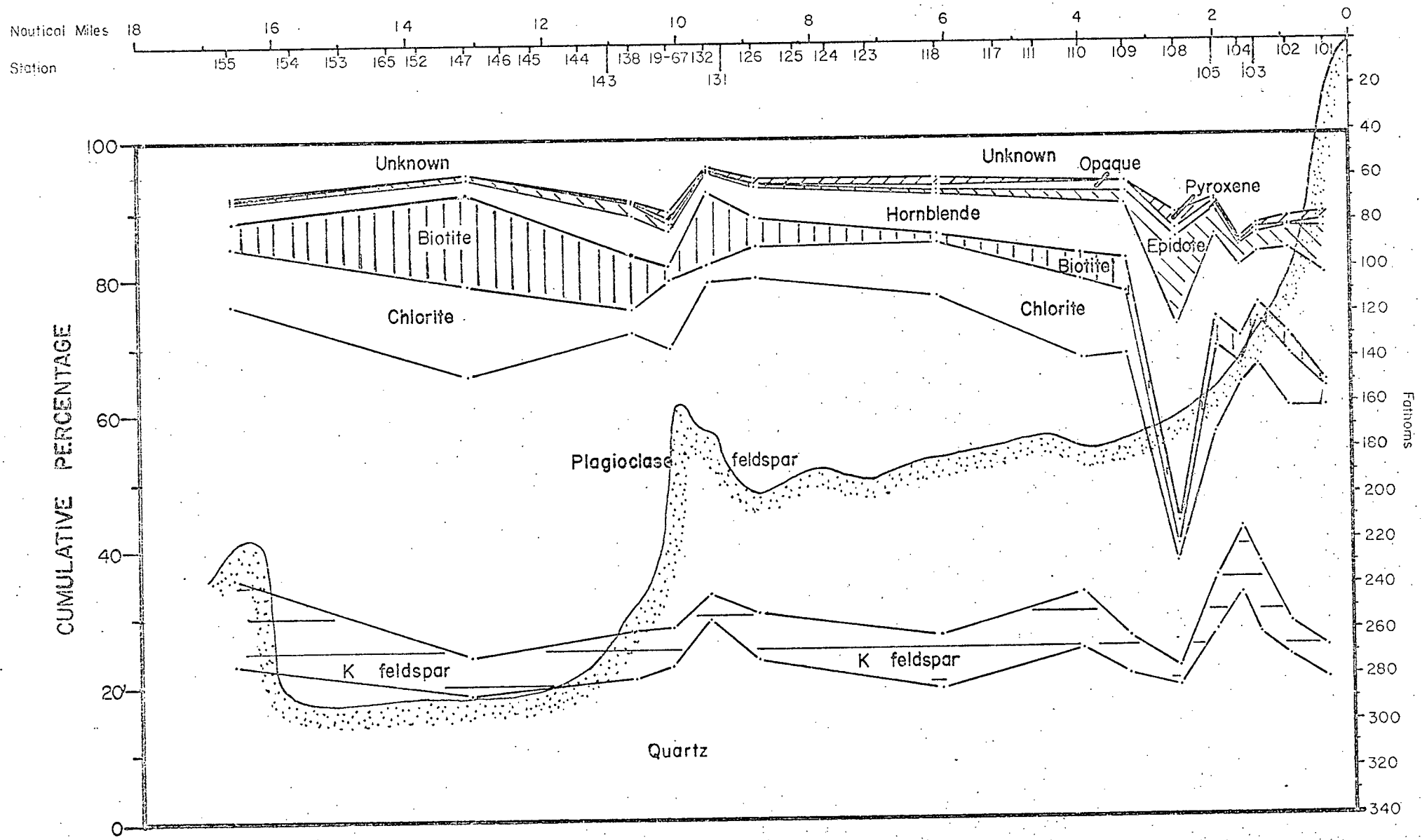

FIG. 19 MINERAL DISTRIBUTION ALONG AXIS OF UPPER JERVIS INLET

known. From the head of the inlet to Station J-118, hornblende was the only amphibole present. However, from J-118 to the end of the study area, tremolite-actinolite was also found, although never with the same abundance as hornblende.

Even though sediment is being added to the inlet elsewhere than at the head, the relatively uniform sediment mineralogy from Station J-110 down the inlet indicates most sediment sources have a similar mineralogic composition.

The exception to the approximately uniform trend in mineralogy occurs at the head of the inlet between Stations J-101 and J-110. Here it appears that slumping plays a major role in sediment distribution. The break in slope occurring at J-108 corresponds with a marked increase in heavy minerals and a decrease in micaceous minerals.

3) Clay Size Material

Mineralogic analyses of clay size particles were made for each of the samples for which the mineralogy of the sand and cobble fraction was determined. Table 5 gives the results of these analyses. Interpretation of abundances from diffractograms was made with reference to three sample interpretations

made by Dr. L. M. Lavkulich (Department of Soil Sciences, University of British Columbia.) The following scale of abundance was used:

5	Dominant	65 - 100%
4	Major	35 - 65%
3	Minor	10 - 35%
2	Trace	0 - 10%
1	None	

Clay mineral identification was based on X-ray diffraction data only. The relative amounts of Fe, Mg, and Al in the chlorites was based on diffraction patterns given by Weaver (1958). Some peaks which appeared on the diffractograms could not be identified, but the magnitude of these indicated trace abundances. A list (Table 4) of the recognized mineral species and their [001] peaks (in Angstroms) according to treatment appears on the following page.

MINERAL	K	K 300°C	K 500°C	Mg	Mg & Glycerol
Chlorite	14	14.2	14.2	14.2	14.2
Illite	10	10	10	10	10
Vermiculite	10-13	10	10	14-15	14
Montmorillonite	12-14	10	10	12.8-14	17-18
Illite-montmorillonite	10-14	10	10	10-14	10-18
Illite-vermiculite	10-13	10	10	10-15	10-14
Illite-chlorite	10-14	10-14	10-14	10-14	10-14
Plagioclase	3.18	3.18	3.18	3.18	3.18
Quartz	3.3	3.3	3.3	3.3	3.3
Amphibole (hornblende)	8.40	8.40	8.40	8.40	8.40
K-feldspar	3.24	3.24	3.24	3.24	3.24

Table 4 [001] Peaks (in Angstroms) of Minerals in Clay Size Fraction

Plagioclase feldspar, quartz and amphibole (principally hornblende) were present in nearly constant proportions for the length of the inlet. K-feldspar occurred as a trace mineral in considerably lesser quantities than plagioclase and quartz. As with some of the minerals in the coarser fractions, K-feldspar content increases significantly at Station J-118 where the influence of Princess Louisa Inlet would be expected.

Several interesting trends were noted in the clay mineral abundances. There is insufficient information to determine whether or not the observed trends are geochemically significant. Many investigators (Grim, 1968) have concluded that variations in settling rates of clay mineral species are adequate to explain variations in abundances in situations like upper Jervis Inlet where there is a dominant sediment source. With increase in salinity the settling velocity of illite and kaolinite has been found to increase rapidly while that of the smectites (e.g. montmorillonite) is little affected.

The most noticeable trend is the disappearance of montmorillonite and illite-montmorillonite

intergrade by Station J-103, i.e. shortly after the material enters the marine environment. With the disappearance of these species, vermiculite and an illite-vermiculite intergrade appear. The illite-vermiculite intergrade occurs with an approximately constant abundance for the remaining length of the study area. Vermiculite gradually increases in abundance until, on the sill, it becomes the dominant clay mineral. For the remaining samples analyzed, vermiculite remains one of the dominant or near-dominant types. The overall trend is thus an increase in vermiculite with distance from the head of the inlet with the increase being accentuated on the sill. The only other type trend noted was the appearance of an illite-chlorite intergrade at Station J-118. This intergrade occurs in most samples taken farther down the inlet, but only in trace amounts.

The two dominant clay minerals are Fe and Fe-Mg chlorite and illite. There is no noticeable trend in abundance of these.

Montmorillonite is a dominant clay mineral in sediments collected from the inlet head. Therefore, if differential settling of the clay mineral

species is occurring, it is likely to be doing so on a smaller scale than on which upper Jervis Inlet was sampled. The apparent rapid disappearance of montmorillonite and illite-montmorillonite intergrade with deposition in the saline inlet environment suggests that potassium and magnesium are being absorbed from sea water by the montmorillonite. Absorption of these elements collapses the montmorillonite structure resulting in the formation of illite and chlorite.

TABLE 5 RELATIVE ABUNDANCES OF CLAY MINERAL SPECIES

J-101	Illite	3-4	J-102	Fe chlorite	4
	Fe chlorite	3-4		Illite-montmor.	3
	Illite-montmor.	3-4		Illite	3
	Montmorillonite	3		Montmorillonite	3
	Amphibole	2		Plagioclase	2
	Plagioclase	2		Amphibole	2
	Quartz	2		Quartz	2
J-103	Fe Chlorite	3-4	J-104	Mg-Fe chlorite	4
	Illite	3-4		Illite	3-4
	Vermiculite	3		Vermiculite	3
	Illite-vermic.	3		Vermic.-illite	3
	Plagioclase	2-3		Plagioclase	2
	Quartz	2-3		Quartz	2
	Amphibole	2		Amphibole	2
J-105	Fe chlorite	3-4	J-108	Fe chlorite	4
	Illite	3-4		Illite	3-4
	Vermiculite	3-4		Vermiculite	3
	Illite-vermic.	3		Illite-vermic.	3
	Plagioclase	2		Plagioclase	2
	Quartz	2		Quartz	2
	Amphibole	2		Amphibole	2
J-109	Mg-Fe chlorite	4	J-110	Mg-Fe chlorite	3-4
	Illite	3-4		Vermiculite	3-4
	Vermiculite	3		Illite-vermic.	3-4
	Illite-vermic.	3		Illite	3
	Plagioclase	2		Plagioclase	2
	Quartz	2		Quartz	2
	Amphibole	2		Amphibole	2
	Illite-chlorite	2			
J-118	Mg-Fe chlorite	3-4	J-123	Mg-Fe chlorite	4
	Illite	3-4		Illite	3-4
	Vermiculite	3-4		Vermiculite	3-4
	Illite-vermic.	3		Illite-vermic.	2-3
	Plagioclase	2		Illite-chlorite	2
	Quartz	2		Quartz	2
	Amphibole	2		Plagioclase	2
	Illite-chlorite	2		Amphibole	2

TABLE 5 (contd.)

J-126	Vermiculite	4	J-19-67	Vermiculite	3-4
	Mg Fe chlorite	3		Fe chlorite	3-4
	Illite	3		Illite	3
	Illite-vermic.	3		Illite-vermic.	2-3
	Quartz	2		Quartz	2
	Illite-chlorite	2		Plagioclase	2
	Plagioclase	2		Amphibole	2
	Amphibole	2		Illite-chlorite	2
J-132	Fe chlorite	4	J-138	Fe chlorite	3-4
	Vermiculite	3-4		Illite	3-4
	Illite	3		Vermiculite	3
	Illite-vermic.	2-3		Illite-vermic.	2-3
	Quartz	2		Illite-chlorite	2
	Plagioclase	2		Quartz	2
	Amphibole	2		Plagioclase	2
	Illite-chlorite	2		Amphibole	2
J-147	Vermiculite	4	J-155	Fe chlorite	3-4
	Mg Fe chlorite	3-4		Illite	3-4
	Illite	3-4		Vermiculite	3-4
	Illite-vermic.	2-3		Illite-vermic.	2-3
	Plagioclase	2		Quartz	2
	Quartz	2		Plagioclase	2
	Amphibole	2		Amphibole	2
	Illite-chlorite	2		Illite-chlorite	2

VI. GRAIN SIZE DISTRIBUTION

The grain size distribution and corresponding parameters were calculated with a computer program developed by Dr. A. J. Sinclair of the Department of Geology, University of British Columbia. Calculations were based on a cumulative curve plotted with arithmetic ordinates and developed by joining successive data points with straight lines. A minimum grain size was needed in the program and was arbitrarily set at 0.06/u (14 Ø)

The following is a list of parameters calculated for each sample.

Mean	Arithmetic Graphic (Folk) Graphic (Inman)
Standard Deviation	Arithmetic Graphic (Folk) Graphic (Inman) Inclusive Graphic Phi Quartile
Sorting Coefficient(Trask)	
Skewness	Moment Phi Quartile Graphic Inclusive Graphic
Kurtosis	Moment Graphic Transformed Graphic

Parameters used for interpretation in this study

were the graphic mean (Folk), graphic standard deviation (Folk), inclusive graphic skewness, and graphic kurtosis. These parameters were the more efficient with respect to the average grain size distribution of the sediment analyzed and the laboratory methods used. The majority of the sediment in upper Jervis Inlet contains abundant material in the silt and clay size fractions. Hydrometer analyses were taken as far as 0.98/u (10 Ø) with the result that a considerable percentage of the material (up to 34%) was not directly analyzed, i.e., was of diameter less than 0.98/u. The usefulness of grain size parameters in such an environment is therefore suspect. However, certain trends did show up in longitudinal profiles.

The graphic mean as proposed by Folk reflects the average particle diameter of a sediment. Since the Ø diameter is defined as $-\log_2$ (particle diameter in millimeters) a trend showing an increase in Ø value would indicate a decrease in particle size. This parameter is calculated from the following equation:

Folk and Ward (1957) $M_z = \frac{Ø16 + Ø50 + Ø84}{3}$

where Ø16, Ø50 and Ø84 are the Ø values taken from

a cumulative curve for the appropriate percentiles. However, the graphic mean gives no indication of the range of the grain size diameters and for interpretive purposes the inclusive graphic standard deviation must be considered simultaneously. The equation of this parameter, which gives the "sorting" or dispersion of the population is:

Folk and Ward (1957) $O_1 = \frac{(\emptyset 84-\emptyset 16)}{4} - \frac{(\emptyset 95-\emptyset 5)}{6.6}$

The inclusive graphic skewness and the graphic kurtosis should also be considered as a pair. The equations of these parameters are:

Folk and Ward (1957)

Skewness $S_{kl} = \frac{\emptyset 84-\emptyset 16+2\emptyset 50}{2(\emptyset 84-\emptyset 16)} + \frac{\emptyset 95-\emptyset 5-2\emptyset 50}{2(\emptyset 95-\emptyset 5)}$

Kurtosis $K_G = \frac{\emptyset 95 - \emptyset 5}{2.44(\emptyset 75-\emptyset 25)}$

Skewness and kurtosis are measures of non-normality of a distribution. The degree of asymmetry is measured by the skewness parameter. A negative value indicates a distribution curve asymmetric to the left (i.e. excess of coarse material), while a positive value indicates asymmetry to the right, (i.e. excess of fine material). A skewness value is a pure number and the absolute limits are -1.00 and +1.00.

Kurtosis is a measure of peakedness of a curve, and is a ratio between sorting in the tails and sorting in the central portion. Low values for kurtosis (i.e. 0.9) indicate better sorting in the tails than central portion. A distribution with low kurtosis is often bimodal. As with skewness, a kurtosis value is a pure number. The absolute limits of the measure a +0.41 and infinity, but most samples fall in the 0.60 to 5.0 range (Folk 1961).

Figure 20 (in pocket) shows the distribution of sediments according to grain size based on Shepard's (1954) classification. Figure 21 (in pocket) shows the clay size particle distribution in upper Jervis Inlet and Figures 22 and 23 are longitudinal profiles of grain size distribution parameters.

Frequency curves plotted from the grain size analyses indicate that the surficial sediments in upper Jervis Inlet can generally be divided into two dominant modes. The coarse mode usually falls in the 250 to 63 μ (2Ø to 4Ø) range, while the finer mode in the 16 to 4 μ (6Ø to 8Ø) range. These ranges represent the fine to very fine sands and

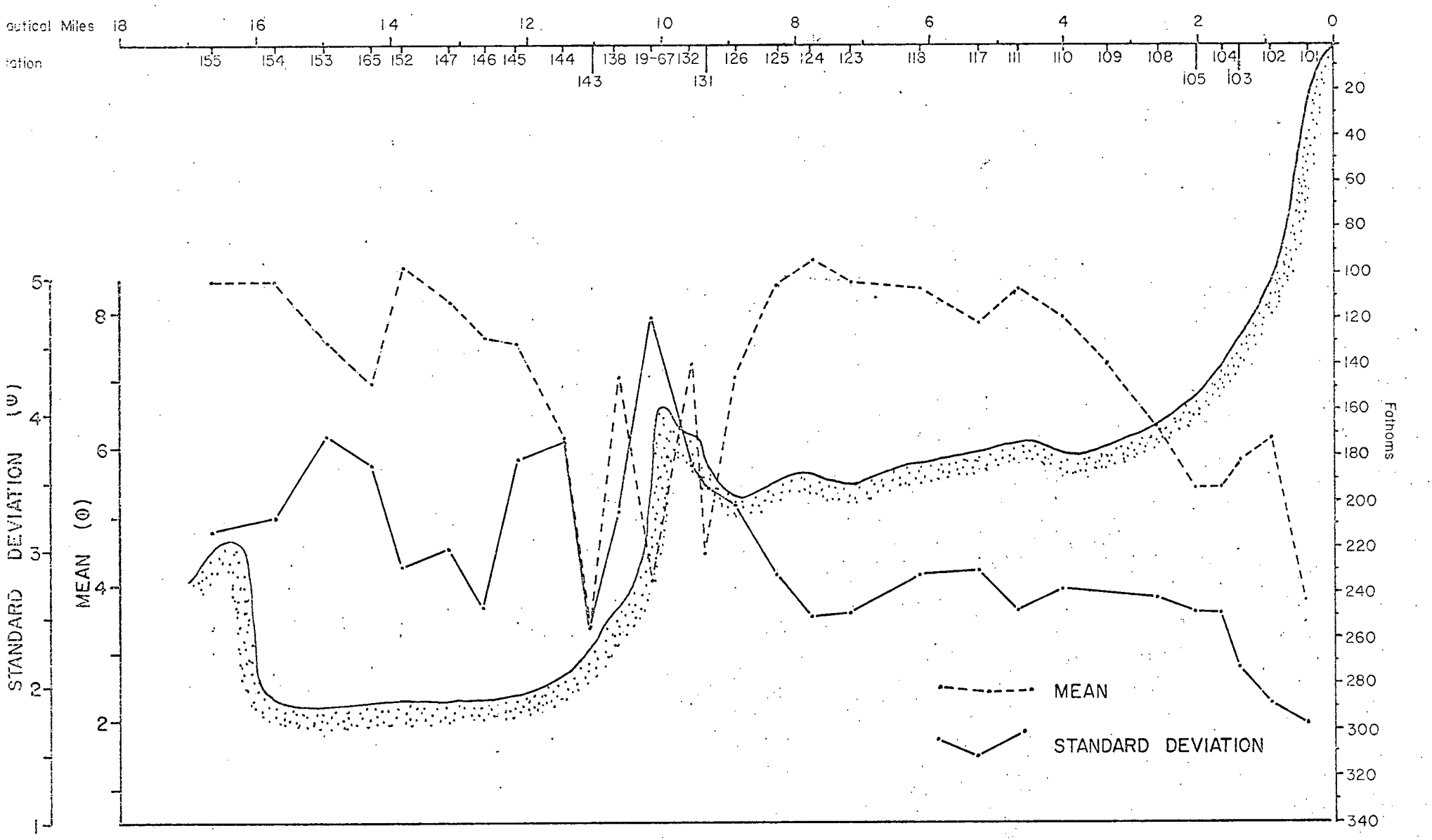

FIGURE 22 MEAN AND STANDARD DEVIATION OF GRAIN SIZE OF SURFICIAL SEDIMENTS ALONG AXIS OF UPPER JERVIS INLET

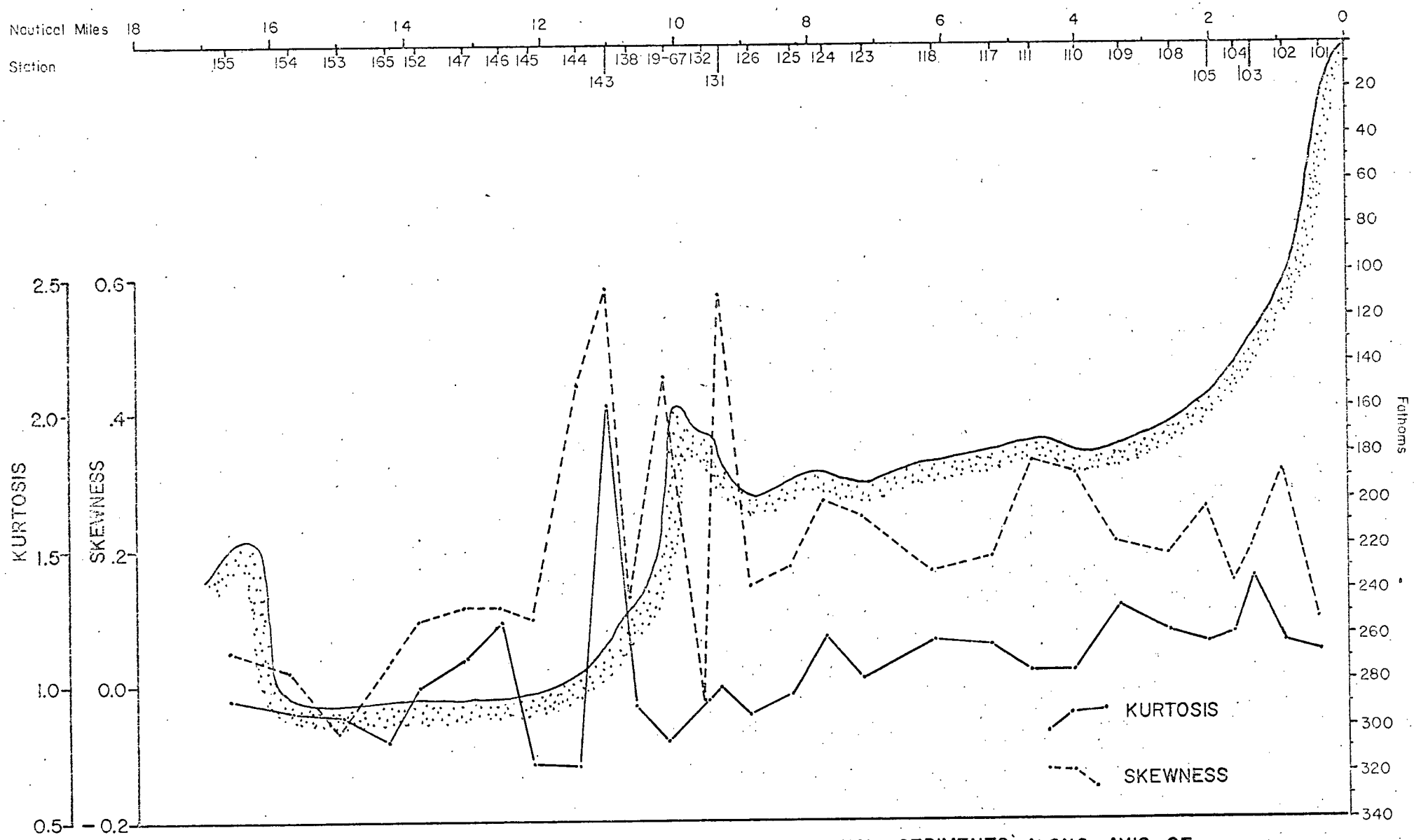

FIGURE 23 KURTOSIS AND SKEWNESS PARAMETERS OF SURFICIAL SEDIMENTS ALONG AXIS OF UPPER JERVIS INLET

and medium silts to clays respectively. The parameters presented in Figures 22 and 23 can be interpreted in terms of varying proportions of these two modes.

Most noticeable on the map showing sediment type distribution was the uniform decrease in average particle diameter with distance from the head of the inlet within the upper basin. The cumulative curves and histograms, in Figure 24 also illustrated this. The particle size distribution of sample J-111 represented an approximate average for the upper basin (0.9% sand, 51.9% silt, 47.2% clay). For the sediment collecting on the floor of the upper basin, the graphic mean (in Ø values)increased while the inclusive graphic standard deviation remained approximately constant. Overall, kurtosis followed a slowly decreasing trend, and skewness an approximately constant trend. The principal source of sediment within the upper basin would therefore be interpreted as being the river and river delta at the inlet head. However, an appreciable amount of material is being added from Princess Louisa Inlet and the deltaic deposit formed along the shore

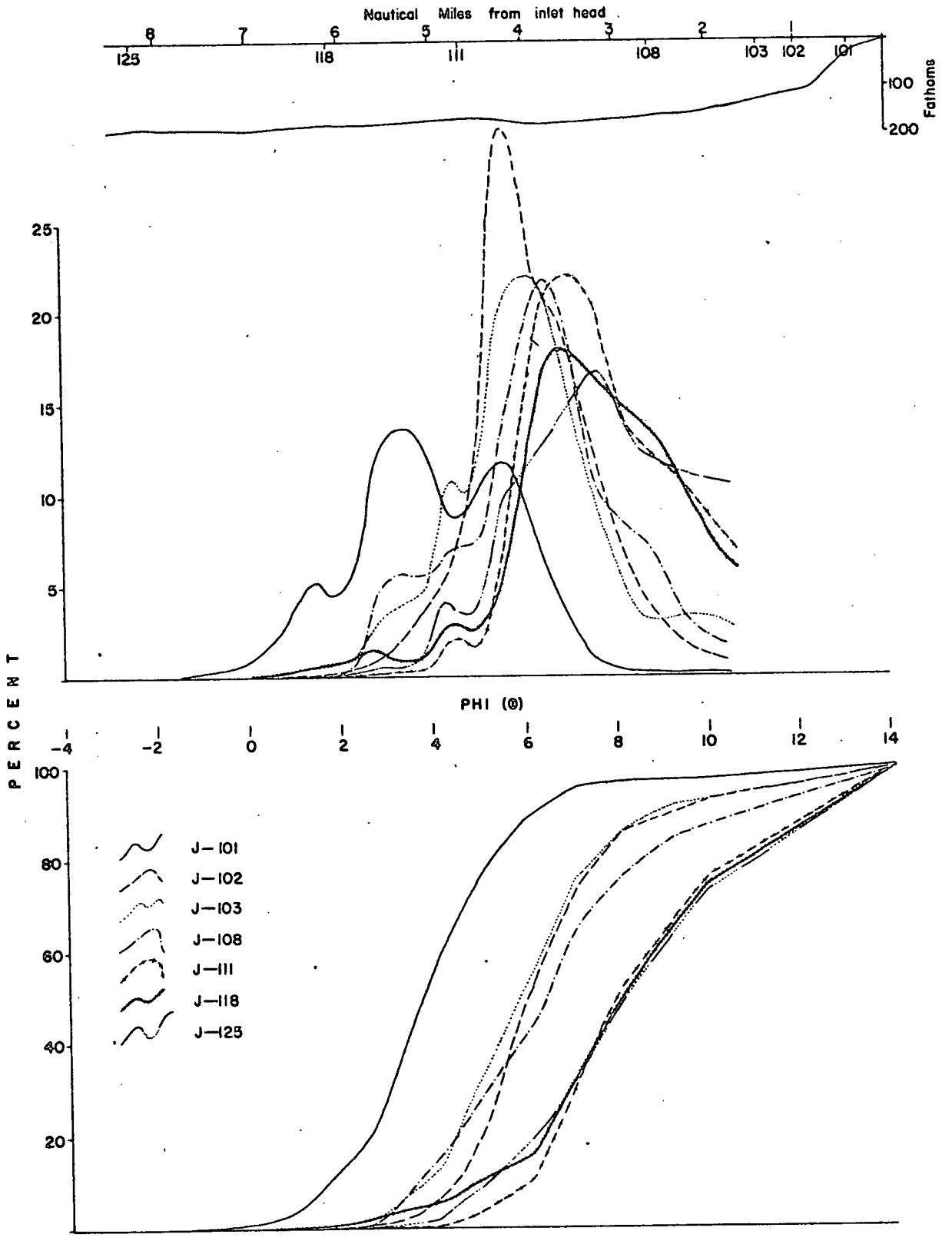

FIGURE 24 LONGITUDINAL PROFILE OF QUEENS REACH - CUMULATIVE AND FREQUENCY CURVES OF SURFICIAL SEDIMENTS

of Jervis Inlet at the point where the two inlets are connected (Malibu Rapids). Figures 22 and 23 indicate that addition of fine sand and silt is occurring in the vicinity of Station J-117. The mineralogy of the material being added closely resembled that of the sediment originating from the inlet head, probably indicating a common glacial origin. On an ebb tide, a vigorous tidal current (maximum velocity 10-12 knots, where 10 knots is equivalent to 520 cm/sec.) flows from Princess Louisa Inlet into Jervis Inlet. This tidal jet, at the point of maximum velocity, would be sufficient to carry cobble or boulder-sized material. Even though the velocity would attenuate rapidly once the water spread into Jervis Inlet, considerable reworking of the deltaic sediments would likely occur. The finer sands and smaller material would be deposited as foreset beds or carried in suspension by the weak estuarine circulation and deposited elsewhere. Subsequent slumping of the delta would carry the fine sands to the depths of the basins.

Figure 25 presents the cumulative and frequency curves for a transverse section of Queen's Reach at a point above Malibu Rapids. The abundance of the

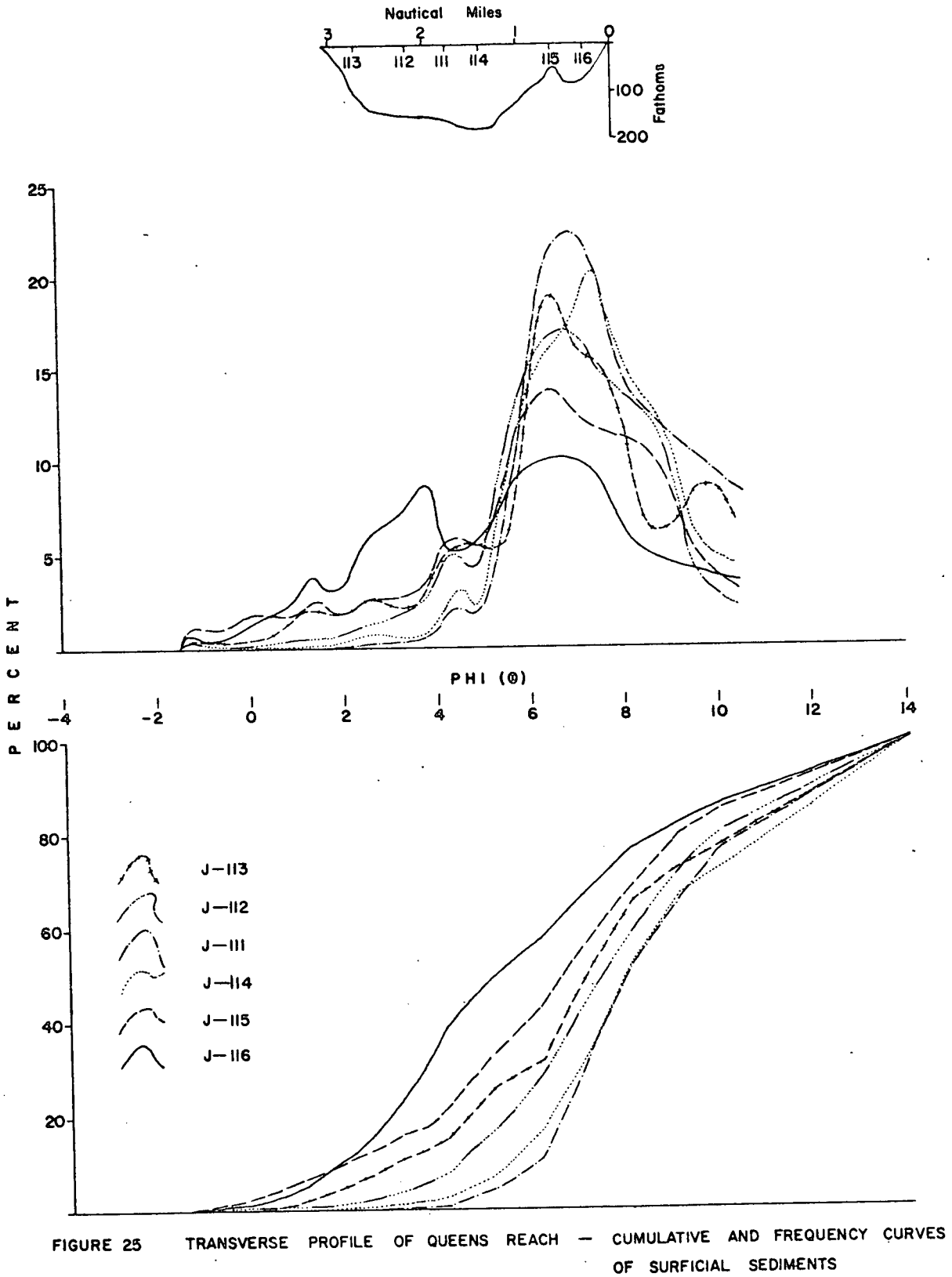

FIGURE 25 TRANSVERSE PROFILE OF QUEENS REACH — CUMULATIVE AND FREQUENCY CURVES OF SURFICIAL SEDIMENTS

Bottom Photographs

The scale of the photographs depends on the camera to sea floor distance. Where present, the compass assembly can be used as a scale indicator. The diameter of the compass dome is 3 in. (7.5 cm.) and the length of the vane is 10 in. (25 cm.) On an average, the photographs cover an area of about 3 feet by 4 feet (approx. 1 m. x 1.3 m).

Figure 26 a Note hummocky microtopography. Whether this is due to the presence of animals or to depositional processes is not known.

b Note shadow of compass. This different aspect of the microtopography is likely due to difference in camera angle.

Figure 27 a Note the skate partially concealed in the bottom sediments. Hummocky microtopography still prominent.

b

All photographs approx. 1/8 true scale

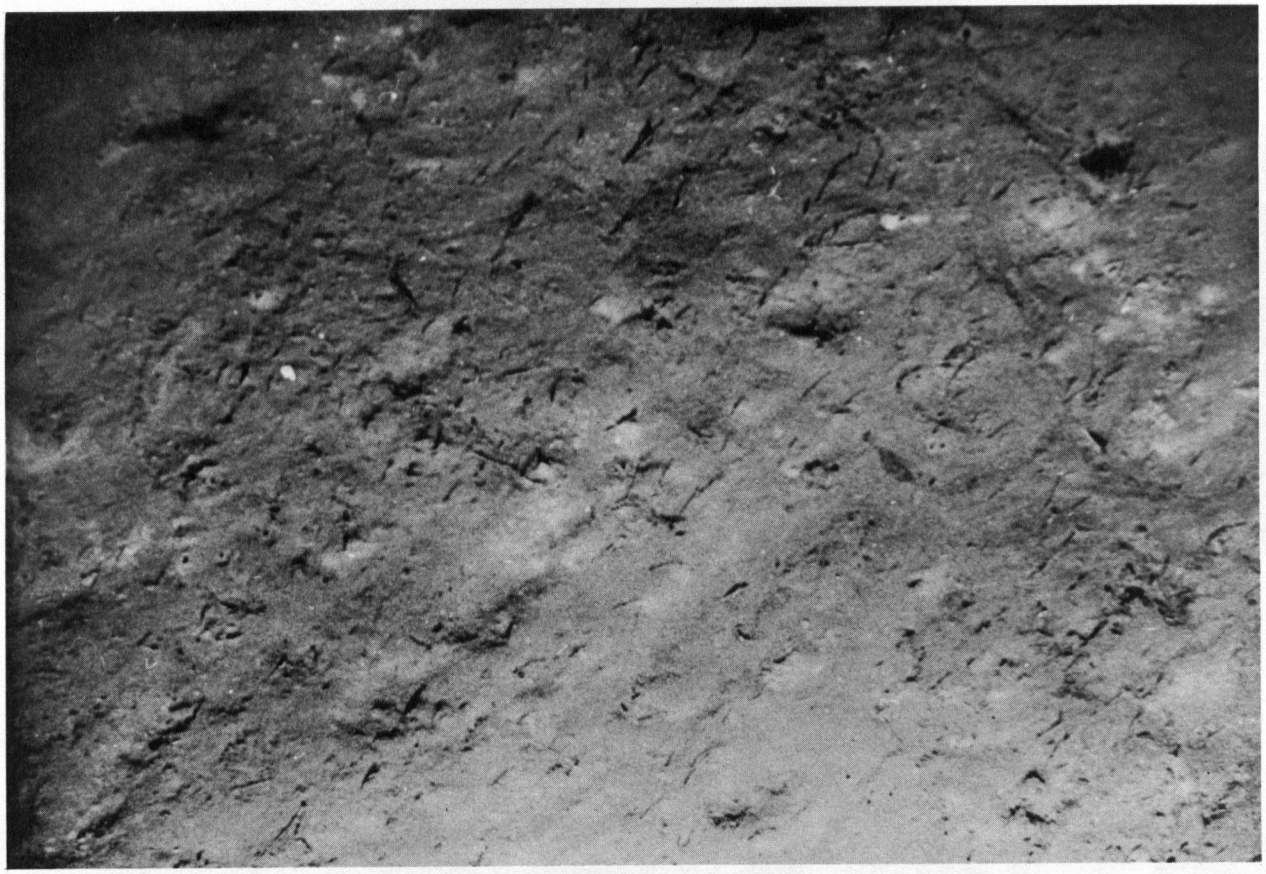

a

FIGURE 26 BOTTOM PHOTOGRAPHS – STA. J–126

b

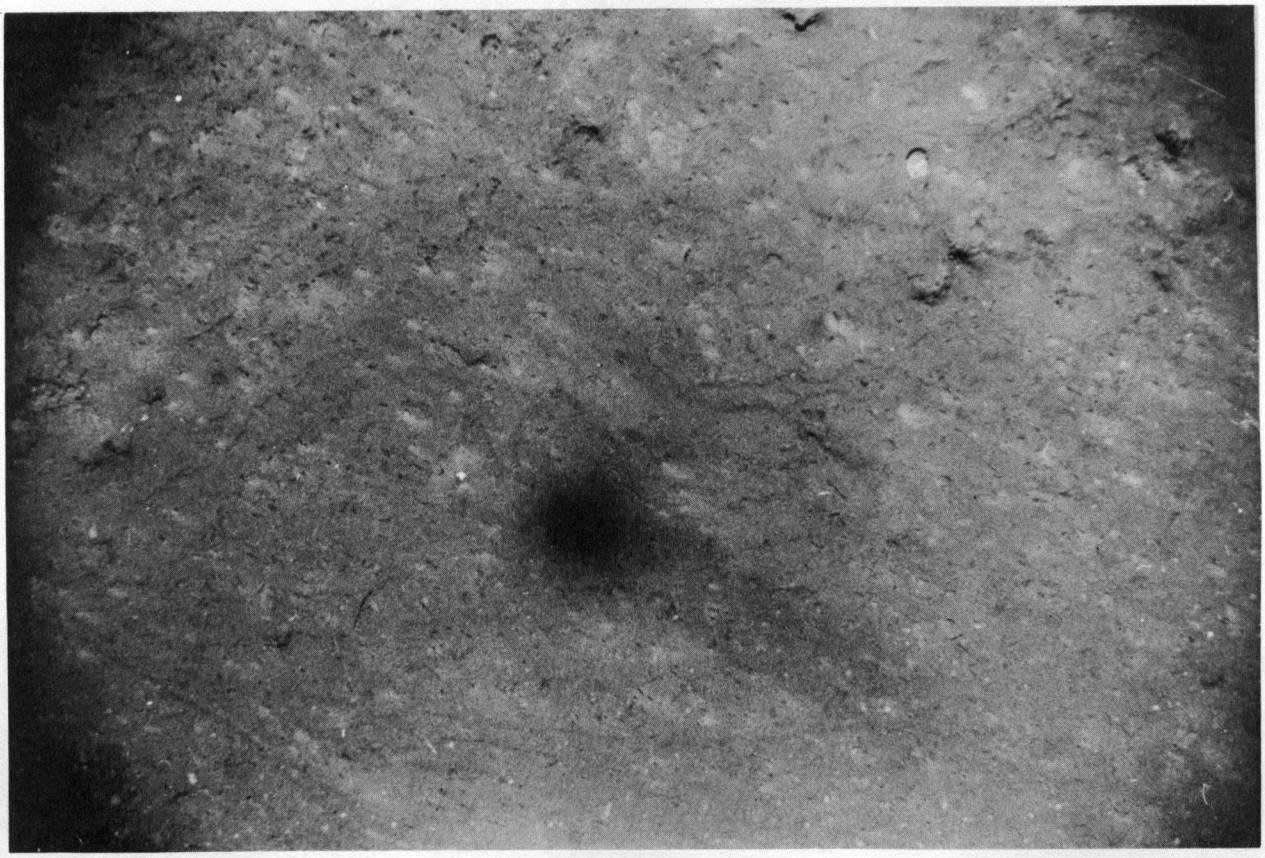

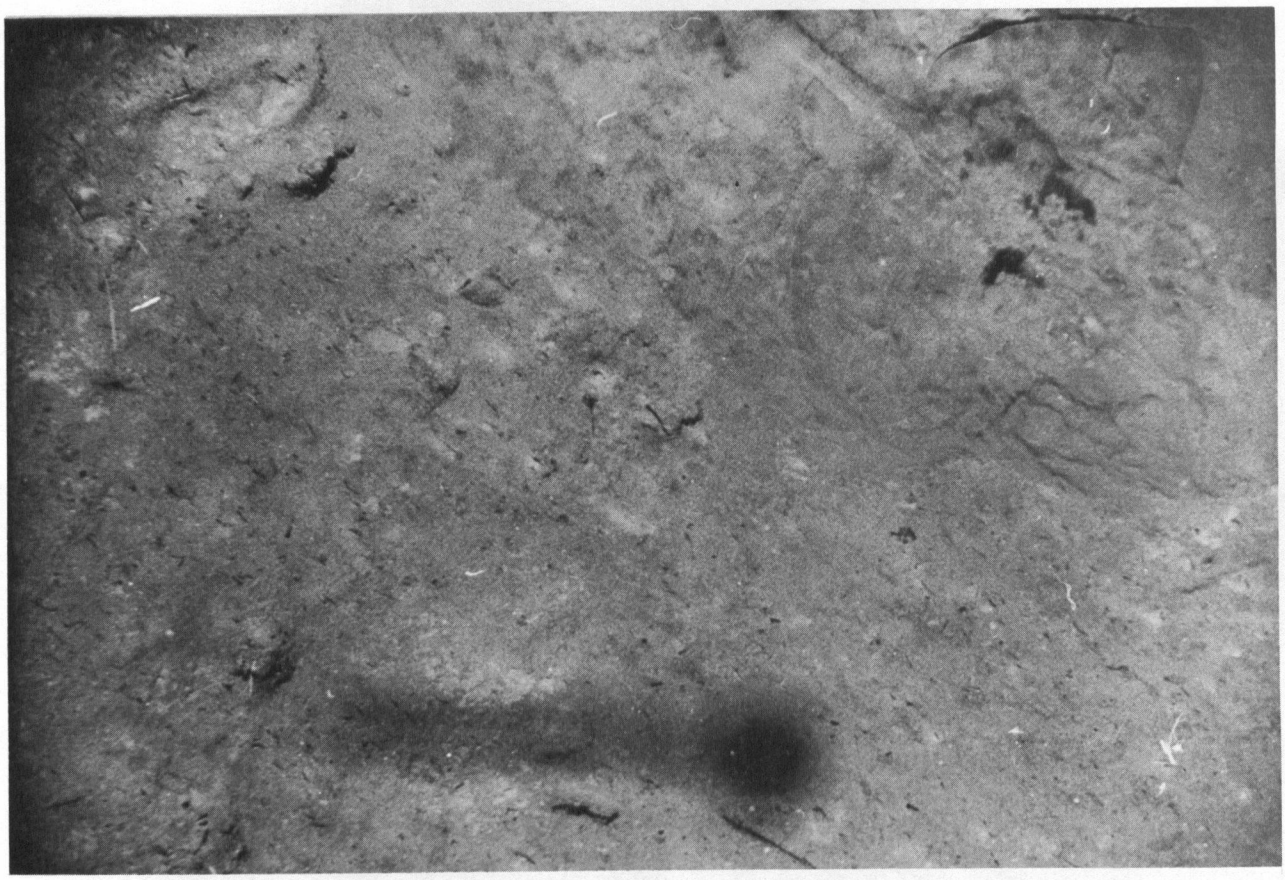

a

FIGURE 27 BOTTOM PHOTOGRAPHS – STA. J–126

b

coarse mode decreases with depth, while that of the finer mode increases.

Figures 26 and 27 are bottom photographs taken at Station J-126. These were taken at a depth of 180 fathoms (330 meters) which is the maximum depth in the upper basin. Each photograph covers an area measuring about 3 by 4 feet, (1 by 1.3 meters). The microtopography appears hummocky. The origin of these hummocks is not known, but animals obviously have some effect as shown by Figure 27a in which a skate had just partially buried itself in the sediment. However, photographs taken in an area where slumping is almost certainly occurring (Figures 34 and 35) show a similar topography. Thus, slumping is also a possible explanation for the topography pictured. Photographs of better quality, covering a larger area and preferably as stereo pairs would be very advantageous to such interpretation.

Perhaps the most interesting area, even from a sedimentologic point of view, is Patrick Sill. The medial depression or V-notch and the flanks of the sill in line with the notch are apparently areas of sediment reworking. Figure 28 illustrates how the sediment characteristics change in passing from the upper to the lower basin over Patrick Sill. The

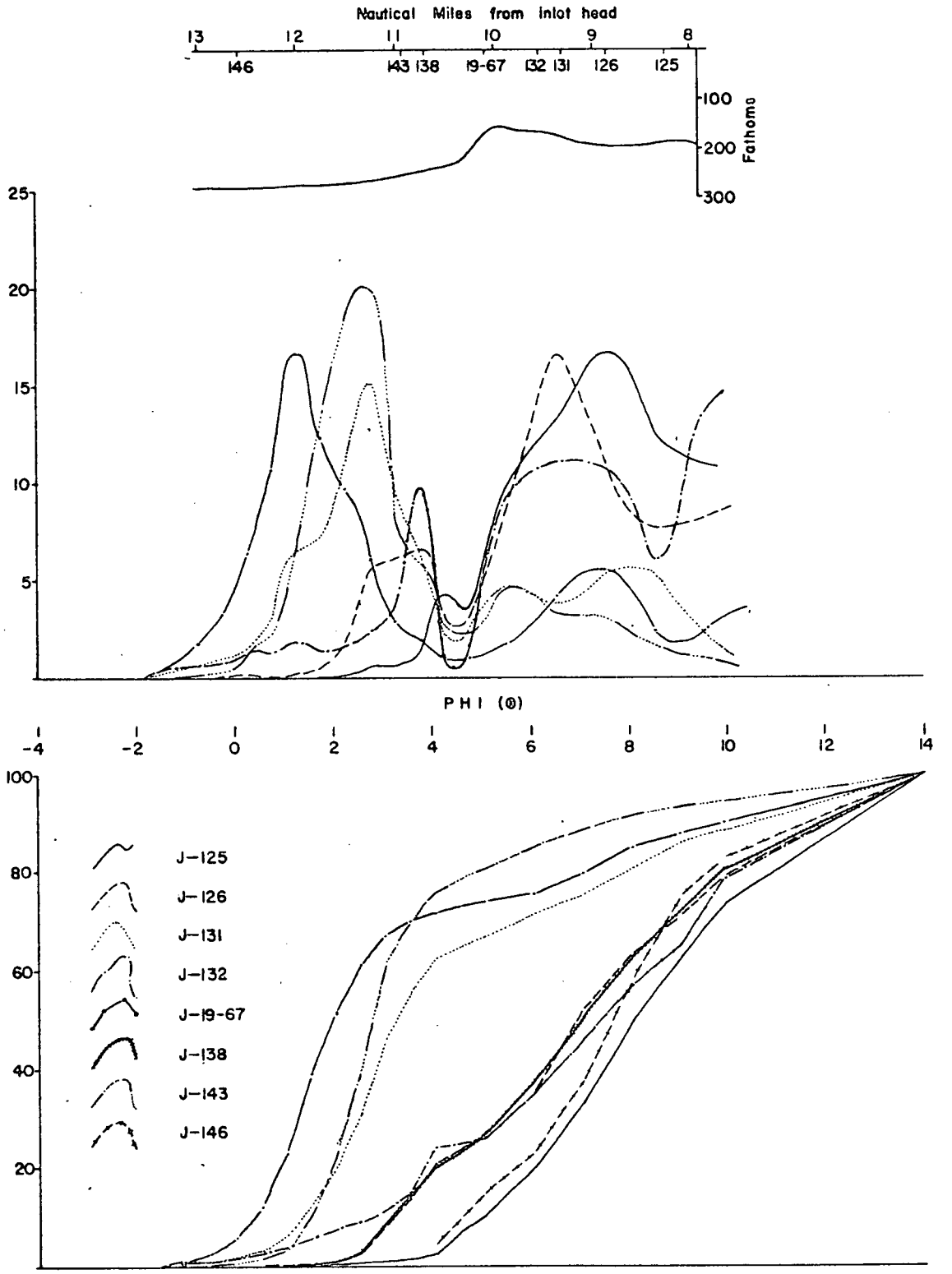

FIGURE 28 LONGITUDINAL PROFILE OF LOWER QUEENS REACH AND UPPER PRINCESS ROYAL REACH — CUMULATIVE AND FREQUENCY CURVES OF SURFICIAL SEDIMENTS

sediments collected above and below the sill (Stations J-125 and J-146 respectively) are very similar. The concretion locality (Station J-19-67) sediments have a mean diameter of 63/u (4Ø) with a high standard deviation. Skewness is high and kurtosis is low. Apparently a current is winnowing the sediment, leaving a lag deposit of material with a dominant mode in the 250 to 125/u (2Ø to 3Ø) range. This sediment is noticeably coarser than any other collected in the study area from depths greater than 100 fathoms (183 meters). The photographs in Figures 29 and 30 were taken near the nodule locality. The rock out-cropping in Figure 29a may be a glacially rafted boulder, but appears to be bedrock. The current direction would be perpendicular to the plane in which the gorgonian coral is growing. Figures 29b and 30a show the lag deposit and Figure 30b a more typical bottom sediment, near but not in the medial depression, indicating the maximum intensity of the current is confined to the medial depression.

Sediments collected on the sill flanks at Station J-131 and J-143 were similar in grain size

Figure 29 a Bedrock or large boulder in vicinity of concretion locality. Low rates of sediment deposition in this area allow animal growth. Plane of gorgonian coral in background is normal to current direction. (approx. 1/8 X)

b Lag deposit in area of concretion locality. Note abundance of squat lobsters. (approx. 1/8 X)

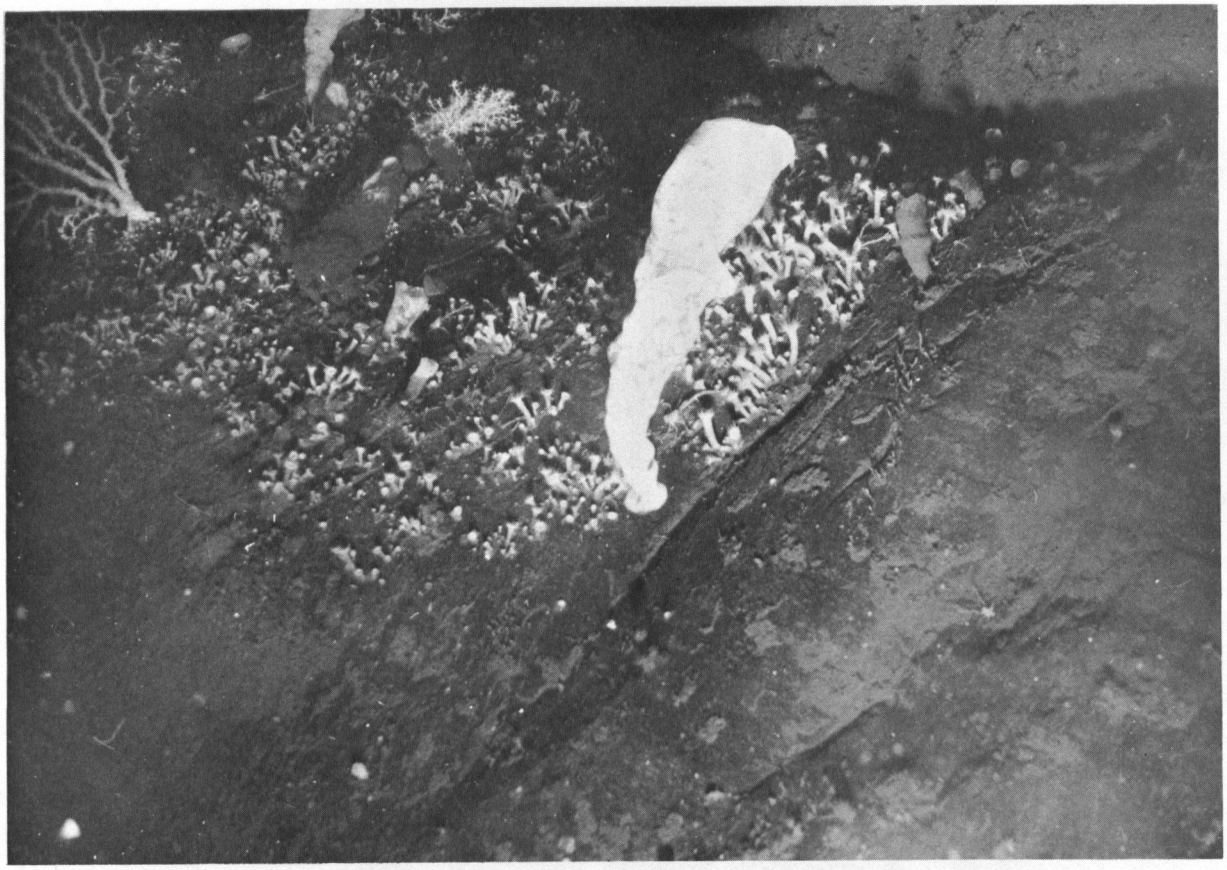

a

FIGURE 29 BOTTOM PHOTOGRAPHS - STA. J-19-67

b

Figure 30 a Photograph taken on slope of medial depression. A low sedimentation rate is indicated by the presence of siliceous sponges etc. (approx. 1/8 X)

b Photograph taken on slope of medial depression to the east of the concretion locality. A low sedimentation rate is indicated as well as minor influence of bottom currents (approx.1/8X).

a

FIGURE 30 BOTTOM PHOTOGRAPHS - STA. J-19-67

b

distribution. If the origin of the dominant mode in the 250 to 125 μ (2Ø to 3Ø) range were the crest of the sill, a current velocity of at least 25 cm/sec. must flow in the medial depression. Slumping may carry the material derived from the sill to the flanks as the current velocity within the medial depression probably would not be maintained over the flanks. The two-way action of the current through the depression indicated by sediment parameters and size distribution curves, suggests a tidal origin. However, current action in the south easterly direction apparently is more pronounced.

Cumulative and frequency curves plotted for sediments collected on the sill along a line transverse to the medial depression are presented in Figure 31. Most noticeable is the very poor sorting, especially for samples collected on either side of the medial depression. The deeper the sample station, the more dominant is the coarse fraction. This trend is the reverse of that pictured in Figure 25. The very poor sorting and wide range of grain sizes indicates that the surficial sediments of the sill are probably of a glacial origin and, with exception

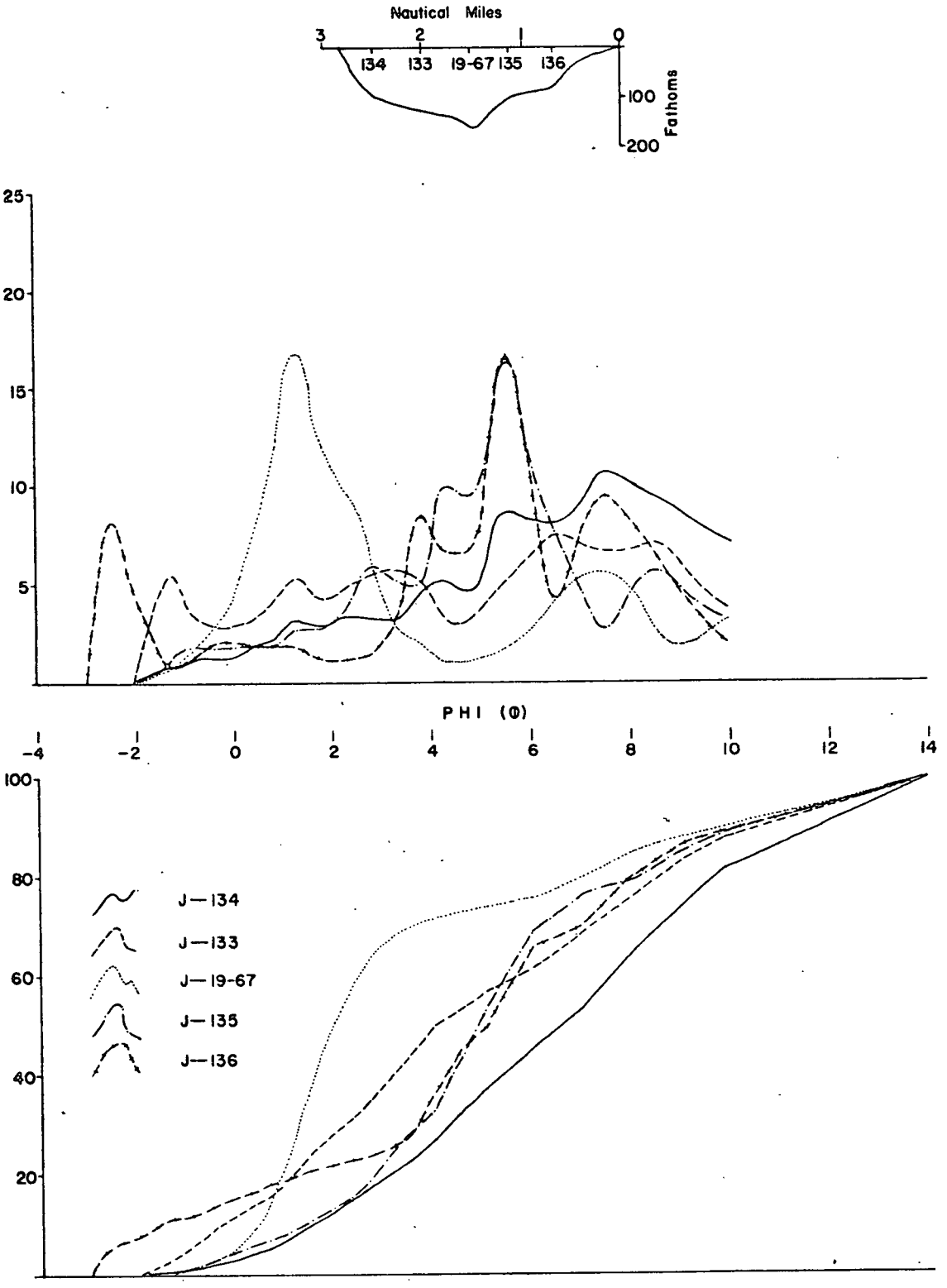

FIGURE 31 TRANSVERSE SECTION OF QUEENS REACH (OVER PATRICK SILL) — CUMULATIVE AND FREQUENCY CURVES OF SURFICIAL SEDIMENTS

of those sediments in the medial depression, have been little affected since initial deposition in Pleistocene time.

The distribution characteristics of sediments collected along the axis of Princess Royal Reach (lower basin) are presented in Figure 32. The two dominant sediment modes apparent on a similar longitudinal profile for the upper basin (Figure 24) are apparent in sediments from the lower basin. However, the material collecting in the lower basin is originating from many sources, each with a localized effect, whereas that in the upper basin comes from one dominant source. This is even more apparent in Figure 20 (in pocket).

Evidence of slumping was obtained from Station J-160. Figure 33 presents cumulative and frequency curves for a section approximately transverse to the axis of Princess Royal Reach. Depth recordings made while attempting to collect a sample on Station J-160 indicate that the south wall of Princess Royal Reach is much steeper than shown on the Hydrographic Service charts. The sediment sample collected on Station J-160 at a depth of 285 fms.(522 meters) contained abundant shallow and mid-depth faunal

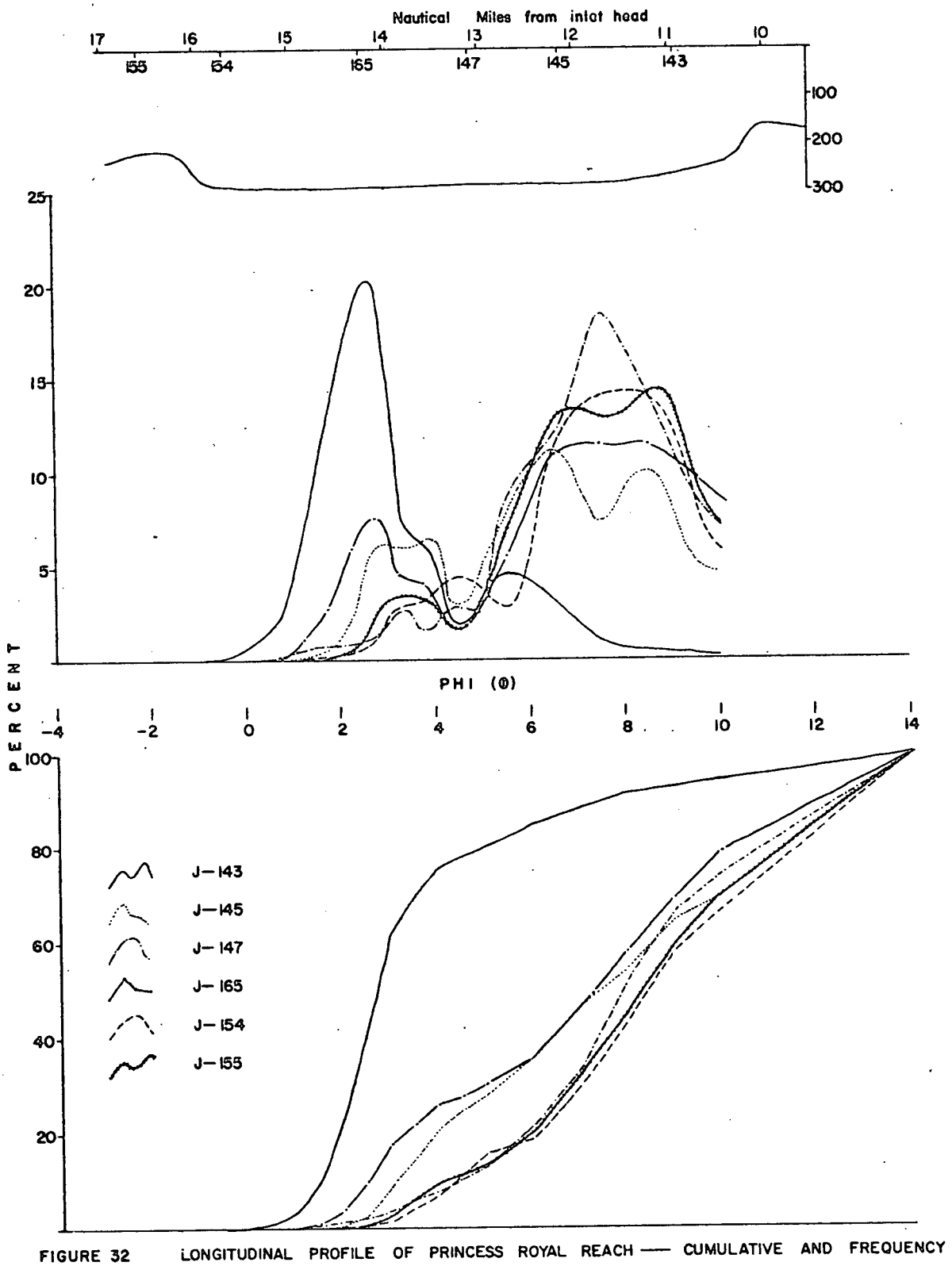

FIGURE 32 LONGITUDINAL PROFILE OF PRINCESS ROYAL REACH — CUMULATIVE AND FREQUENCY CURVES OF SURFICIAL SEDIMENTS

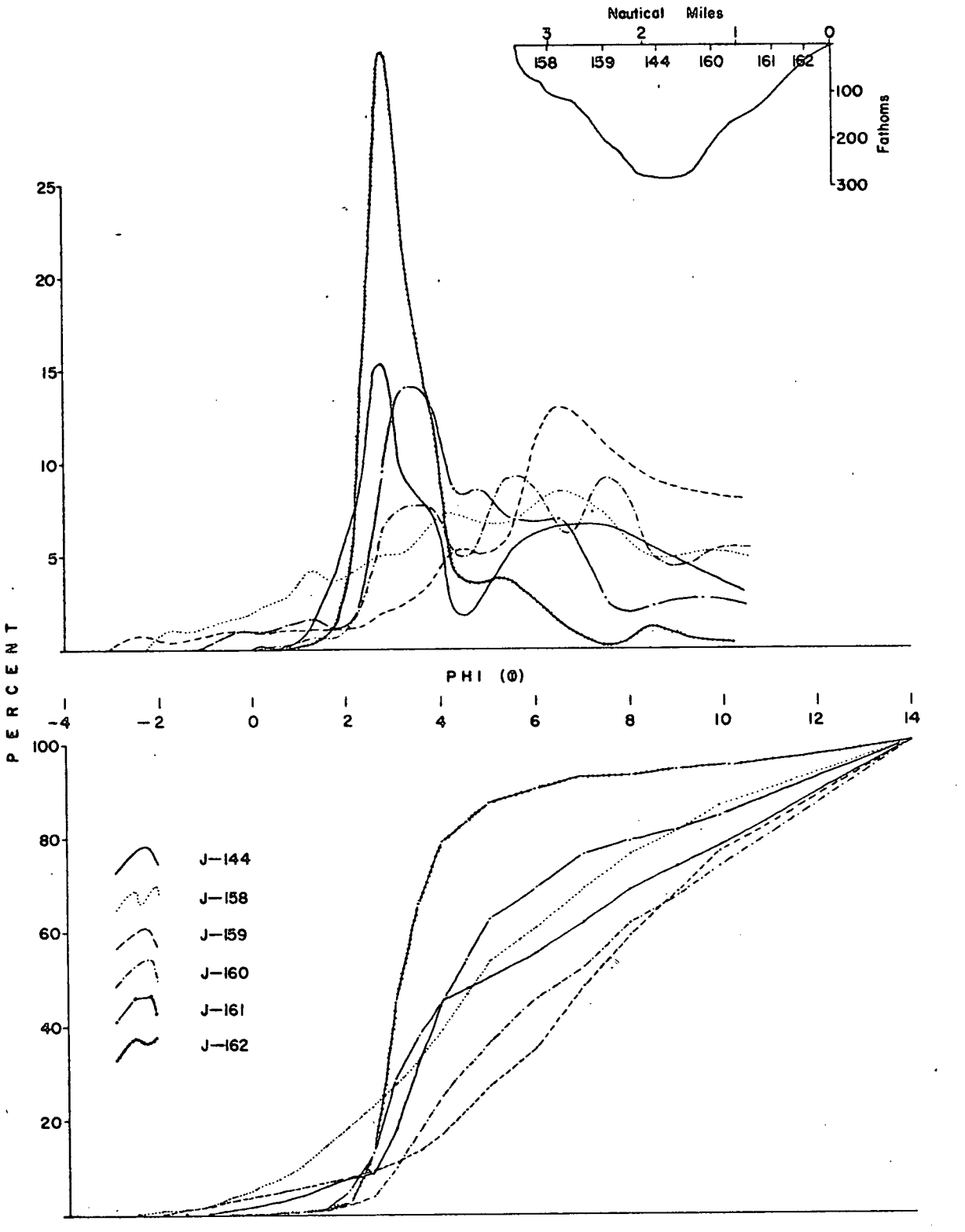

FIGURE 33 TRANSVERSE PROFILE OF PRINCESS ROYAL REACH — CUMULATIVE AND FREQUENCY CURVES OF SURFICIAL SEDIMENTS

remains. Identified as contributors to the shell debris were blue mussels (Mytilus edulis), brachiopods (Laqueus californicus vancouverensis), pelecypods (Thyasira cygnus and an unidentified pectin), scaphopods (Cadulus tolmei) and numerous solitary corals (Balanophyllia elegans and Caryophyllia alaskensis). Also included in the organic debris were numerous wood fragments. One of the photographs taken showed a partially decomposed tree trunk embedded in the sediment. Figures 34 and 35 are bottom photographs taken on Station J-160. The hummocky topography resembles that appearing in Figures 26 and 27 taken on Station J-126.

Sediment collected at Station J-162 was predominantly medium to fine sand, likely deposited as a delta by the large stream flowing into the inlet nearby (Figure 33). Sample J-161 was collected further offshore from J-162 at the top of the steep slope leading to the basin floor. Sediments collected from J-161 resemble those deposited further inshore (J-162) but with a less pronounced medium to fine sand mode and a greater abundance of silt size material. However, the sediment collected at Station J-160 near the bottom of the slope

Figures 34, 35 Photographs taken in area where abundant shallow water faunal remains were recovered. The depth this station was 285 fathoms (522 meters).Note disordered, hummocky topography. All photographs approx. 1/8 X true scale.

a

FIGURE 34 BOTTOM PHOTOGRAPHS - STA. J-160

b

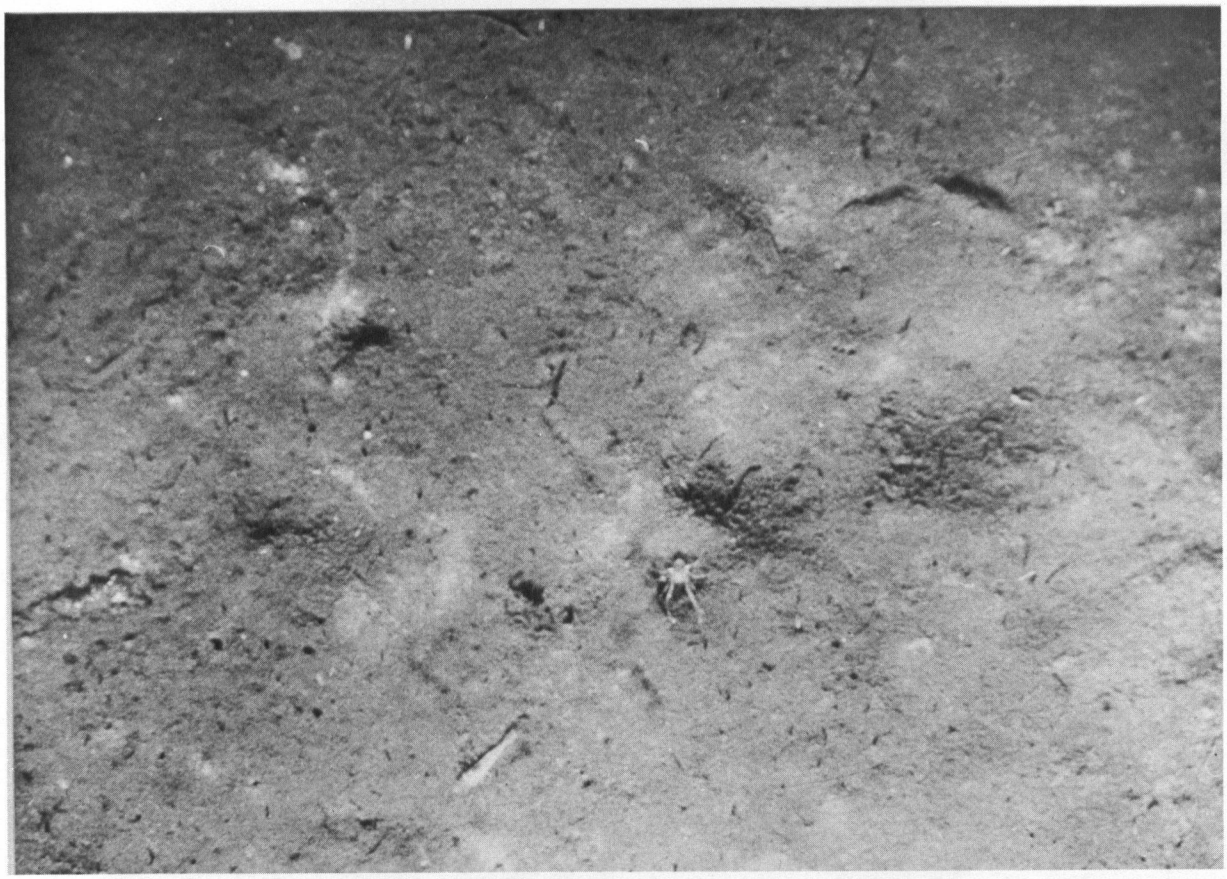

a

FIGURE 35 BOTTOM PHOTOGRAPHS – STA. J-160

b

only vaguely resembles that of Station J-161. As Station J-162 is located near the south foot of the sill, perhaps the sediment accumulating there has more than one source. The pronounced double mode in the silt-clay region of particle size distribution also occurs in the sediment collected further down the inlet at Station J-145 (Figure 32).

VII. Characteristics with Depth

Four gravity cores, taken at sites shown in Figure 36, were split as previously described and logged visually. Generally the cores appear featureless. The average colour of the three cores taken in the upper basin matches that of the surficial sediments and was best described as grayish olive(10Y4/2). The core taken from the lower basin was a noticeably darker olive gray (5Y3/2). The majority of structures shown in Figure 36 appear as slight changes in hue which were most visible just after the core had been split and the surface smear washed away. The average grain size of the core material resembles that of the corresponding surficial sediments, i.e. the three collected in the lower part of the upper basin are silty clays, whereas the core material from the lower basin is a clayey silt with minor fine sand.

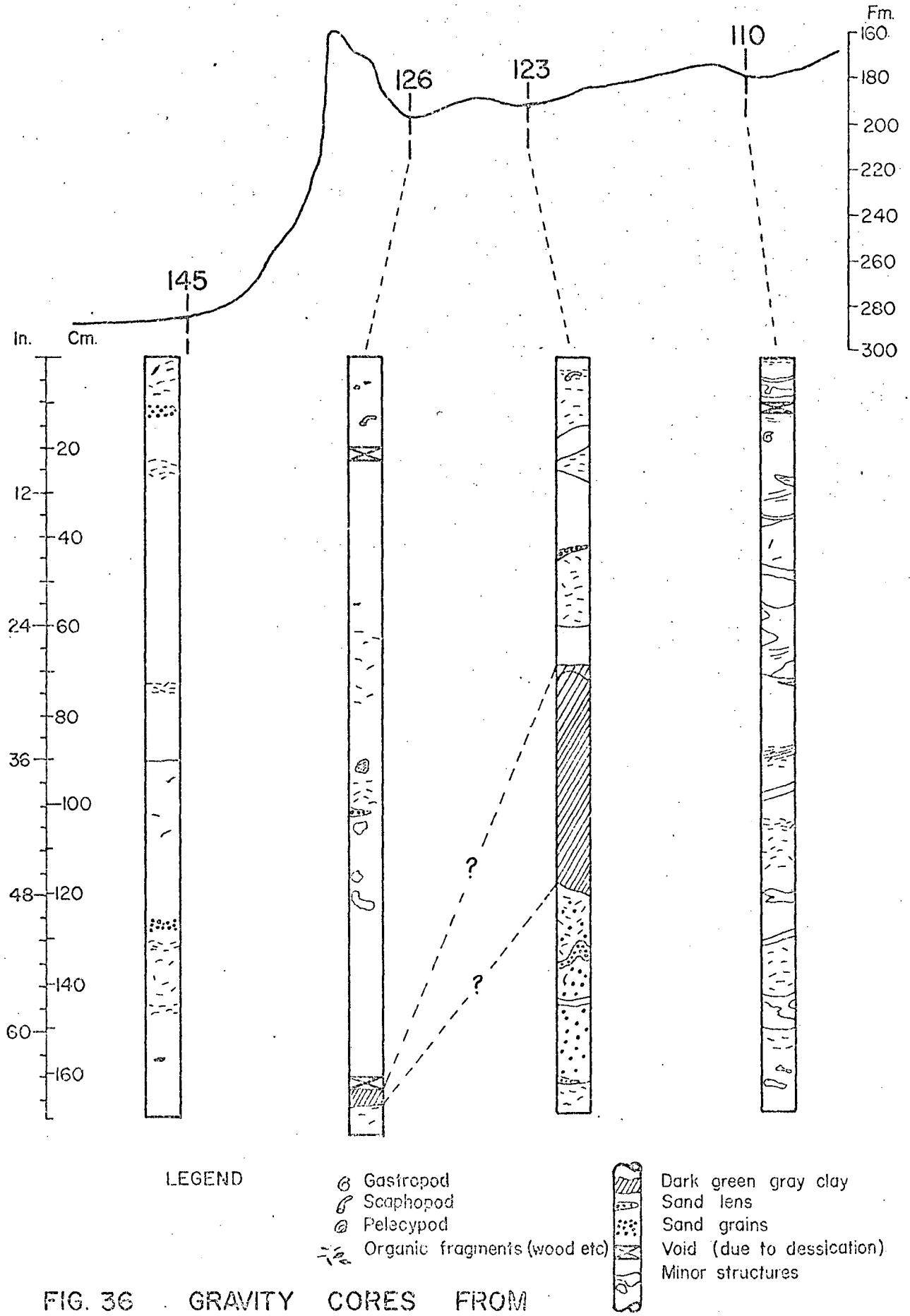

FIG. 36 GRAVITY CORES FROM UPPER JERVIS INLET.

The core taken at Station J-123 contained three distinct, but thin, layers of fine sand and a two-foot layer of a green-gray clay. The core taken at J-126 contained a single thin sand layer and a much thinner layer of green-gray clay. This clay represented the only lithology that may be useful as a reference horizon. The sand layers appeared to represent discontinuous lenses.

The competency under stress of the green-gray clay is much less than that of the more typical gray-olive to olive-gray sediment. Thus the material may be quite mobile as the sediment column compacts. This may explain the thick section in core J-123 but minor occurrence in core J-126 and absence in core J-110. Small diameter (Phleger) cores taken by Dr. E. V. Grill on and in the vicinity of the concretion locality on Patrick Sill contained green-gray clay starting at depths of 12 to 24 inches (30 to 60 centimeters). If large areas of the surficial sediments on the sill are underlain by this clay it would likely promote decollement and slumping into the basins on either side.

Wood fragments were the most abundant coarse material. These were not evenly distributed throughout

the core, but tended to be abundant in particular horizons. Generally the fragments occurred with their long axis parallel or sub-parallel to the bedding indicating a non-turbulent deposition. However, in some layers within the cores, the fragments were randomly oriented indicating a turbulent deposition as in a slump (e.g. core J-123 4'00" to 4'02"). A few shells and shell fragments were visible in the cores. Recognizable were gastropod, scaphopod, and pelecypod shells. The latter two belonged to the same species recovered in the surficial sediment samples (i.e. Cadulus tolmei and Thyasira cygnus respectively).

Possibly more information could have been derived from longer cores. The collection of these would present no problem if the sediment mechanical characteristics at greater depths do not change markedly from those of the cores already taken.

CHAPTER 7

SEDIMENTATION IN JERVIS INLET

Studies in the Fraser Valley by Armstrong and Brown (1965) revealed that much of the late Pleistocene sediments are fossiliferous stony, silty clays. The stony clays are mixtures of varying proportions of marine drift and normal marine clays. Basal sediments are marine drift but these decrease in abundance upwards and are replaced by normal marine clays. This transition occurred with the waning of the continental ice sheet. Marine drift was carried by and deposited from shelf, berg and sea ice. As the ice disappeared, rivers became the principal method of transport. The river-borne materials were deposited as normal marine clays.

The total depth of sediments within the basins studied was determined from seismic profiles, but the sedimentation rate cannot be calculated because of its time dependence. The average rate for the entire inlet of 14 inches (35 centimeters) per 1000 years estimated by Pickard (1960) for present sediment accumulation is still the most valid available. As Pickard mentions, this rate is likely higher within the upper reaches of the inlet where most of

the sediment is added to the system. Material added by slumping from the inlet sides would increase this estimated rate.

The green-gray clay was an anomalous lithology within the cores. The depths of this clay may be misleading because the incompetent nature of the material may allow horizontal and vertical movement as the total sediment column compacts. The green-gray clay was found within typical olive-gray marine sediments. Cores taken elsewhere along the continental shelf (e.g. Barclay Sound and Queen Charlotte Sound) also penetrate a horizon of green-gray clay. The significance of this clay is not known but in view of its apparently widespread distribution further study may prove rewarding.

Sediment is being transported to the basin floors by several mechanisms. These include settling through the water column of fine-grained fluviatile material and periodic slumping of coarser grained material from the steep inlet walls with the possible initiation of turbidity currents. The optical turbidity data presented by Pickard indicates that a major percentage (up to about 50%) of suspendable material added to the inlet waters from the river at the head is carried down the inlet within the low

salinity surface waters. There is however, a marked increase in turbidity on the bottom waters of the upper basin. In explanation Pickard suggested bottom currents or turbidity currents.

Slumping almost certainly occurs from the steep inlet walls which have an average slope of about 35°. The abundance of shallow water faunal remains at the base of a steep submarine cliff in the lower basin (Princess Royal Reach) attests to this. Other active areas are the large deltaic deposit off Malibu Rapids, which is swept by the tidal jet through the narrows, and perhaps all the smaller deltas which likely became unstable during periods of rapid sediment accumulation. Slumping is also thought to occur at the inlet head and perhaps on the south facing flank of Patrick Sill where long unbroken slopes may result in the formation of turbidity currents.

Gravity cores collected within the upper basin were examined only visually and revealed no distinctive graded bedding. Future examination by X-ray or by thin-section may give more information.

The lack of orientation of elongate organic fragments within certain horizons in the cores suggests deposition under turbulent conditions.

Sand lenses within the cores taken from the upper basin likely represent the influence of slumping from the nearby inlet walls rather than from the inlet head. Bottom photographs taken in the upper basin show a hummocky non-oriented topography. These support Pickard's conclusion that bottom currents are probably not the cause of the turbidity pattern described. If bottom currents were sufficiently strong to stir up the sediments, bed forms with a distinct orientation should have been visible in the photographs.

There is a marked difference in grain size distribution between the upper and lower basins. Patrick Sill forms a boundary between these basins. To explain the depositional patterns, one must postulate either that the sill arrests the dominant depositional mechanism influencing the upper basin, or that the streams flowing into the lower basin have a much greater effect than those which flow into the upper basin. The relief of the sill is not sufficient to act as such an effective barrier if the majority of sediment is being added to the upper basin by the settling of particles through the water column. However, the sill is high enough that it would likely bar the passage of a density or turbidity current.

CHAPTER 8

AUTHIGENIC MINERALS

I. MANGANESE CONCRETIONS

1) Source Area

Manganese concretions occur in the medial depression or V-notch on the south-facing slope of Patrick Sill. (Figure 37 - in pocket). Depth of the locality is between 175 and 190 fathoms and the areal extent is estimated to be 36,000 square yards (30,000 square meters). As mentioned, the sill is thought to be a bedrock feature mantled by post-Pleistocene sediments of varying thickness. There is little possibility these sediments pre-date the last major glacial advance in view of the estimated thickness of the ice sheet which passed over the area.

The sediments collected with the concretions were generally similar to those collected elsewhere within the area studied. However, some sediment samples recovered from the concretion locality indicated the presence of a flocculant red-brown surface layer, one to several centimeters in thickness. The sediment within this layer often had a predominant coarse-grained component which is thought to represent a

lag deposit. If the abundant fine sand noted at Station J-143 came from the concretion area, then the current within the V-notch must attain velocities of about 25 centimeters/second in order to move the sand. Underwater television observations of the locality substantiated the existence of a bottom current of approximately the velocity calculated. Bottom photographs taken on the sill show what appears to be a lag deposit associated with the concretions. Lag deposits are not evident in photographs taken near, but not on the concretion locality. Apparently, the strongest currents in the area occur where the concretions are forming. Sedimentation rates here should be correspondingly low. The total extractable iron and total carbon contents of the sediments recovered with the concretions were anomalously low. The low carbon content would reflect the sweeping away of the light organic material by the current. Figures 38 and 39 are photographs of the concretion locality.

2) Age and Growth Rates

The maximum age of the concretions would be determined by the time of ice retreat after the last major advance during the Pleistocene. This is

Figures 38, 39 Photographs taken on the concretion locality. The rounded, exposed to partially buried masses are manganese concretions. Note general coarse texture of surficial sediments. All photographs approx. 1/8 X true scale.

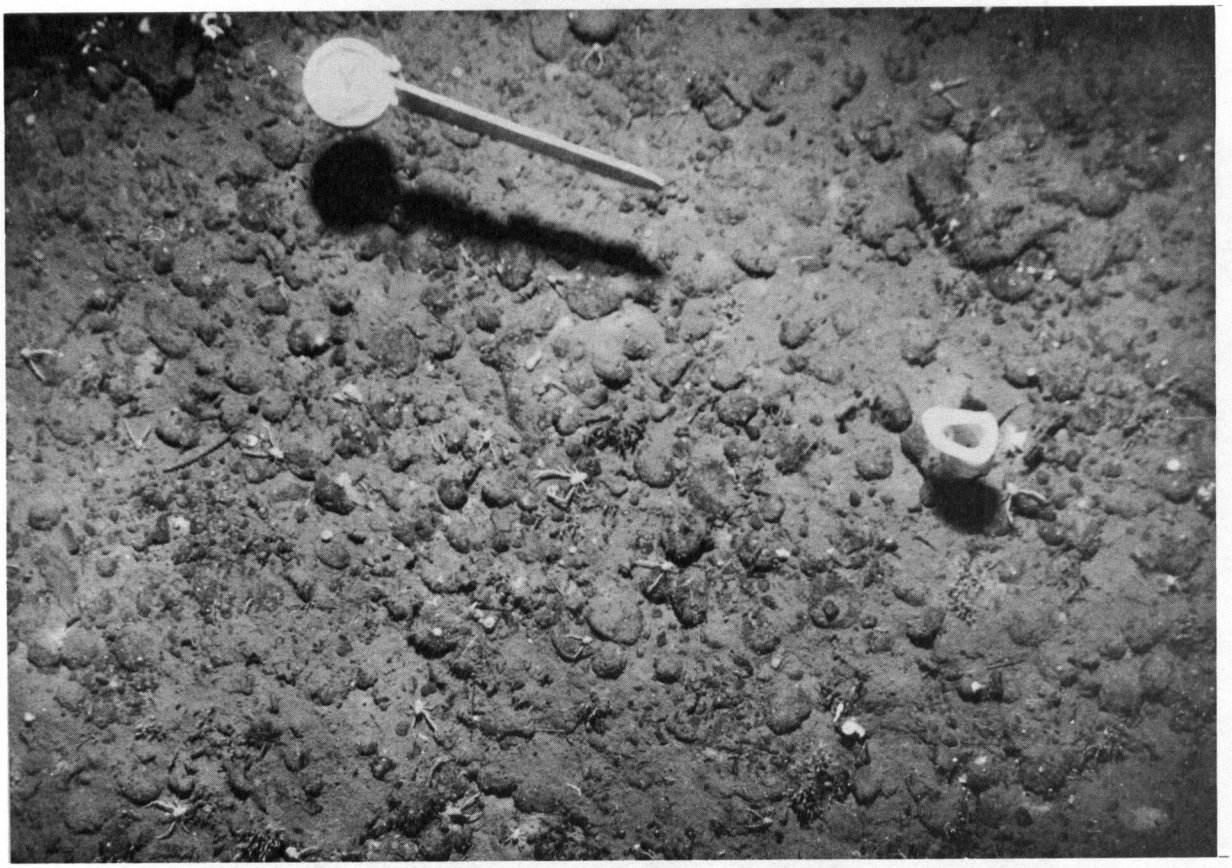

a

FIGURE 38 BOTTOM PHOTOGRAPHS - CONCRETION LOCALITY

b

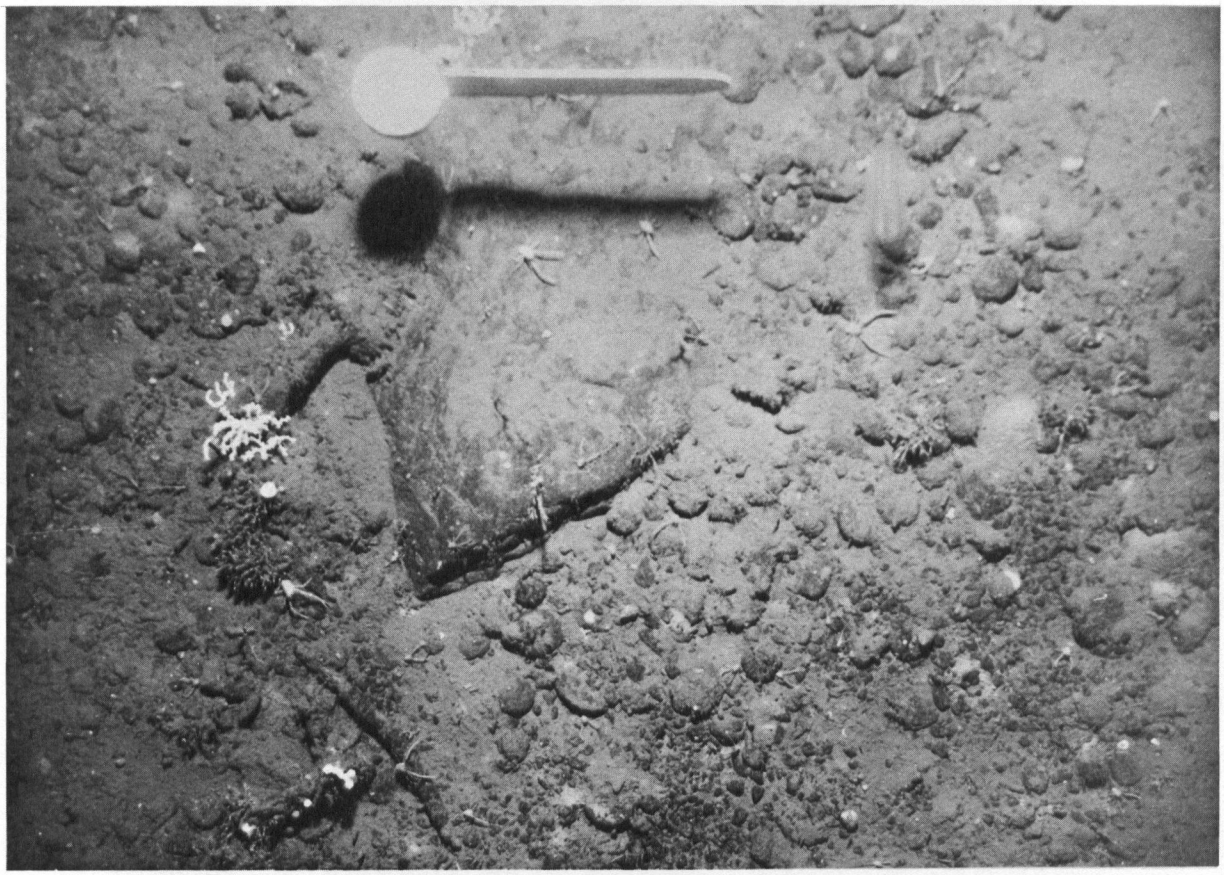

a

FIGURE 39 BOTTOM PHOTOGRAPHS - CONCRETION LOCALITY

b

estimated to be about 12,000 B.P.(Armstrong et al). Evidence that the concretions formed in situ is provided by the recovery of siliceous sponges having a thick manganese-iron oxide coating. The discoid shape and friable nature of the concretions precludes transport.

The maximum thickness of oxide material measured on any one concretion was 1.4 inches (35 millimeters). The accumulation rate of oxide material is highest in the horizontal plane. Assuming the age of the concretions to be 12,000 years, the apparent growth rate would be in the neighbourhood of 3 millimeters/ 1000 years or less. This value is somewhat lower than the general accumulation rate of 10 to 1000 millimeters/1000 years suggested by Manheim (1965) for shallow marine concretions. However, Manheim noted that concretion development in nearshore environments may be very irregular with wide variations over small areas. The porous nature and wide variation in lamination thickness of Jervis Inlet concretions suggests the deposition rate was erratic, and, when deposition was occurring, much more rapid than the average rate of 3 millimeters/1000 years.

3) Structure

The concretions occur in two distinct shapes -- discoidal and spheroidal. Discoidal masses are usually larger and range up to 6 inches (15 centimeters) in diameter. Rock fragments, mostly granitic, form the nucleus of all specimens examined. The upper surfaces of the concretions are dark red-brown to brown, the under surfaces light yellow-brown. Brachiopods, serpulid worm tubes, bryozoan plates, siliceous sponges and corals may be attached to the upper surfaces.

The discoidal concretions frequently exhibit several interesting features. A side view (Figure 40a) reveals the typical shape of this variety with a rock nucleus surrounded by a skirt of oxide material. The under-surface of the skirt is usually even, and flat or concave downwards in contrast to the upper surface which is often very irregular. Some specimens of discoidal concretions have apparently been rotated about a horizontal axis at one time during their formation. On one side of the nucleus the oxides have accumulated in two lobes or skirts to form a lip-like structure while the opposite side

Figure 40 a Side view of a large discoidal manganese concretion. The nucleus is a granitic boulder. Major diameter 5.5 inches (13.1 cm.)

b Small diameter (1.2 inches or 3 cm) spheroidal concretion with attached siliceous sponge.

c Coalescence of two ~~discoidal~~ spheroidal concretions. Major diameter approx. 3 inches (7.5 cm.)

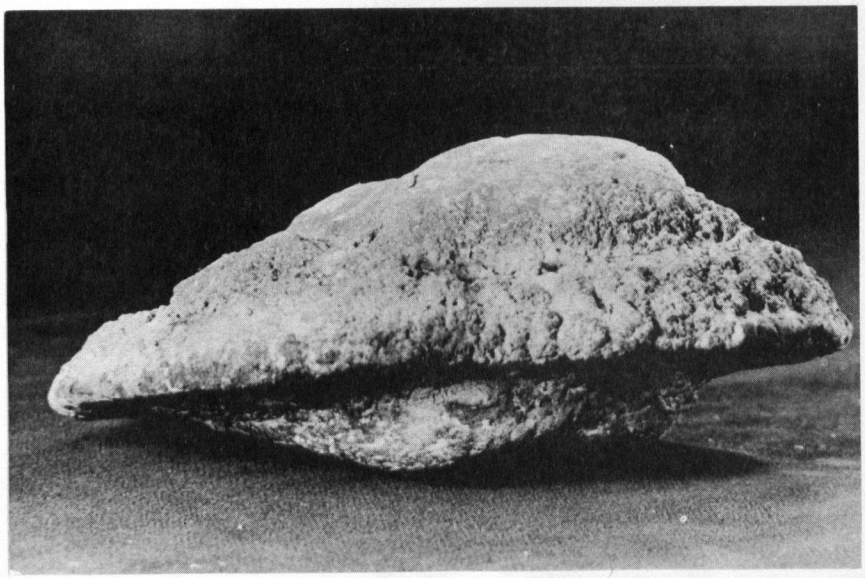

a

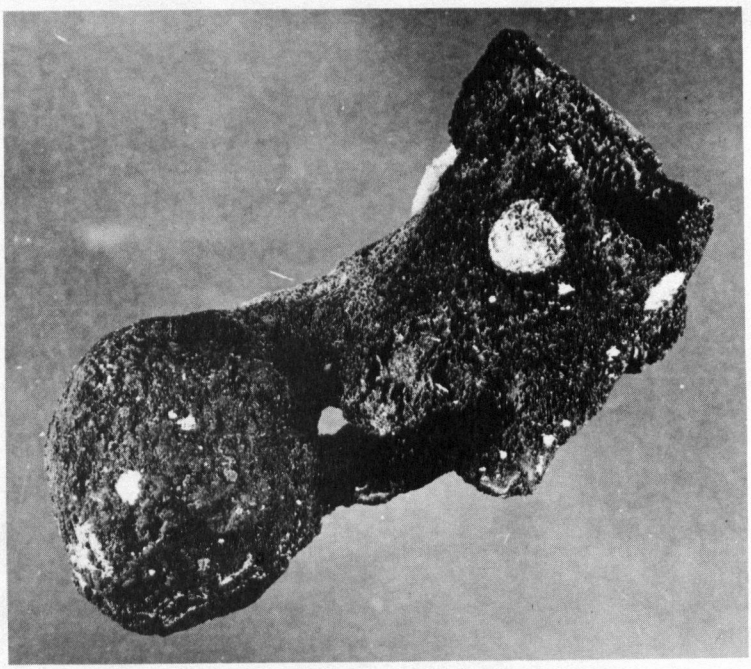

b

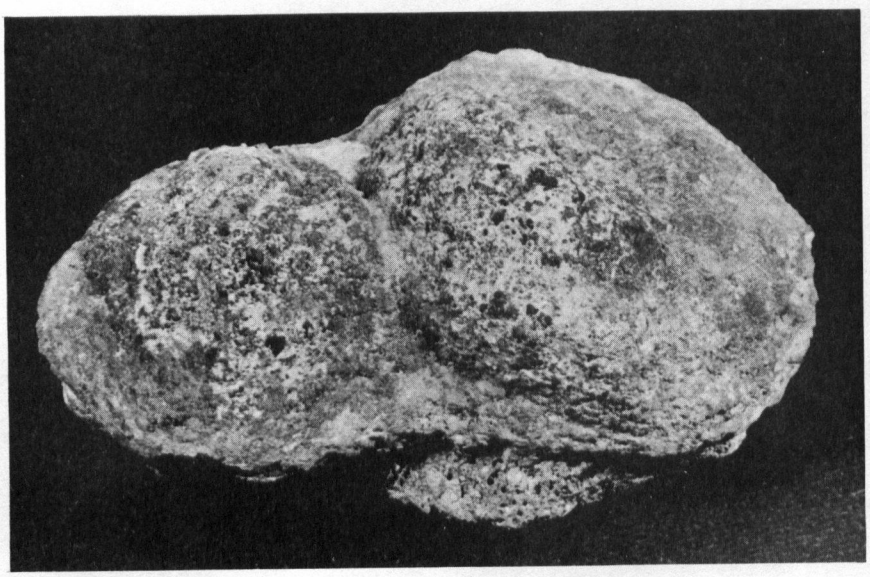

c

FIGURE 40

of the nucleus is nearly devoid of oxides. Oxide materials are apparently deposited about a nucleus in a plane paralleling the sediment water interface. The asymmetry in plan view of the oxide skirt of many of the specimens indicates a favoured direction for greatest growth. This orientation is also exhibited by the oxide crusts which have formed as plateaus on dead siliceous sponges which have toppled.

The nuclei of spheroidal concretions are completely enclosed by oxides. The difference between spheroidal and discoidal types may be due in part to the size and shape of the nucleus. The generally smaller and more equidimensional nuclei of the spheroidal types perhaps allow these to be rolled about the bottom by currents or animals. Figure 40c shows two spheroidal masses which have coalesced with the formation of a surrounding skirt. Since coalescense, this mass has behaved as a discoidal concretion.

Cross sections of concretions are pictured in Figures 41 and 42. The dark laminations correspond to finer-grained material and are generally much thinner than the lighter coloured layers. The lighter coloured laminations include most of the

Figure 41 a Cross-section of discoidal manganese concretion (approx. 5.5 X). The nucleus is an angular fragment of granitic rock.

b Corresponds to area outlined in photograph 'a'. Textural, colour and thickness differences between successive layers of oxide materials likely indicate erratic growth rates. (approx. 44 X)

c Corresponds to area outline in photograph 'a'. The unconformity shown may have been the result of tilting of the concretion with subsequent change in preferred growth direction. (approx. 44 X)

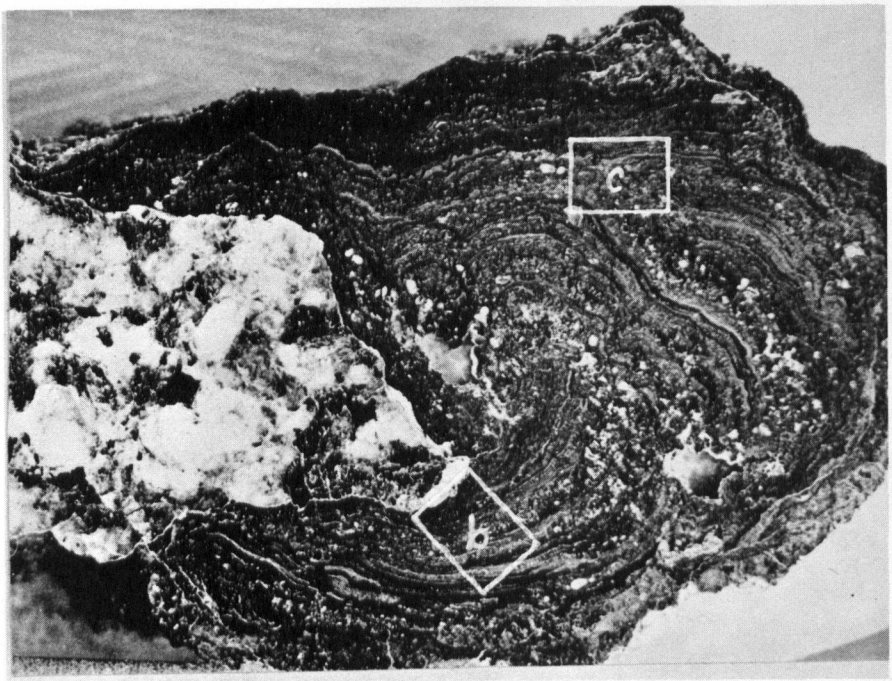

a

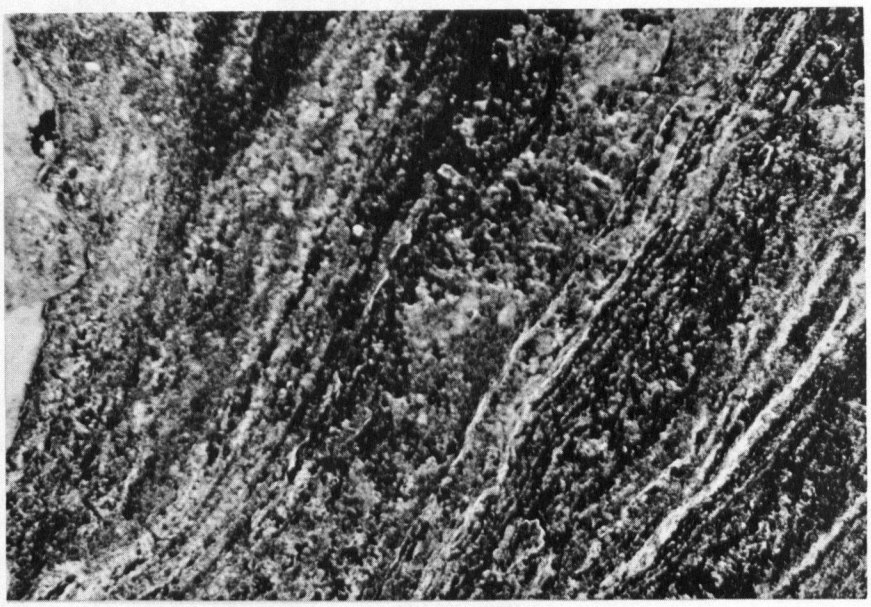

b

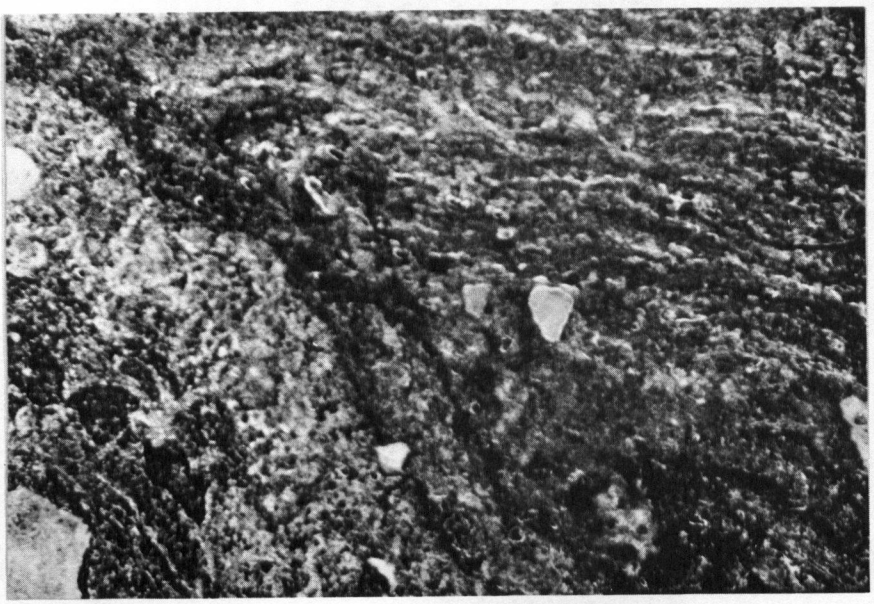

c

FIGURE 41

Figure 42 a Cross-section of middle portion of discoidal concretion which had nucleus completely enclosed by oxide materials (approx. 4.3 X). Early layers of oxides were preferentially deposited on left side of nucleus as it appears in the photograph.

b Enlargement from concretion pictured in 'a' showing detrital mineral included in accreted oxide materials. Detrital minerals are generally most abundant in the porous, lighter coloured oxide layers (approx. 43 X).

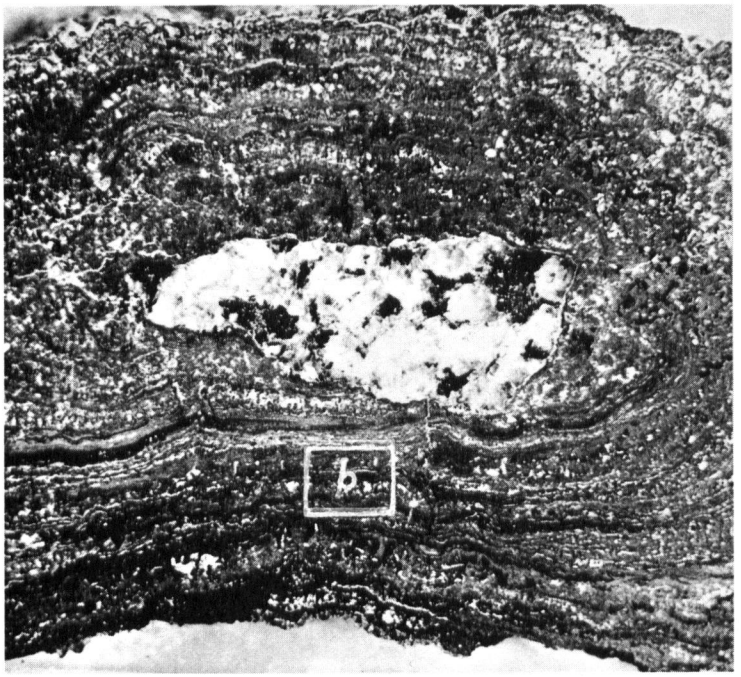

a

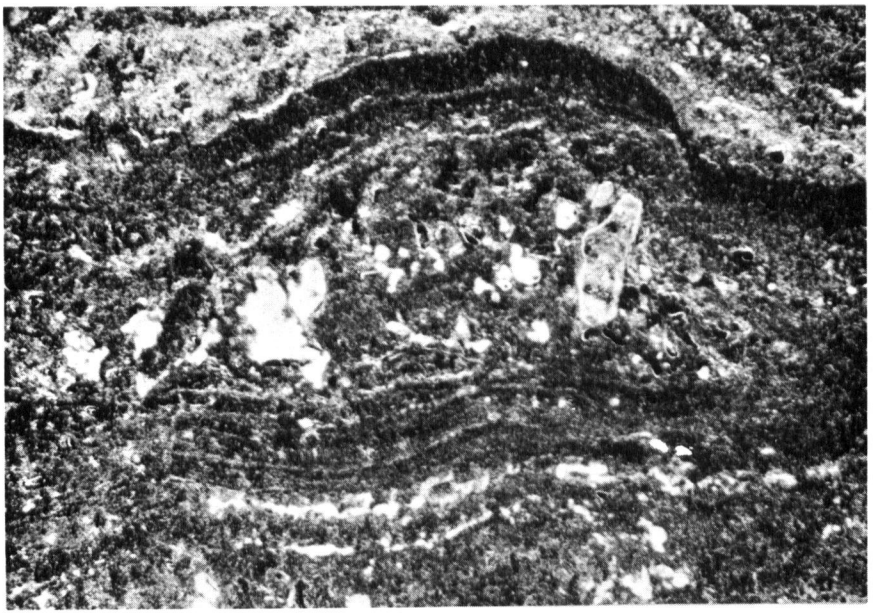

b

FIGURE 42

detrital material. Apparently the darker layers represent periods of slow deposition. In a vertical section the laminations are shown to be reasonably symmetrical about a horizontal plane. Figure 41c shows the effect of either periods of erosion of oxide materials followed by renewed deposition or of changes in position of the concretion. The latter idea is favoured because unconformities are not evident.

Detrital minerals included by oxides are predominantly quartz and feldspars. These also dominate in the underlying sediments.

4) Chemical Composition

The chemical composition of the concretions was determined by Dr. E. V. Grill of the Institute of Oceanography (Table 6). For purposes of comparison, Table 7 gives the average compositions of deep ocean and Baltic Sea concretions and the composition of shallow water concretions from the Vermilion Sea off Baja California (Manheim 1965 and Mero 1965).

Total carbon analyses of Jervis Inlet concretions indicated a carbon content equal to or slightly less than that of the underlying sediments (which had an average content of 1.26 per cent).

Table 6 Chemical Analyses of Jervis Inlet Concretions

(Analyses by Dr. E. V. Grill, I.O.U.B.C.)

Sample	A*		B	
% Soluble	81.75		81.09	
Fraction	Soluble	Insoluble	Soluble	Insoluble
Fe_2O_3	7.65	3.06	6.55	2.45
FeO	-	1.79	-	1.23
MnO	51.70	0.10	52.31	0.10
SiO_2	2.3	64.9	-	67.1
Al_2O_3	0.41	15.8	0.71	15.3
TiO_2	0.096	0.62	0.085	0.58
P_2O_5	0.94	0.11	0.72	0.16
Na_2O	1.06	2.27	1.05	2.37
K_2O	1.11	1.52	1.18	1.51
MgO	3.19	2.24	3.36	1.66
CaO	1.55	3.19	1.56	3.17
BaO	0.27	0.55	0.36	0.83
MoO_3	0.041	0.007	0.049	0.006
V_2O_5	0.028	-	0.043	-
CoO	0.020	-	0.022	-
NiO	0.040	-	0.060	-
CuO	0.0084	-	0.014	-
ZnO	0.0029	-	0.0056	-
PbO	ND	-	ND	-
TeO_2	0.018	-	0.020	-
SO_3	0.18	-	-	-
CO_2	0.56	-	-	-
NaCl	1.09	-	1.09	-
Active O	10.12	-	10.09	-
H_2O -110	8.81	0.93	8.84	0.94
H_2O+110	8.63	2.94	8.29	3.17
Sum	99.82	100.03	96.41	100.58

All analyses are presented as weight percentages on an air dried basis. A dash indicates no analysis and ND means not detected.

*Sample A (the unfractionated crust) also contains 0.0012% Cr_2O_3.

Table 7 Comparison of Elemental Analyses of Manganese Concretions

	Jervis Inlet A	Jervis Inlet B	Baltic Sea Average	Deep Ocean (est.average)	V.S.78
Al	1.70	1.83	1.54	8.57	1.90
Ca	1.33	1.33	1.21	1.57	1.16
Co	.013	.014	.016	0.28	.010
Cu	.0055	.0091	.0048	0.40	.010
Fe	5.01	4.21	22.4	11.7	.86
K	.98	1.03	.076	.68	.96
Mg	1.82	1.83	.57	1.38	-
Mn	32.72	32.82	14.0	19.0	38.9
No	.023	.027	.013	.038	.022
Na	.95	.97	.35	2.08	-
Ni	.026	.038	.075	.58	.045
P	.34	.27	.70	.19	-
Pb	ND	ND	.0038	.10	.025
Ti	.096	.089	.11	.47	.07
Te	.012	.013	-	-	-
Zn	.0019	.0036	.008	0.04-0.40	.023

Jervis Inlet A Discoidal type - Grill 1968
B Spheroidal type

Baltic Sea Average - Manheim 1965
Deep Ocean (estimated average) - Manheim 1965
V.S. 78 (Vermilian Sea) - Mero 1965

However, the carbon analyses represent an average over the depth of penetration of the sampler (about 12 inches) and therefore are only an indication.

The ratio of manganese to iron ($Mn/_{Fe}$) has been correlated with depth and used in an attempt to distinguish and classify concretion localities (Mero, 1965). These ratios can be extremely variable with a considerable range sometimes occurring within a single specimen. In general, concretions from neritic and lake environments have a $Mn/_{Fe}$ ratio of less than unity. A majority of pelagic nodules have a ratio of greater than unity. Jervis Inlet concretions have an average $Mn/_{Fe}$ ratio of 5, there being little variation between samples. While this ratio does not follow the norm for shallow water concretions, it is by no means unique. Some nodules close to the North and South American coasts and near Japan have $Mn/_{Fe}$ ratios ranging from 12 to 50 (Price, 1965). As more analyses are published, the less evident becomes the supposed relationship between depth and $Mn/_{Fe}$ ratio.

The oxidation state of the manganese was calculated by Grill (Grill, Murray and Macdonald,1968) to be $MnO_{1.87}$ for sample A and $MnO_{1.86}$ for sample B, assuming all the active oxygen was associated with higher oxides of manganese. This O/Mn ratio is somewhat higher than the average value for neritic areas (1.55) and lower than that for the pelagic areas (1.9 - 2.0) (Manheim, 1965). Unlike the $^{Mn}/_{Fe}$ ratio, the $^{O}/_{Mn}$ ratio apparently has a significant covariance with depth (Manheim 1965). However, a considerable overlap of $^{O}/_{Mn}$ ratios exists between shallow and deep-water concretions.

The minor element content of Jervis Inlet concretions approximates that of other neritic occurrences. Elements of economic concern such as Ni, Cu, Zn, and Co have abundances ranging from 1 to 2 orders of magnitude below the estimated deep ocean average. Lead was not detected while molybdenum occurred with an abundance similar to that of deep sea concretions. The original analyses by Grill (Table 6) were given as oxide percentages of the soluble and insoluble (in a heated solution containing 10 ml of hydrochloric acid and 10 g. of hydroxylamine hydrochloride) fractions. The major

elements in the insoluble fraction were silicon, aluminum, iron, calcium, magnesium and sodium. These likely formed the detrital silicate minerals which were included within the ferromanganese oxide crusts. The phosphorus content of manganese concretions is thought to be related to their association with stagnant or semi-stagnant sediments (Manheim 1965). Jervis Inlet concretions, which are associated with semi-stagnant sediments, contained approximately 0.3 per cent phosphorus which is considered common for shallow marine forms. Tellurium was detected in the soluble fractions of both the Jervis Inlet samples analyzed.

5) Mineralogy

Todorokite was identified as the principal manganese mineral in Jervis Inlet concretions (Grill, Murray and Macdonald 1968). The suggested composition (Straczek, Horen, Ross and Warshaw, 1960) is:

$$(Ca,Na,Mn^{+2},K)\ (Mn^{+4},Mn^{+2},Mg)_6\ O_{12}\ .3H_2O$$

Calculation of atomic proportions (the number of atoms per unit cell) of Mn^{+4}, Mn^{+2}, Mg (including Co, Cu), Ca (including Ba, Sr), Na and K for soluble Jervis Inlet material agrees with similar data presented for todorokite by other authors.(Grill et al 1968).

6) Formation of Concretions

The mechanism of formation of manganese concretions can only be postulated. Many workers (e.g. Manheim, 1965 and Price, 1967) consider the growth of concretions to be due to the precipitation of elements from the interstitial waters of the underlying sediments. Metals present in low concentrations in sea water are deposited as oxides or as ions adsorbed on clay and organic particles. Release of these metals to the interstitial waters would occur with sediment burial due to the reducing effect of the organic matter. The resulting high concentration of elements in the interstitial waters as well as electrochemical differences between the adjacent reducing and oxidizing environments will set up a diffusion potential so causing the upward movement of these elements (Price, 1967).

This mechanism could produce a variety of concretion habits. Manheim (1961) suggests that in areas where the sediment water interface is neutral or reducing, nodules will not form but the trace-element content of the bottom waters will be increased. Conversely, in areas where the surficial sediments are highly oxidized, pea ores may form within the sediment

itself (Gripenburg, 1934). The most common habit is the discoid concretion (Kindle, 1932,Gripenburg, 1934, Manheim,1965).

Although the basic mechanisms for the formation of concretions in the shallow water and open ocean environment are believed similar, the concentration of many minor metals such as Cu, Co, Ni, Pb, and Zn tends to be one to several orders of magnitude less in shallow than in the deep ocean varieties. This trend is thought to be due to differing concentrations and types of organic matter present in the two environments. In neritic and lacustrine conditions, burial of the sediment and reduction in the presence of organic material releases most Mn, Pb, and Zn to the interstitial waters while the loss of Fe, Ni, Co and Cu is smaller and possibly due to retention of these elements in iron sulphides (Price, 1967). Water soluble organics, amino acids and humic acids within the sediments are also thought to affect metal concentrations of shallow water concretions by modifying the inorganic uptake of minor metals such that Pb, Zn, and Cu are not sorbed by the manganese-iron phases. In the open ocean environment the low abundance of organic matter in the

sediments would likely minimize the mobility and upward diffusion of manganese and other elements during sediment burial.

7) Abundance and Value

Figure 43a shows manganese-iron concretions as they were recovered in a grab sampler. The bulk of the sample is coarse to fine-grained sediment on which the concretions form. Figure 43b is an approximate average sample recovered from one lowering of the grab on to the locality. The square outline within which the concretions are pictured represents the area covered by the open jaws of the sampler.

The total air dried weight of the concretions pictured was 1.97 pound (.894 kilograms) of which 72.9 per cent or 1.43 pounds (.684 kilograms) was oxide material. Since the area within the open jaws is approximately 0.2 square yards (.17 square meters) the concentration of oxide material, assuming total recovery, would be 7.1 pounds/square yard (3.9 kilograms/square meter). If the area of the deposit is taken to be 36,000 square yards (30,000 square meters) the tonnage of oxides present would be 128 short tons (117 metric tons). This estimate could

Figure 43 a Petterssen grab sampler on deck with recovered manganese concretions and sediment substrate.

b An average density of manganese concretions. Black outline represents area covered by open jaws of Petterssen grab sampler. The area is 1/6 meter^2..

c Top view of large discoidal concretion. Note the preferred direction for accretion of oxides. (Major diameter is 5.5 in. or 13.1 cm.)

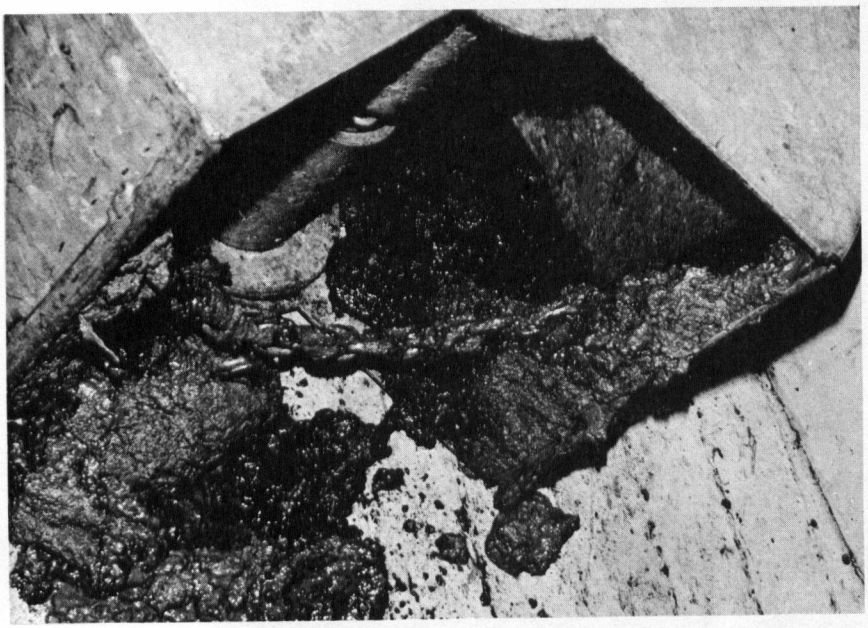

a

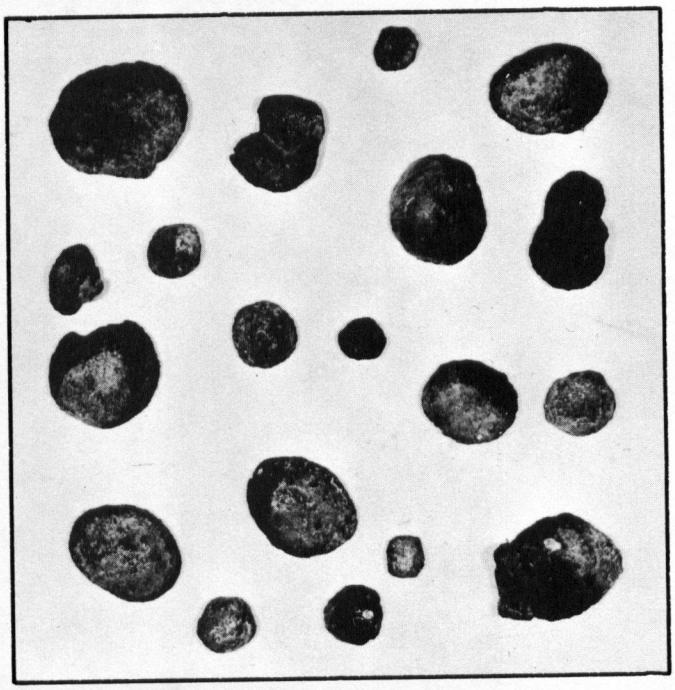

b

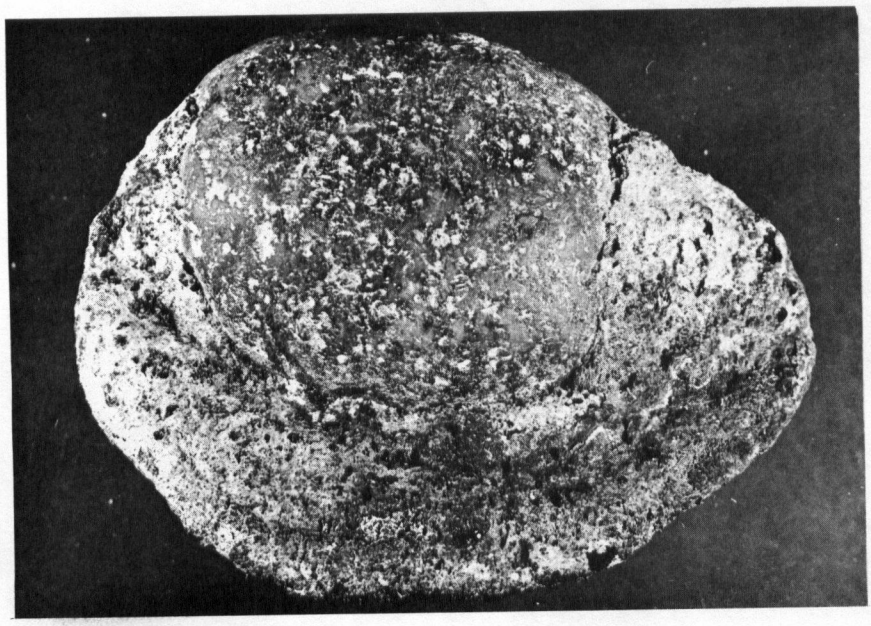

c

FIGURE 43

be in error by a considerable amount (perhaps ± 50 per cent) as the area of the locality is poorly known and only one sample which, from photographs, appeared to represent an average sample, was weighed.

While the above method of determining reserves of authigenic oxides on Patrick Sill is accurate within itself, many similar samples will have to be taken in order to estimate reasonably accurately the total tonnage. Perhaps a better method to determine this information would be to combine a small underwater camera and light source with the grab sampler. If the camera was triggered 10 feet or so off the bottom the concentration of concretions within the grab sampler could be extrapolated to the much larger area covered by the photograph. Underwater television was tried as a method to determine concentrations but concretions could not be distinguished from barren boulders with the system available.

II. Iron Crusts

Maintaining station over the concretion locality was difficult and only about 50 per cent of the attempts to obtain samples were successful. One attempt, which proved to be too far to the west by about 100 to 200 feet resulted in the sampler hitting

either bedrock or very large boulders. However, within the grab sampler were ferruginous crusts (Figure 44) which had been broken off the rock surface.

The external surfaces of the crusts vary from smooth to irregular. Cross sections reveal a distinct layering. The surface or outer layer is rind-like and varies in thickness from about .04 to 0.6 in. (1 to 15 mm). The colour is red brown to dark brown and black. The material is non-porous and has a vitreous to opaline lustre as if deposited as a gel. On dessication at room temperature the thicker portions have cracked forming interlocking polyhedral masses. Deposition of the gel-like material must have occurred reasonably rapidly as large bubble-like cavities were formed (Figures 44b, c). The principal mineral forming this outer layer is goethite (FeOOH).

The bulk of the material forming the crust is reddish yellow to yellow-brown, fine-grained, loose and very porous. An X-ray powder diffraction pattern indicated the principal minerals to be quartz, feldspar and goethite. This material likely

Figure 44 a Iron crust as recovered from rock face near but not on (i.e. within about 100 meters) the concretion locality. (approx. 1.6 X)

b,c Bubble-like structure shown by some of the iron crusts recovered from vicinity of concretion locality. Note layering within material of bubble and base and fragments of sponges within bubble. Approx. 1.6 X

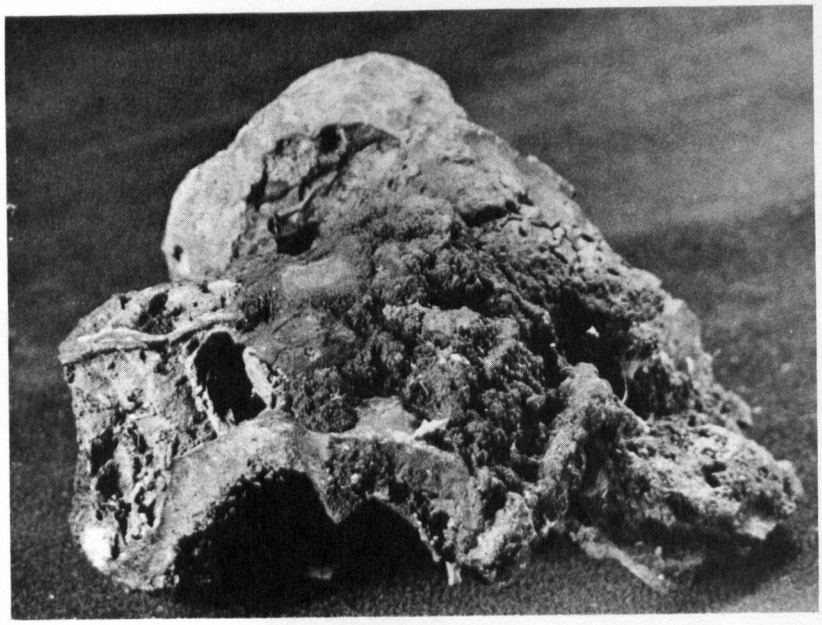

a

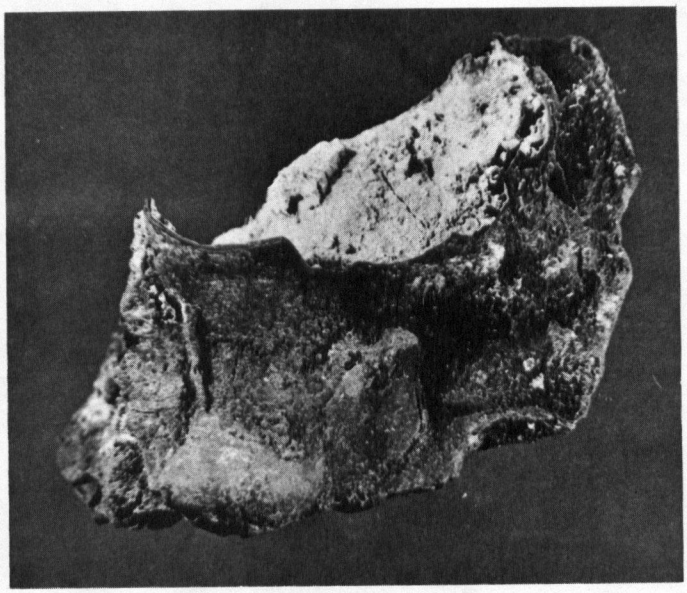

b

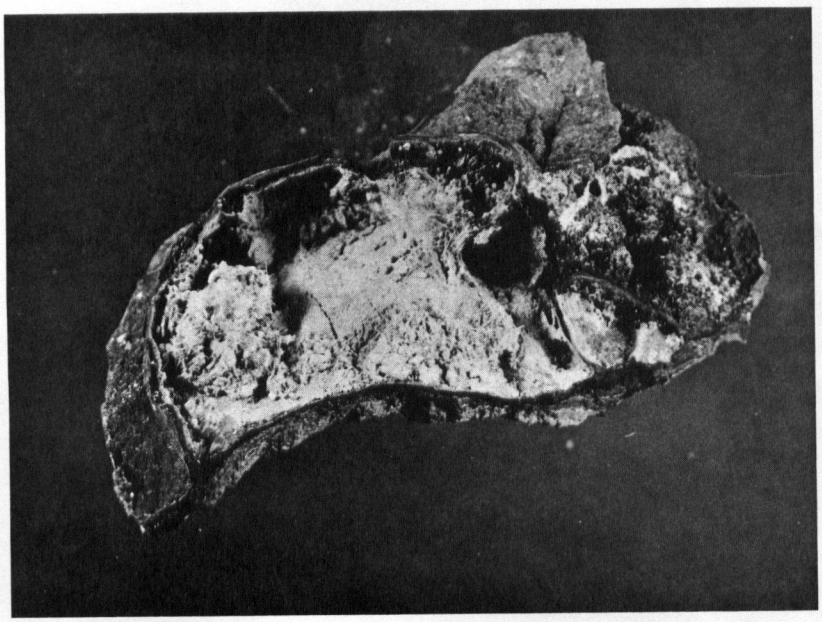

c

FIGURE 44

represents sediments which accumulated and were then included in the structure of the crusts by the deposition of the gel-like material. The layering mentioned is due to alternating layers of loose porous and vitreous materials. The nature of the material which formed the bond with the rock surface is not known.

There is no feature of the crust which would give an indication of age.

III. "Glauconite-Montmorillonoid" Pellets

Murray and MacIntosh (1968) described interstratified glauconite-montmorillonoid pellets from Queen Charlotte Sound. Mineralogic and morphologic studies of Jervis Inlet sediments revealed the presence of physically identical pellets (Figure 18d). These pellets were found over a considerable area of the sill as well as in localized areas on the sides of the lower basin. Pellets were not noted in samples collected from the upper basin. No X-ray or chemical analyses have been made of these pellets to date.

The pellets are generally spheroidal and light yellow-green to gray-green in colour. In the fractions examined, the pellets are most abundant in the fine sands (i.e. 88 to 63/u or 3.5 to 4 Ø) but some

samples contained pellets in the 500 to 350/u (1.0 to 1.5 Ø) range. Both these fractions of sample J-135, which is near but not on the concretion locality, were estimated to be 40% pellets. The finer fraction of sample J-164 was also about 40% pellets. Sediments collected with concretions were about 15% pellets for the fractions examined. Often recovered with the pellets were sponge spicules and radiolarian tests.

1V DISCUSSION

The sill environment, especially on and near the medial depression is mineralogically unique within the study area. Why manganese concretions and iron crusts should form there and apparently not elsewhere within upper Jervis Inlet is not known. The area of the medial depression is affected by a bottom current with an approximate velocity of 25 centimeters/second. This current limits the deposition of detritus, both minerogenic and organic, and in some areas is capable of winnowing, with subsequent formation of lag deposits. The surficial sediments of the concretion locality are a dark red-brown colour for a depth of about 1 to 2 centimeters. Below this layer the sediments are generally a typical olive-green. The

colour of the surficial sediments indicates oxidizing conditions probably due to the constant renewal of overlying waters and the lower organic matter content of the sediments.

Iron is being deposited as goethite crusts on exposed rock surfaces within the medial depression of the sill. Apparently simultaneously and in close proximity, manganese concretions are forming around rock fragments resting on sediments. Whereas the source of the goethite is likely a gel formed in the seawater, the concretion-forming manganese is apparently derived from the substrate. Further studies which might prove interesting would be determination of the concentration of iron on the surface versus the underside of concretions and, although possibly not yet feasible, the determination of groundwater circulation within the sill.

What are thought to be "glauconite-montmorillonoid" pellets are also forming within upper Jervis Inlet, but they are not unique to the sill. Certain samples collected from the wall of the lower basin contained these pellets in considerable quantity, but no pellets were found in the sediments of the upper basin.

Whether these pellets form on or beneath the sediment-water interface is not known. The depth zonation noticed by Porrenga (1966) in which goethite occupies the 0 to 50 meter zone and glauconite the 30 to 2000 meter zone is only partly applicable in this area. However, since it is not known if the goethite crusts and pellets are forming presently or what the fluctuations in sea level have been since Pleistocene time, little can be said. More thorough sampling might necessitate revision of ideas about distribution patterns.

V EXPLORATION

If, at some time in the future, the mining of concentrations of shallow marine concretions becomes profitable, the question will arise as to how to locate these deposits. At present, the best guide would probably be bathymetry. Favourable conditions appear to be achieved on the crests of banks and sills or on basin margins. All presently known local occurrences of concretions have been found in the 100 to 200 fathom range. However, the significance of depth is not known. Movement of the overlying waters is needed to maintain a low sediment accumulation rate and oxidizing conditions within the bottom waters and top centimeter or so of the sediments. The occurrence

of a stagnant to semi-stagnent basin adjacent to the elevated area is thought to be important (Price 1967). To date, not enough is known about trace element concentrations within sea water and sediment in areas where concretions form to enable one to use such data for exploration.

Bibliography

Armstrong, J. E. and W. L. Brown, 1954, Late Wisconsin Marine Drift and Associated Sediments of the Lower Fraser Valley, British Columbia, Canada. Bull. Geol. Soc. Amer., Vol. 65: 349-364

Armstrong, J. E. et al, 1965, Late Pleistocene Stratigraphy and Chronology in Southwestern British Columbia and Northwestern Washington. Bull. Geol. Soc. Amer., Vol.76: 321-330

Bacon, W. R., 1957, Geology of Lower Jervis Inlet, B. C. Dept.of Mines and Petroleum Resources Bulletin 39

B. C. Natural Resources Conference, 1956, British Columbia Atlas of Resources

Carter, N. M. 1934 Physiography and Oceanography of Some British Columbia Fjords, Proc. Fifth Pacific Sci. Cong. 1933, Vol.1: 721-733

Cockbain, A. E. 1963, Distribution of Sediments on the Continental Shelf off the Southern B. C. Coast, Manuscript Report 15, I.O.U.B.C.

Dobrin, M.B., 1960, Introduction to Geophysical Prospecting McGraw-Hill, 446 pp.

Folk, R. L. 1961, Petrology of Sedimentary Rocks, The University of Texas, 154 pp.

Folk, R. L. 1966, A. Review of Grain Size Parameters, Sedimentology 6: 73-93

Folk, R. L. and W.C. Ward, 1957, Brazos River Bar, a Study in the Significance of Grain Size Parameters, J. Sediment. Petrol., 27: 3-27

Grill, E.V., J. W. Murray and R. D. Macdonald 1968, Todorokite in Manganese Nodules from a British Columbia Fjord, Nature, Vol.129,No.552: 358-359

Grim, R. E., 1968 Clay Mineralogy, McGraw-Hill,596 pp.

Gucleur, S.M. and M.G. Gross,1964, Recent Marine Sediments in Saanich Inlet, a Stagnant Marine Basin, Limn.and Ocean., Vol.9, No.3: 359-375

Holland, S.S., 1964, Landforms of British Columbia, B. C. Dept.of Mines and Petroleum Resources, Bull. No.48

Kittrick, J.A. and E.W. Hope, 1963, a Procedure for the Particle Size Separation of Soils for X-ray Diffraction Analysis, Soil Science 96: 319-325

Lazier, J.R.N., 1963, Some Aspects of the Oceanographic Structure in the Jervis Inlet System, M.Sc. Thesis, University of British Columbia

LeRoy, O.E., 1908, Preliminary Report on a Portion of the Main Coast of British Columbia and Adjacent Islands, Geologic Survey of Canada, Report No.996: Publications 1908 Vol. 1

Manheim, F. T., 1965, Manganese-Iron Accumulations in the Shallow Marine Environment, Symposium on Marine Geochemistry, Narragansett Marine Laboratory, University of Rhode Island, Occas. Public. No. 3 - 1965: 217-275

Mero, J. L. 1965, The Mineral Resources of the Sea, Elsevier Publishing Company, 312 pp.

Murray, J.W. and E.E.Mackintosh, 1968, Occurrence of Interstratified Glauconite-Montmorillonoid Pellets, Queen Charlotte Sound, British Columbia, Canadian Jour. of Earth Sciences, 5: 243-247

Pantin, H.M. 1969, The Appearance and Origin of Colours in Muddy Marine Sediments Around New Zealand, New Zealand Jour.of Geol. and Geoph., Vol. 12, No.1: 51-56

Peacock, M. A. 1935, Fjord-Land of British Columbia, Bull. Geol. Soc.of Amer.46: 633

Pickard, G. L.,1961, Oceanographic Features of Inlets in the British Columbia Mainland Coast, Jour. Fisheries Research Board of Canada, Vol. 18, No. 6: 907-999

Pickard, G.L. and G.K.Rodgers, 1959, Current Measurements in Knight Inlet, British Columbia, Jour. of Fisheries Research Board of Canada, 16: 635-678

Pickard, G.L. and L.F. Giovando,1960, Some Observations of Turbidity in British Columbia Inlets, Limn. and Oceanog. 5 (12): 162-170

Porrenga, D.H., 1966, Glauconite and Chamosite as Depth Indicators in the Marine Environment. Marine Geology 5: 495-501

Postma, H., 1967, Sediment Transport and Sedimentation in the Estuarine Environment in Estuaries, Amer. Assoc. Adv. of Science Publ.No.83:158-180

Price, N.B., 1967, Some Geochemical Observations on Manganese-Iron Oxide Nodules from Different Depth Environments, Marine Geology 5; 511-538

Roddick, J.A. 1965, Vancouver North, Coquitlam and Pitt Lake Map Areas, British Columbia, G.S.C. Memoir 335 : 376 pp

Shepard, F.P., 1954, Nomenclature Based on Sand-Silt-Clay Ratios, Jour. Sedimentary Petrology, Vol. 24: 151-158

Soren, R.K. 1967, Manganese Nodules: Nature and Significance of Internal Structure, Economic Geology, Vol. 62, No.1:

Tiffin, D.L. and J.W. Murray, 1966, Mapping Offshore with Continuous Seismic, Oil Week, Nov.7,1966

Toombs, R.B.,1956, Bute Inlet Sediments, Trans.Roy. Soc. Canada, Ser. III,50: 59-65

Trask, P.D., 1938, Organic Content of Recent Marine Sediments, Recent Marine Sediment - A Symposium, Dover Publications, 736 pp.

Trites, R.W.,1965, A Study of the Oceanographic Structure in British Columbia Inlets and Some of the Determining Factors, PhD Thesis, University of British Columbia, Vancouver, B.C.

Weaver, C.E.,1958, Geologic Interpretation of Argillaceous Sediments, Part I, Origin and Significance of Clay Minerals in Sedimentary Rocks, Bull.Amer. Assoc. Pet. Geol.,Vol.42, No.2: 254-271

JERVIS INLET (Northern Portion)

FIGURE 3

SAMPLE STATION LOCATIONS

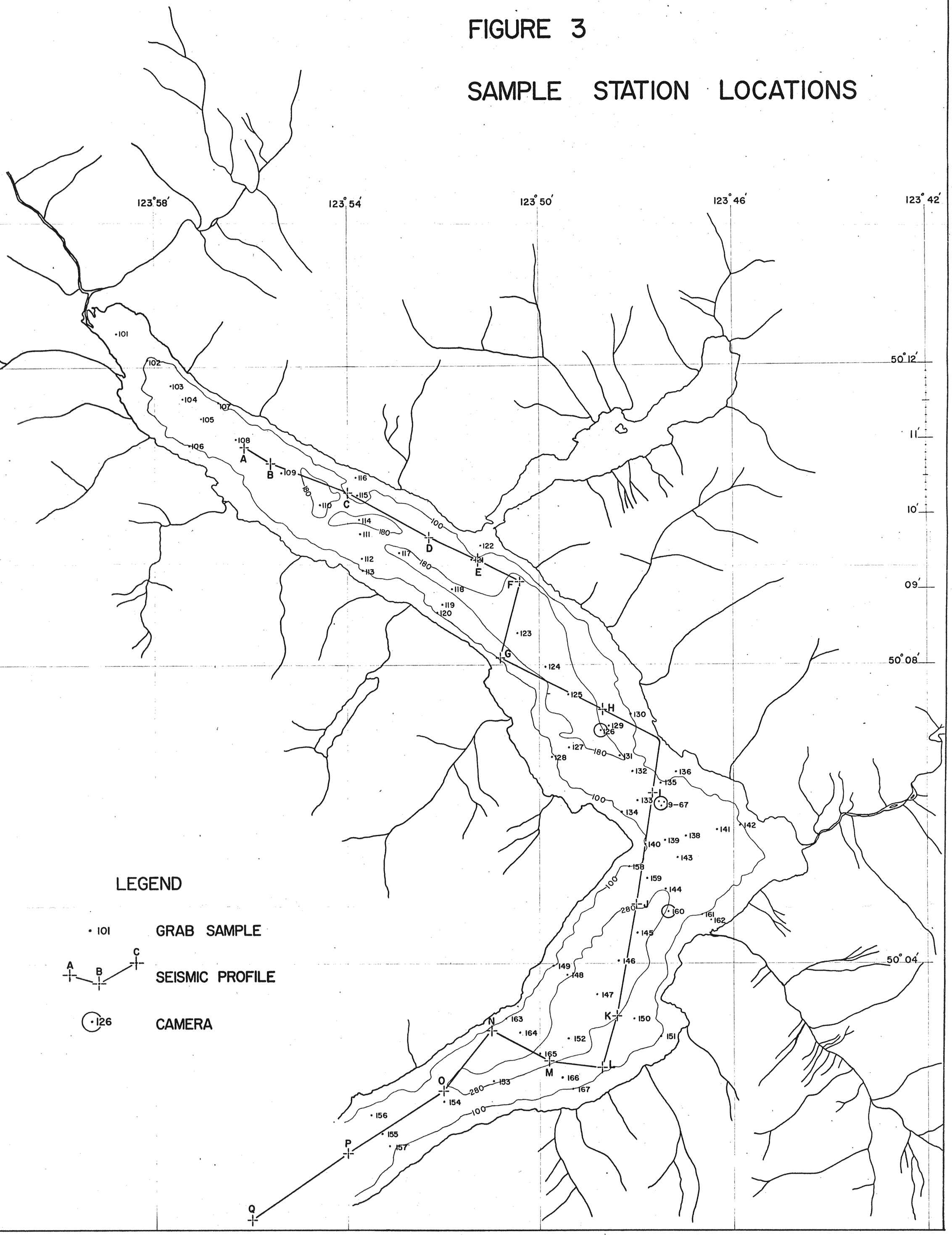

LEGEND

- 101 — GRAB SAMPLE
- A, B, C — SEISMIC PROFILE
- 126 — CAMERA

Robert D. MacDonald

JERVIS INLET (Northern Portion)

Ref: Canadian Hydrographic Service Field Sheet 2228-L

CONTOUR INTERVAL - 20 FATHOMS

FIGURE 6

LOCATION AND BATHYMETRY

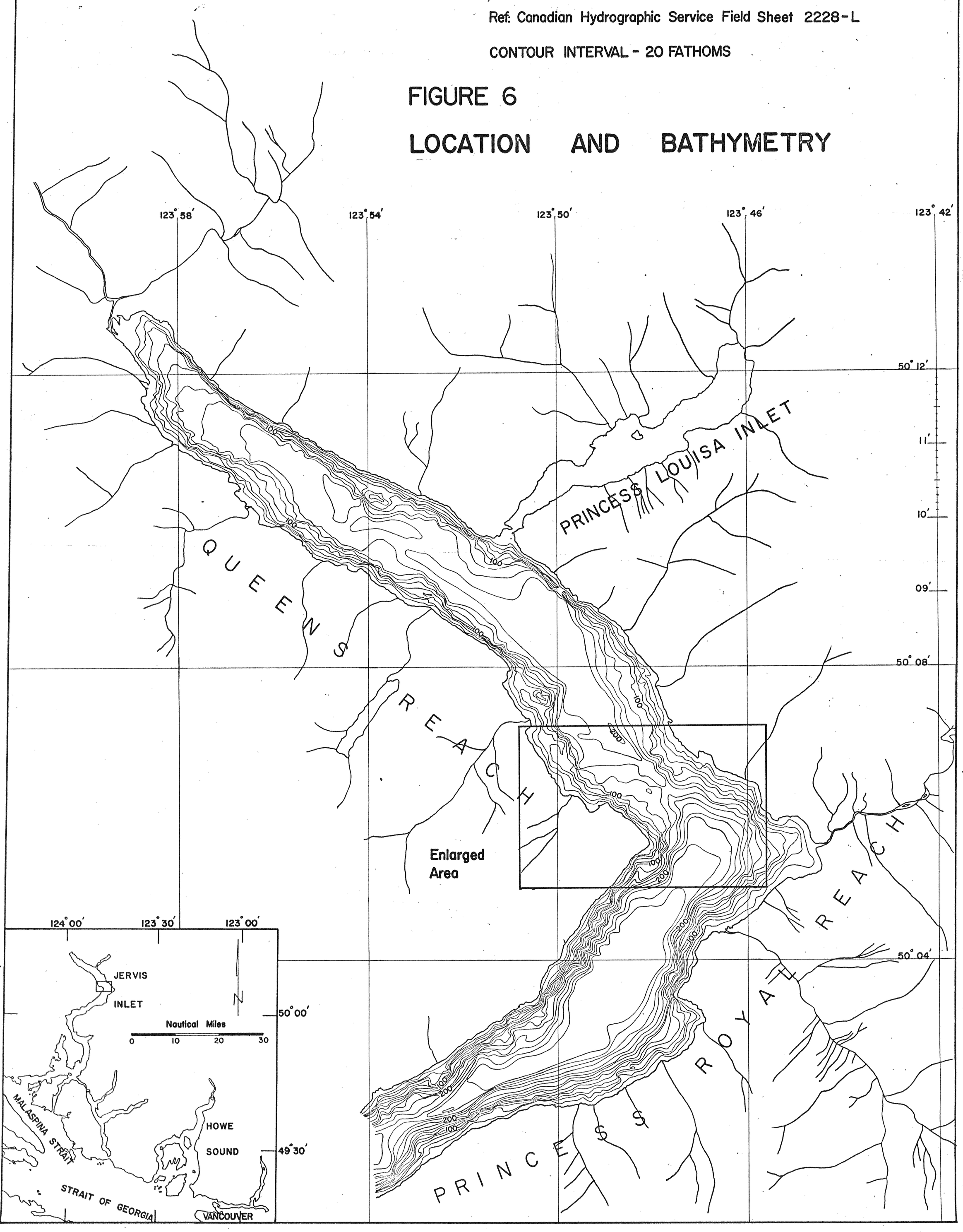

Robert R. MacDonald -

JERVIS INLET (Northern Portion)

FIGURE 14

TOTAL CARBON PERCENT

123°58′ 123°54′ 123°50′ 123°46′ 123°42′

50°12′ 11′ 10′ 09′ 50°08′ 50°04′

LEGEND

< 2%

2-3%

3-4%

> 4%

Robert N. MacDonald

JERVIS INLET (Northern Portion)

FIGURE 20

SEDIMENT-TYPE DISTRIBUTION

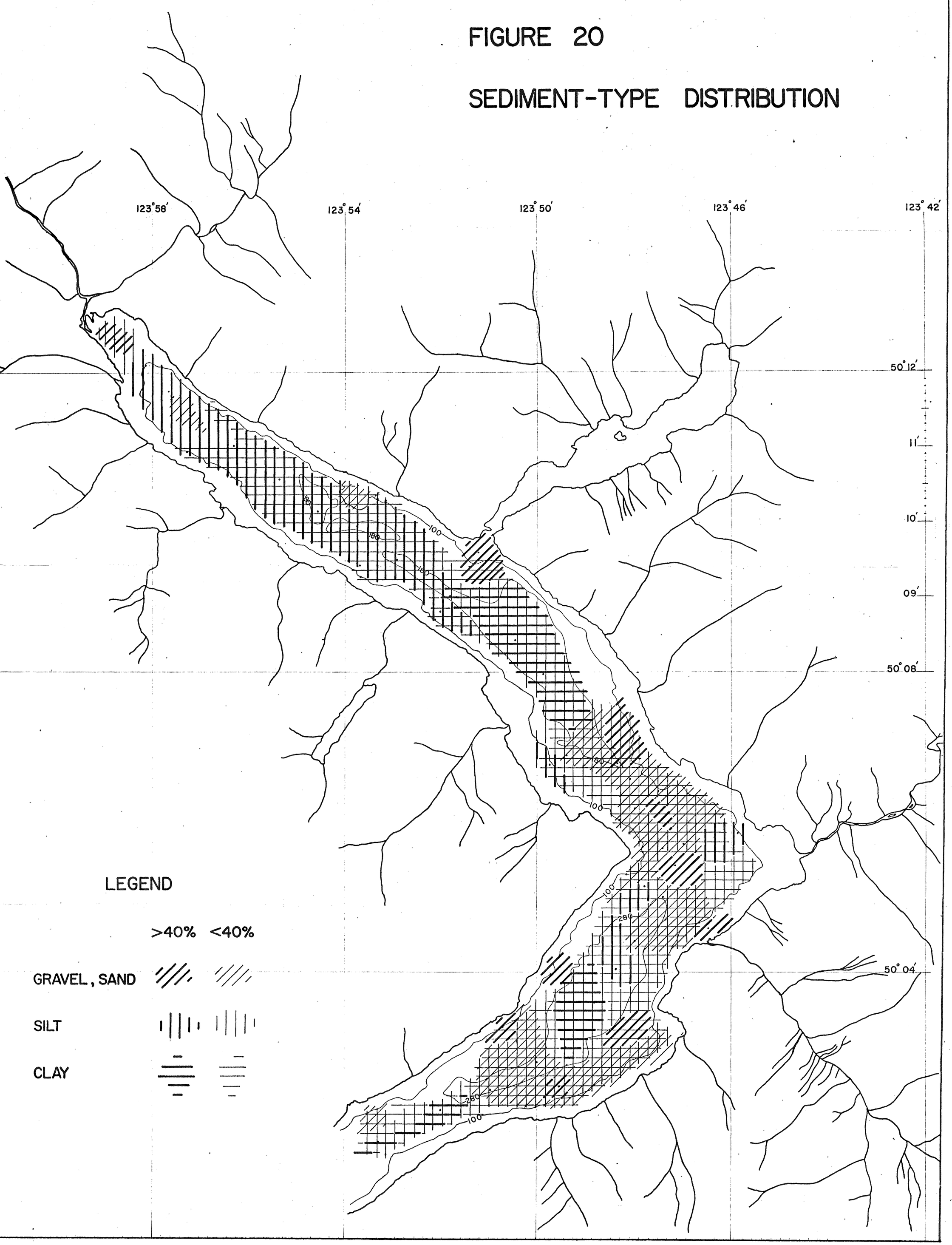

Robert W. Macdonald

123° 50′ 00″ 123° 48′ 00″ 123° 46′ 00″

50° 07′ 00″ 50° 07′ 00″

50° 06′ 00″ 50° 06′ 00″

50° 05′ 00″ 50° 05′ 00″

123° 50′ 00″ 123° 48′ 00″ 123° 46′ 00″

PATRICK SILL

JERVIS INLET (Northern Portion)

Contour Interval – 10 fathoms

Manganese Locality

FIGURE 37

Robert H. MacDonald

JERVIS INLET (Northern Portion)

FIGURE 21

CLAY SIZE PARTICLE PERCENT

123°58′ 123°54′ 123°50′ 123°46′ 123°42′

50°12′ 11′ 10′ 09′ 50°08′ 50°04′

LEGEND

< 20%

20-30%

30-40%

40-50%

> 50%

Robert H. MacDonald